DEVELOPMENT OF A HIGH THROUGHPUT ASSAY TO OPTIMIZE HEMATOPOIETIC DIFFERENTIATION OF HUMAN PLURIPOTENT STEM CELLS

Joel Thomas Outten

A DISSERTATION

in

Bioengineering

Presented to the Faculties of the University of Pennsylvania in Partial Fulfillment of the Requirements for the Degree of Doctor of Philosophy

2012

Supervisor of Dissertation:

Signature_____
Dr. Scott L. Diamond, Arthur E. Humphrey Professor of Chemical and Biomolecular Engineering

Graduate Group Chairperson:

Signature_____
Dr. Beth Winkelstein, Professor of Bioengineering

Dissertation Committee:

Dr. Casim A. Sarkar	*Committee Chair*, Assistant Professor in Bioengineering
Dr. Deborah L. French	Director, hESC/iPSC Core Facility, Children's Hospital of Philadelphia
Dr. Christopher S. Chen	Skirkanich Professor of Innovation in Bioengineering

DEVELOPMENT OF A HIGH THROUGHPUT ASSAY TO OPTIMIZE HEMATOPOIETIC DIFFERENTIATION OF HUMAN PLURIPOTENT STEM CELLS

Acknowledgements

As with most undertakings in science, this work represents much more of a team effort than the single authorship implies. Firstly, I would like to thank my advisor, Scott Diamond. After spending my first year on a project that was failing miserably, I told Scott that I'd like to start something new. He was extremely supportive throughout this transition and helped create the vision that eventually became this work. Scott has always been enthusiastic, encouraging, patient, and trusting for whatever direction I wanted to take my research. I greatly appreciate his support for bringing an entirely new area (stem cell biology) into his lab.

I would like to thank all members that have been associated with the Diamond Lab during my tenure. Huiyan Jing has assisted with many different day to day lab procedures and is always extremely happy to help in whatever way she can. I greatly appreciate the initial cell culture assistance provided by Dave Fein, Greg Barker, and Renee Randazzo. Sean Maloney deserves infinite thanks for keeping many of the lab operations running smoothly. I can't express how much I enjoyed the entertainment provided by the personalities of Keith Neeves and Dave Fein and how they kept me going when research was floundering. Thank you to Dan Jaeger for handling the IT aspects of the lab and being there anytime I couldn't figure out how to turn my computer on. I am extremely thankful for both Olga Lozysnka and Edinson Lucumi for always being up for talking about things other than research. Thank you to Viraj Kumat for stem cell assistance and for continuing to upkeep the stem cell aspect of this lab. Finally, although you may not have been as directly involved with this research, thank you to

Hana Oh, Andrew Dolan, Matt Flamm, Tom Colace, Ryan Muthard, Melissa Myint, and Manash Chatterjee for being such delightful lab mates.

Peter Davies, Marvin Jackson, and Janell Petzko ran the IME during this project and each significantly. Peter directed the training grant that funded much of this research and has always been highly interested in this research. I am very thankful for Janell's assistance with admin duties and for discussing pottery and ceramics techniques. Marvin has been extremely helpful in numerous ways…I greatly appreciate everything he has done from encouraging me to give a chalk talk to throwing happy hours to being up for grabbing Indian buffet lunches.

I cannot express enough gratitude and appreciation for the entire staff of the CHOP hESC/iPS Core. This project began after Scott mentioned that CHOP had just hired a stem cell group interested in doing blood research. I met with both Debbie French and Paul Gadue, who were both extremely enthusiastic about the endeavor. Deb and Paul have both been amazing mentors over the past 4 years. Thank you for providing the expertise and resources necessary for this project to even exist. I can't express enough how much I've enjoyed this collaboration. Thank you to Core Manager Aline Disimone for all the time and effort that you provided…you are amazing. Thanks to Prasuna Palaru, Xin Cheng, and Jay Mills for their constant protocol assistance and for helping me to get new techniques up and running. I am lastly very thankful to everyone in the Core that either fed my cells at some point or simply being a fantastic personality, including Amita Tiyaboonchai, Helen Mac, Spencer Sullivan, Lei Ying, and Lin Lu.

I'd like to express my love and appreciation for the Philadelphia Ultimate Frisbee community for providing a recreational outlet that has expanded into a huge part of my

life. This research may have crashed and burned long ago had I not been able to balance my life with Ultimate and such fantastic group of people. More specifically, thank you to Ruth Strickland, Peter Cline, and Ryan Doherty for being such supportive, understanding, imperfect, and amazing friends throughout the time of this research.

Finally, I'd like to thank my family for always being so supportive. Thank you to Leigh and Scott for being there for me when needed and for serving as such inspirations. I would certainly not have accomplished this goal if it were not for my parents, Fred and Claire, and their support and encouragement from my childhood to always strive to be my best. Thank you both for all that you've done.

ABSTRACT

DEVELOPMENT OF A HIGH THROUGHPUT ASSAY TO OPTIMIZE HEMATOPOIETIC DIFFERENTIATION OF HUMAN PLURIPOTENT STEM CELLS

Joel Thomas Outten

Advisor: Scott L. Diamond

Human embryonic stem cells (hESCs) offer the potential to develop *in vitro* protocols for the generation of any human somatic cell. In order for protocols to allow for both comprehension of underlying developmental mechanics and future clinical application, they will need to rely upon efficient differentiation of cells without the reliance upon animal-derived components. This thesis presents the development of a 96-well plate culture system that allows 4-color, flow cytometry based high throughput screening of defined, serum-free hESC differentiation conditions. In the first portion, broad applicability is proven by demonstrating highly efficient differentiation toward the three primary germ layers. Using four separate biomarkers, we were able to distinguish between ectoderm, endoderm, mesoderm and pluripotent hESCs. We demonstrated the ability to perform both cytokine screens and siRNA-mediated knockdown in this assay. In the second portion, we establish conditions to apply this assay to study hematopoietic differentiation. We performed numerous cytokine and inhibitor screens to develop a stepwise protocol that generates high yields of primitive megakaryocyte-erythromyeloid progenitors and megakaryocytes after 8 and 11 days of embryoid body differentiation, respectively. This work provides a novel tool to streamline the development of hESC

differentiation protocols and advances the hematopoietic field towards future hESC-derived therapies.

Contents

List of Tables

List of Figures

1. Introduction

1.1 Human embryonic stem cells

The isolation of human embryonic stem cells (hESCs) in 1998 [1] has revolutionized the field of regenerative medicine. hESCs, isolated from human blastocysts, exhibit pluripotency and can thus be theoretically induced to generate any somatic human cell. These cells offer new approaches to study human development and organogenesis, screen candidate drug molecules for toxicities, treat previously incurable pathologies, generate lines of desired cell types, and study disease mechanisms. Studies are increasingly being undertaken in all of these areas. While these cells have vast scientific and medical potential, progress relies on scientists to identify repeatable techniques to control differentiation outcome. Initial studies identified basic conditions to differentiate cells to the three primary germ layers [2, 3]. Somatic adult cells, in contrast, require lengthy differentiation pathways that must be tightly controlled and are infrequently understood. Increasingly more studies focus on defining protocols by which to differentiate hESCs to target cell lineages.

1.2 Mammalian development

hESCs are extracted from the inner cell mass of the approximately 6 day old blastocyst [3]. In mammalian development, the inner cell mass develops into the epiblast within a few days. The onset of gastrulation is marked by the formation of the primitive streak on the surface of the epiblast around day 14. Epiblast cells begin to migrate

through the primitive streak and differentiate into either mesoderm or definitive endoderm. Epiblast cells that do not migrate through the streak will form the ectoderm. These three germ layers eventually differentiate into all the cells and tissues of the body [4].

Gastrulation, as well as the entire process of development, is a highly coordinated, delicate interplay of growth factors and cytokines secreted and received at just the right moments. The primitive streak itself is initiated by coordinated expression of the transforming growth factor-beta (TGF-β) family members Nodal and bone morphogenic protein 4 (BMP4) and members of the Wnt family. The local concentration of these growth factors induces streak cells to migrate and begin differentiating toward the mesoderm and endoderm lineages. The extraembryonic endoderm secretes BMP4 during gastrulation. A BMP4 diffusion gradient is thus formed in which posterior primitive streak cells receive the highest exposure and anterior cells receive the lowest. BMP4 promotes mesoderm, inducing posterior streak cells to differentiate down this lineage. Conversely, high concentrations of Nodal, secreted by the node by late-streak stage, promote anterior streak cells to become definitive endoderm. Members of the fibroblast growth factor (FGF) family, including FGF4 and FGF8, are also required for primitive streak formation and gastrulation. The signaling pathways utilized during development are thoroughly reviewed in Gadue et al. [5] and Murry and Keller [6].

In vitro experiments aim to recapitulate hESC development by mimicking the *in vivo* environment. Developmental signals and cues *in vivo* can be utilized to structure differentiation protocols of hESCs. Therefore, studies aim to follow developmental principles and pathways when differentiating to various lineages. Conversely, hESC

studies can help elucidate pathways and developmental mechanisms to give a greater understanding of *in vivo* embryogenesis.

1.3 Differentiation systems

Although scientists frequently know what target cell they aim to generate, the most appropriate path of differentiation is generally more elusive. Three primary methods have been utilized to support differentiation systems: 1) embryoid body (EB) suspension culture, 2) adherent culture, and 3) co-culture with another cell line. Although the technique of choice depends upon the goal, the vast majority of studies have relied upon EB culture, and many protocols incorporate multiple methods.

1.3.1 Embryoid body culture

When undifferentiated hESCs are seeded in suspension (generally as clumps of cells), cells aggregate and form spherical three-dimensional clusters called embryoid bodies. Depending on external signaling cues, cells within EBs differentiate to one of the three primary germ layers as the EBs increase in size during differentiation. EBs are generally cultured in one of four systems: 1) hanging drops 2) liquid suspension culture 3) methylcellulose medium, and 4) large-scaleable bioreactors [7]. Each method carries advantages and disadvantages. As a general principle, studies have shown that results are more reliable, dependable, and controllable when homogenous EBs of known sizes are utilized .

Hanging Drops

Although becoming less common, hanging drops have traditionally been widely used as a reliable method of generating consistent EBs of known size[8]. Individual drops of medium containing cells at a known density are attached to the underside of a plastic petri dish lid. Cells aggregate in the rounded bottom of each drop and form an EB of defined cell number. This method is becoming less common due to the time required to seed and harvest EBs.

Liquid suspension culture

Many studies have relied on seeding single cells or clumps of ESCs into 6 to 24-well culture plates. EBs are formed either from spontaneous aggregation or from non-dissociated clusters of cells [2, 9]. Due to the uncontrolled environment, EBs tend to be heterogenous in these systems[7]. EBs also have the potential to aggregate together during differentiation [10]. Rotary culture of EBs during differentiation has been demonstrated to induce homogenous EBs and increase yield and differentiation efficiency, albeit through an unknown mechanism [11]. More recently, groups have utilized micro-scale conical-patterned well inserts to generate hundreds of thousands of EBs from centrifugation of cells prior to seeding EBs in liquid suspension differentiation culture [12]. Similar technologies are now commercially available.

Methylcellulose culture

Semisolid methylcellulose culture has been utilized to avoid uncontrolled aggregation and ensure the formation of single cell-derived EBs [13]. This method has

been used mostly for hematopoietic differentiation, but has become less frequent due to the difficulty of harvesting cells from methylcellulose.

Large scale bioreactors

Many commercial and therapeutic applications of ESC protocols will require extremely large amounts of cells, negating the reliance on standard cell culture systems. Bioreactor systems can be scaled to meet such demands. As with liquid culture systems, multiple EBs can aggregate in such systems, reducing the homogeneity of EB populations. In order to minimize this phenomenon, EB formation is completed ahead of time, for instance in hanging drops[14], and then transferred to bulk stirred suspension cultures.

1.3.2 Adherent and stromal cell co-culture

While EB culture supports ESC differentiation toward numerous lineages, several alternative approaches have been utilized to re-create a more developmentally-realistic stem cell niche. Both adherent and stromal cell co-culture aim to accomplish this goal. Adherent methods entail culturing ESCs as a two-dimensional monolayer on extracellular matrix proteins and allow for more control and generally exhibit less variability than EB protocols. However, such protocols can not be scaled-up to bioreactor culture and have only been demonstrated to be applicable for a small number of differentiation pathways. Numerous animal stromal cells have been demonstrated to induce efficient differentiation. Stromal cells derived from the murine aorta-gonad-mesonephros (AGM),

the fetal liver, and the bone marrow have all been utilized to efficiently differentiate ESCs towards the hematopoietic lineage [15].

1.4 Serum-free differentiation media

Early ESC protocols relied on the use of serum containing media due to the enhanced viability and efficient differentiation [1, 16-18]. However, serum contains a plethora of unknown factors, is significantly variable between lots, and is not clinically applicable. To overcome these limitations, more recent feeder-free studies have focused on identifying serum-free media formulations [19-21]. Numerous combinations of cytokines, growth factors, and siRNA molecules are being evaluated in order to understand signaling pathways utilized during differentiation and to optimize differentiation protocols to target cell types. By precisely activating or inhibiting the TGFβ family, FGF, Wnt, and other pathways at specific times, the developing embryo directs differentiation to all somatic cells of the body [5]. *In vitro* hESC differentiation systems attempt to recapitulate these developmental pathways by utilizing controlled concentrations of cytokines and inhibitors. As differentiation proceeds down specific lineages, the possible number of cytokine combinations dramatically increases.

1.5 Small scale platforms

In an effort to reduce the requisite time and materials needed to assess a large array of conditions and cytokine combinations, several groups have developed small-

scale culture platforms. Ng et al. have developed a 96-well spin embryoid body (EB) technique in which hESCs are spun down to form a single EB of a defined size within each well [22, 23]. This technique has been utilized to optimize differentiation to various stages in the hematopoietic lineage[24, 25]. Koike et al. have developed a 96-well murine ESC (mESC) differentiation system and explored effects of EB seeding density upon differentiation to cardiomyocytes [26, 27]. Both of these systems allow for a high degree of control over the medium environment, enabling precise identification of extrinsic factors that may influence EB differentiation. However, due to the small seeding density utilized by both methods to generate single EBs and the tendency for cell counts to drop over the first five days of differentiation [24], it is unclear if enough cells would be available for readouts such as 96-well flow cytometry analyses without pooling wells. Furthermore, these systems cannot be scaled up to larger platforms, limiting the number of EBs that can be produced. Several studies have utilized an adherent 384-well plate format to screen for small molecule inhibitors or enhancers of ESC differentiation [28, 29]. Although these confocal microscopy-based assays have been utilized to screen several thousand small molecules, they are not conducive to multi-color flow-cytometry or live cell sorting and would only be applicable to adherent culture protocols.

2. Materials and Methods

2.1 hESC maintenance

HES2 (passage 26-34) and H9 cells (passage 35-65) were maintained on irradiated mouse embryonic fibroblasts (MEFs) in hESC maintenance medium consisting of DMEM/F12 50:50 (Mediatech) supplemented with 20% Knockout Serum (Invitrogen, Carlsbad, CA), 1x non-essential amino acids (Invitrogen), 0.55 mM β-mercaptoethanol, 1% penicillin/streptomycin, 2 mM glutamine (Invitrogen), and 20 ng/mL bFGF (R&D Systems, Minneapolis, MN). Cells were passaged at 1:3-1:6 ratios using 0.25% trypsin/EDTA (Mediatech, Manassas, VA) or TrypLE Express (Invitrogen). For siRNA experiments, a previously established HES2 line was utilized that expresses a red fluorescent protein (RFP) from the *hROSA26* locus (HES2-R26) [30].

2.2 hESC differentiation

2.2.1 Germ layer differentiation

A 6-day differentiation procedure was utilized (Fig. 3.1A). Prior to differentiation, hESCs were trypsinized and replated on matrigel (Becton Dickinson, Franklin Lakes, NJ) in hESC maintenance medium. Serum-free differentiation (SFD) medium consisted of 75% IMDM (Invitrogen), 25% F12 (Mediatech), 0.5x N-2 supplement (Invitrogen) 0.5x B27 without retinoic acid (Invitrogen), and 0.05% BSA (Sigma, St. Louis, MO). Upon 75% confluency, cells were trypsinized, harvested with a

cell scraper, spun down, and resuspended in SFD medium supplemented with penicillin/streptomycin, 2 mM glutamine, 0.5 mM ascorbic acid (Sigma), $1.5x10^{-4}$ M monothioglycerol (Sigma), and the specified concentrations of cytokines as indicated (summarized in Table 2.1). Day 0 media was supplemented with: 10 ng/mL BMP4 (R&D Systems) for endoderm/mesoderm or 10 μM SB431542 (Tocris, Ellisville, MO), 500 ng/mL BMPR1A (R&D Systems), and 5 ng/mL bFGF (R&D Systems, Minneapolis, MN) for ectoderm. $2x10^6$ cells were seeded into 10-cm petri dishes and cultured at 5% CO_2/5% O_2/90% N_2. After 24 hours, EBs were harvested, manually disrupted, and seeded into 100 μL Day 1 medium into low-cluster 96-well plates (Corning, Corning, NY) at $2x10^5$ cells/mL ($2x10^4$ cells/well). *Endoderm* Day 1 medium was supplemented with 100 ng/mL activin A (R&D Systems), 2.5 ng/mL bFGF, 0.5 ng/mL BMP4. *Mesoderm* Day 1 medium was supplemented with 0.5 ng/mL activin A, 2.5 ng/mL bFGF, and 20 ng/mL BMP4. *Ectoderm* Day 1 medium was supplemented with 5 ng/mL bFGF, 10 μM SB431542, and 500 ng/mL BMPR1A. For growth factor screening experiments, Day 1 media contained 2.5 ng/mL bFGF, and activin A and BMP4 were utilized at concentrations of 0 to 100 ng/mL, as indicated. At Day 4, 200 μL of Day 4 media were added to each well. Day 4 mesoderm and endoderm media were identical to Day 1 media, but with 5 ng/mL bFGF. Day 4 ectoderm medium was identical to Day 1 medium with 20 ng/mL bFGF. For growth factor screening experiments, media were supplemented with 5 ng/mL bFGF, the indicated concentrations of activin A and BMP4, and ± 10 ng/mL $VEGF_{165}$ (R&D Systems). During incubation, 96-well plates were covered with gas-permeable membranes (Breathe Easy, Diversified Biotech, Boston, MA) and stainless steel plate lids (Kalypsys, Inc., San Diego, CA).

Table 2.1. Differentiation media for germ layer induction

	Day 0	Day 1	Day 4
Endoderm	•2 mM Glutamine (Invitrogen) •0.5 mM ascorbic acid (Sigma) •$1.5x10^{-4}$ M monothioglycerol (Sigma) •10 ng/mL BMP4 (R&D Systems)	•2 mM Glutamine •0.5 mM ascorbic acid •$1.5x10^{-4}$ M monothioglycerol •0.5 ng/mL BMP4 •100 ng/mL Activin A (R&D Systems) •2.5 ng/mL bFGF (R&D Systems)	•2 mM Glutamine •0.5 mM ascorbic acid •$1.5x10^{-4}$ M monothioglycerol •0.5 ng/mL BMP4 •100 ng/mL Activin A •5 ng/mL bFGF
Mesoderm	*Identical to Day 0 endoderm*	•2 mM Glutamine •0.5 mM ascorbic acid •$1.5x10^{-4}$ M monothioglycerol •20 ng/mL BMP4 •0.5 ng/mL Activin A •2.5 ng/mL bFGF	•2 mM Glutamine •0.5 mM ascorbic acid •$1.5x10^{-4}$ M monothioglycerol •20 ng/mL BMP4 •0.5 ng/mL Activin A •5 ng/mL bFGF
Ectoderm	•2 mM Glutamine •0.5 mM ascorbic acid •$1.5x10^{-4}$ M monothioglycerol •500 ng/mL BMPR1A (R&D Systems) •10 μM SB431542 (Tocris) •5 ng/mL bFGF	*Identical to Day 0 ectoderm*	•2 mM Glutamine •0.5 mM ascorbic acid •$1.5x10^{-4}$ M monothioglycerol •500 ng/mL BMPR1A •10 μM SB431542 •20 ng/mL bFGF

2.2.2 Hematopoietic differentiation

Cells were harvested from matrigel upon reaching 70-80% confluency by enzymatic cleavage with TrypLE Express for 4 min at RT. Cells were removed with a cell scraper, spun down at 1200 rpm for 3 min, and resuspended in differentiation buffer. Differentiation medium consisted of StemPro-34 serum-free medium (SP34 SFM; Invitrogen) supplemented with penicillin/streptomycin, 2 mM glutamine, 0.5 mM ascorbic acid, $1.5x10^{-4}$ M monothioglycerol, and growth factors and inhibitors as specified in *Results*. Resuspended cell clusters were partially disrupted by pipetting up and down 3-4 times with a serological pipet. Depending upon experiment, the following cytokines and inhibitors were added at specified concentrations at designated stages of

differentiation as described in *Results*: 0-40 ng/mL BMP4, 0-100 ng/mL VEGF, 5-10 ng/mL bFGF, TPO, Flt3-L, IL-3, IL-6 (all R&D Systems), Chir-99021 (Stemgent), and Y-27632 (Tocris). Cells were seeded at 20,000 cells/well into 96-well ultra-low attachment plates. To isolate day 7 single cells for further differentiation and methylcellulose cultures, wells were pooled and EBs allowed to settle for several minutes. Supernatant was then withdrawn to extract single cells. For further hematopoietic differentiation, single cells were transferred to 6-well ultra-low adherence plates and cultured in SP34 based medium supplemented with penicillin/streptomycin, 2 mM glutamine, 0.5 mM ascorbic acid, 1.5×10^{-4} M monothioglycerol, 50 ng/mL SCF, 100 ng/mL TPO, 2 U/mL EPO, 25 ng/mL Flt3-L, 10 ng/mL IL-6, and 10 ng/mL IL-3.

2.3 96-well flow cytometry

2.3.1 Germ layer differentiation

EBs were dissociated, stained, and analyzed via 96-well flow cytometry as described [31]. EBs were transferred to 96-well V-bottom plates, spun down, and dissociated with 0.25% trypsin/EDTA. Antibodies utilized were: rat anti-SSEA-3-Alexa 488 (Biolegend, San Diego, CA, 330306), mouse anti-CXCR4-PE (Invitrogen, MHCCXCR404), mouse anti-NCAM-PE/Cy7 (Biolegend, 318318), mouse anti-KDR-Alexa 647 (Biolegend, 338909), mouse anti-PDGFRα-biotin (Biolegend, 323503), and streptavidin-PE/Cy7 (Invitrogen, SA1012). Cells were acquired directly from 96-well plates using a C6 Flow Cytometer equipped with a 96-well plate C-Sampler (Accuri, Ann

Arbor, MI) and analyzed using CFlow Plus software (Accuri) or FlowJo (Treestar, Ashland, OR). Markers utilized for flow cytometry are given in Table 2.2.

Table 2.2. Extracellular markers used for flow cytometry analyses

Extracellular marker	Alternative names	Expression
KDR (kinase insert domain receptor)	VEGFR2, FLK1, CD309	Many mesoderm subpopulations and on pluripotent stem cells.
SSEA-3 (stage-specific antigen 3)		Pluripotent stem cells and early ectoderm. Expression decreases with advanced differentiation.
CXCR4 (chemokine C-X-C motif receptor 4)		Endoderm and certain mesoderm subpopulations.
NCAM (neural cell adhesion molecule)	NCAM1, CD56	Early ectoderm and many endoderm and mesoderm subpopulations.
PDGFRa (platelet-derived growth factor receptor α)	CD140a	Mesoderm subpopulations. Indicative of paraxial commitment in murine stem cell differentiation.
CD31	PECAM-1 (platelet/endothelial cell adhesion molecule)	Hematopoietic and endothelial cells.
CD34		Many hematopoietic populations.
CD43	sialophorin	Many hematopoietic populations.
CD41	CD41B, GP α_{II}b, integrin α_{II}b	Megakaryocyte progenitors and committed megakaryocytes.
CD42a	GP IX (glycoprotein IX)	Committed megakaryocytes.
CD235a	GYPA (glycophorin A)	Erythrocyte progenitors and committed erythrocytes.
CD45	PRPRC (protein tyrosine phosphatase, receptor type C)	Mature hematopoietic and myeloid cells.
CD18	ITGB2 (integrin beta 2)	Myeloid cells.

2.3.2 Hematopoietic differentiation

EBs were dissociated with either 0.25% trypsin/EDTA or with Collagenase B (Roche) followed by Accutase (Invitrogen). Antibodies utilized were: rat anti-SSEA-3-Alexa 488, mouse anti-KDR-Alexa 647 (Biolegend), mouse anti-CD31 PE/Cy7 (Biolegend), mouse anti-CD34 Alexa 488 (Biolegend), mouse anti-CD43 FITC (Biolegend), mouse anti-CD43 PE (Biolegend), mouse anti-CD41 APC (Biolegend), mouse anti-CD41 PE (Biolegend), mouse anti-CD42a PE (BD Pharmingen), mouse anti-CD45 PE/Cy7 (Biolegend), and mouse anti-CD235a APC (BD Pharmingen). Cells were analyzed with 96-well flow cytometry as discussed previously.

2.4 Real-time quantitative PCR

EBs were collected from wells and dissociated with 0.25% trypsin/EDTA. Cells were lysed with the facilitation of QiaShredder columns and RNA was harvested using an RNeasy Mini-kit and treated with RNase-free DNase (Qiagen, Valencia, CA). Reverse transcription was performed with the iScript cDNA synthesis kit (Bio-rad, Hercules, CA) or the High Capacity cDNA Reverse Transcription kit (Applied Biosystems). Real-time quantitative PCR (qPCR) was performed in triplicate on a Roche Lightcycler 480 using LightCycler 480 SYBR Green I master mix (Roche, Indianapolis, IN) and 500 nM primer concentrations (Table 2.3). All gene expression levels were normalized to the housekeeping gene *GAPDH* [24].

Table 2.3. Primers utilized for real-time quantitative PCR analysis

Gene		Sequence	Amplicon Length
OCT4	forward	GCAAAACCCGGAGGAGTC	113
	reverse	CCACATCGGCCTGTGTATATC	
NANOG	forward	ATGCCTCACACGGAGACTGT	66
	reverse	AGGGCTGTCCTGAATAAGCA	
GSC	forward	ACCTCCGCGAGGAGAAAG	107
	reverse	GTTCCACTTCTCCGCGTTC	
SOX17	forward	CGCCGAGTTGAGCAAGAT	113
	reverse	GGTGGTCCTGCATGTGCT	
FOXA2	forward	CCGTTCTCCATCAACAACCT	89
	reverse	GCCTTGAGGTCCATTTTGTG	
CXCR4	forward	CTGTGAGCAGAGGGTCCAG	60
	reverse	ATGAATGTCCACCTCGCTTT	
CER1	forward	GGGAGACCTGCAGGACAGT	142
	reverse	CAGGAGGTATGGGAGTGCTG	
Brachyury	forward	TTCAAGGAGCTCACCAATGA	108
	reverse	GAAGGAGTACATGGCGTTGG	
KDR	forward	CAGGATGCAGAGCAAGGTG	93
	reverse	TCAAGAGAAACACTAGGCAAACC	
PDGFRα	forward	CCACCTGAGTGAGATTGTGG	83
	reverse	TCTTCAGGAAGTCCAGGTGAA	
PDGFRβ	forward	AGGCTGGCCACTACACCAT	91
	reverse	AGCACTCGGACAGGGACAT	
MEOX1	forward	AAATCATCCAGGCGGAGAA	95
	reverse	AAGGCCGTCCTCTCCTTG	
PAX6	forward	CAAATAACCTGCCTATGCAACC	94
	reverse	TAACTCCGCCCATTCACC	
SOX1	forward	CAGGCCATGGATGAAGGA	65
	reverse	CTTAATTGCTGGGGAATTG	
Nestin	forward	GAGGTGGCCACGTACAGG	86
	reverse	AAGCTGAGGGAAGTCTTGGA	
NCAM	forward	CTGCATTGCTGAGAACAAGG	80
	reverse	CATATGTGATTTTGGGTTTTGC	
CD34	forward	GCGCTTTGCTTGCTGAGT	67
	reverse	GGGTAGCAGTACCGTTGTTGT	
RFP	forward	CTGAAGGGCGAGATCCAC	82
	reverse	TGGCCATGTAGATGGTCTTG	

2.5 siRNA knockdown

HES2 cells stably expressing RFP (HES2-R26 cells) [30] were reverse transfected at the time of 96-well plate seeding at Day 1. $2x10^4$ cells in 100 uL of day 1 endoderm

media were seeded onto a 20 μL transfection volume of Optimem I Reduced Serum Media (Invitrogen) containing 0.2 μL RNAiMax per well (Invitrogen) and 10 nM of either a non-specific scramble siRNA (Applied Biosystems, Foster City, CA) or a siRNA designed to target the *RFP* mRNA (IDT, Coralville, IA). Day 1 total well volume was thus 120 uL. Control samples were seeded into Optimem Media. RNAiMax was utilized due to its high efficiency of delivering siRNA into hESCs [32]. Differentiation was performed as previously described, in which 200 uL medium at Day 4 was subsequently added to each well.

2.6 Colony forming assays

EBs were dissociated as described in *flow cytometry*. 20,000 cells were diluted 600 uL IMDM supplemented with the following cytokines: 10 U/mL EPO (Amgen), 5 ng/mL GM-SCF (R&D Systems), 10 ng/mL IL-3, and 5 ng/mL GM-CSF (R&D Systems). The cell/cytokine cocktail was transferred to 4 mL thawed methylcellulose medium (MethoCult; StemCell Technologies) and vortexed. 1 mL was transferred to each of 3 35-mm Petri dishes and incubated at 37ºC and 5% CO_2 for 12 days.

2.7 Hematologic stains

Selected colonies from methylcellulose culture or cells harvested from suspension differentiation cultures were washed in PBS and spun onto glass slides with a cytospin apparatus (Eppendorf) at 800 rpm for 3 min. Slides were stained for 3 min in May-

Grunwald fixation buffer, washed twice in dH_2O, and stained with Wright-Giemsa stain for 18 min.

3. Development of a 96-well hESC Differentiation Assay

3.1 Abstract

Serum-free differentiation protocols of human embryonic stem cells (hESCs) offer the ability to maximize reproducibility and to develop clinically applicable therapies. We developed a high throughput, 96-well plate, 4-color flow cytometry-based assay to optimize differentiation media cocktails and to screen a variety of conditions. We were able to differentiate hESCs to all three primary germ layers, screen for the effect of a range of activin A, BMP4, and VEGF concentrations upon endoderm and mesoderm differentiation, and perform RNA-interference (RNAi)-mediated knockdown of a reporter gene during differentiation. Cells were seeded in suspension culture and embryoid bodies were induced to differentiate to the 3 primary germ layers for 6 days. Endoderm ($CXCR4^+$), mesoderm (KDR^+), and ectoderm ($SSEA\text{-}3^+/NCAM^+$) differentiation yields were 75 ± 3%, 96 ± 2%, and 62 ± 3%, respectively. Germ layer identities were confirmed by quantitative PCR. Activin A, BMP4, and bFGF drove differentiation, with increasing concentrations of activin A inducing higher endoderm yields and increasing BMP4 inducing higher mesoderm yields. VEGF drove lateral mesoderm differentiation. RNAi-mediated knockdown of constitutively expressed red fluorescent protein did not affect endoderm differentiation. This assay facilitates the

development of serum-free protocols for hESC differentiation to any target lineage and creates a platform for screening small molecules or RNAi during ESC differentiation.

3.2 Introduction

Human embryonic stem cells (hESCs) offer the potential to regenerate any cell in the human body. Initially, many studies utilized serum-containing media to develop differentiation protocols for target cell types [3, 16-18]. Serum, however, contains unknown and variable concentrations of growth factors and proteins. More recently, serum-free differentiation (SFD) protocols have emerged in order to maximize reproducibility and to gain a more thorough understanding of biological pathways activated during differentiation to specified lineages [19-21, 33]. Numerous combinations of cytokines, growth factors, and siRNA molecules are being evaluated in order to understand signaling pathways utilized during differentiation and to optimize differentiation protocols to target cell types. By precisely activating or inhibiting the TGFβ family, FGF, Wnt, and other pathways at specific times, the developing embryo directs differentiation to all somatic cells of the body [5]. *In vitro* hESC differentiation systems attempt to recapitulate these developmental pathways by utilizing controlled concentrations of cytokines and inhibitors. As differentiation proceeds down specific lineages, the possible number of cytokine combinations dramatically increases. A high throughput screening method that streamlines the analysis of various growth factor combinations and their effect upon differentiation would be extremely beneficial.

Only a few groups have developed small scale ESC differentiation systems in order to probe biological pathways and optimize differentiation media cocktails. Ng *et*

al. [22, 23] have developed a 96-well spin embryoid body (EB) technique in which hESCs are spun down to form a single EB of a defined size within each well. This technique has been utilized to optimize differentiation to various stages in the hematopoietic lineage [24, 25]. Koike et al. have developed a 96-well murine ESC (mESC) differentiation system and explored effects of EB seeding density upon differentiation to cardiomyocytes [26, 27]. Due to the small seeding density utilized by both methods to generate single EBs and the tendency for cell counts to drop over the first five days of differentiation [24], it is unclear if enough cells would be available for 96-well flow cytometry analyses without pooling wells. Several studies have utilized an adherent 384-well plate format to screen for small molecule inhibitors or enhancers of ESC differentiation [28, 29]. Although these confocal microscopy-based assays have been utilized to screen several thousand small molecules, they are not conducive to multi-color flow-cytometry or live cell sorting.

RNA interference (RNAi)-mediated gene knockdown has also become a common technique to explore gene involvement in active pathways. siRNA knockdown of reporter genes does not affect pluripotency in hESCs grown on mouse embryonic fibroblasts (MEFs) [34]. Knockdown of *OCT4* and *NANOG* have been shown to induce differentiation and loss of pluripotency in hESCs [35-37]. RNAi has been utilized to elucidate signaling pathways that mediate ESC differentiation to multiple lineages [38]. Despite the potential that RNAi offers for understanding biology and modifying pathway activation, there is little data available regarding any potential off-target effects this technique may have upon targeted hESC differentiation.

We have developed a small scale, flow cytometry-based, high throughput hESC EB differentiation assay. In this study, we differentiate hESCs to the three primary germ layers and demonstrate biomarker profiles unique to each cell type. We obtained high cell yields for each layer with remarkably low well-to-well variability. We also demonstrate the ability to perform small interfering RNA (siRNA)-mediated gene knockdown at this scale without disrupting induced differentiation. These results demonstrate the utility and efficacy of this system for efficiently optimizing SFD conditions and performing siRNA knockdown upon numerous targets.

3.3 Results

3.3.1 EB differentiation in 96-well format

We optimized a 96-well plate, 4-color flow cytometry assay for analyzing surface markers during hESC EB differentiation into target lineages. A stepwise EB differentiation protocol was modified to differentiate the cells for 6 days (Fig. 3.1A) [39]. A 4-color biomarker-based flow cytometry assay to detect cells representative of all three primary germ layers and undifferentiated hESCs in a single sample was developed (Fig. 3.1B). Combinations of the surface markers CXCR4, KDR, NCAM, and SSEA-3 were assessed to differentiate each cell type. CXCR4 is a reliable marker for definitive endoderm [40], but is also expressed in migrating mesoderm [41]. KDR has frequently been utilized to characterize early mesoderm prior to diverging to a KDR^+ lateral lineage or a $PDGFR\alpha^+$ paraxial lineage [42, 43] and is also expressed at low levels by hESCs

[39]. SSEA-3 is a marker of pluripotency expressed by hESCs. Upon differentiation, SSEA-3 expression is lost [44, 45], although expression is maintained at the early neuroectoderm, neural stem cell stage [46]. NCAM (or CD56) is a neural marker whose expression is induced during this early ectoderm stage [46] and is a general marker for ectoderm differentiation [47]. However, NCAM expression is not unique to ectoderm but is expressed by some endoderm and mesoderm cells as well [48, 49]. Therefore, we utilized SSEA-3^{+}NCAM^{-} expression to characterize hESCs, CXCR4^{+}KDR^{-} expression for endoderm, SSEA-3^{+}NCAM^{+} expression for ectoderm, and KDR^{+}SSEA-3^{-} expression for mesoderm.

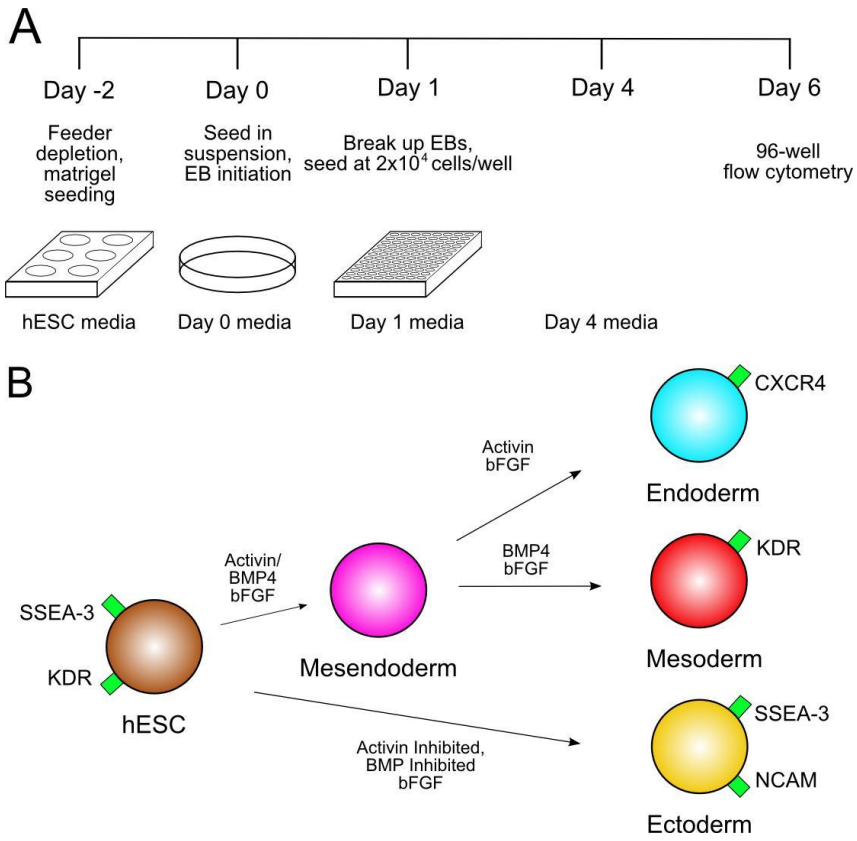

Figure 3.1. Experiment schematic and differentiation model. **(A)** 6-day stepwise hESC EB differentiation schematic. Differentiation protocols were established in which cells were fed at days 0, 1, and 4. Cells were seeded into 96-well plates at day 1 and analyzed by 96-well flow cytometry at day 6. **(B)** Differentiation and biomarker expression model. A four-biomarker combination was designed in which hESCs and cells representing the three primary germ layers could be analyzed in a single sample.

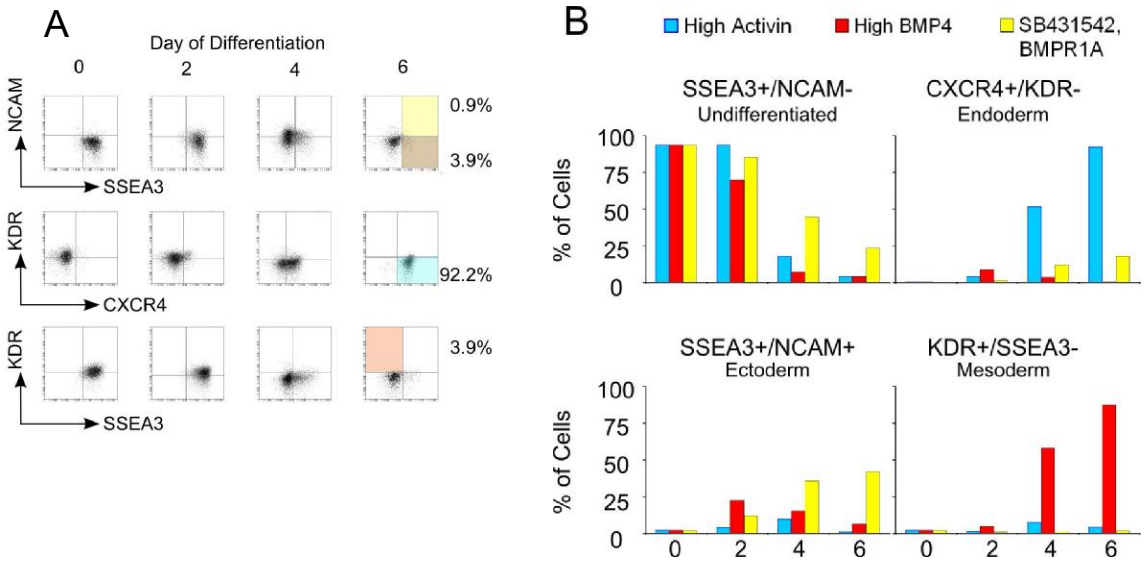

Figure 3.2. Biomarker time-course analysis. Germ layer differentiation was initiated at day 0. SSEA-3, NCAM, CXCR4, and KDR surface marker expression was assessed with flow cytometry at days 0, 2, 4, and 6. **(A)** Endoderm differentiation flow cytometry profiles. Colored quadrants represent undifferentiated cells (brown) and differentiation to endoderm (blue), ectoderm (yellow), and mesoderm (red). Similar mesoderm and ectoderm plots are given in Figure S1. **(B)** Marker expression profiles for all differentiation conditions over 6 days of differentiation

In order to examine inter-well variability and percent differentiation, one 96-well plate was partitioned into 3 induction media zones: endoderm, mesoderm, and ectoderm. We utilized high activin A with bFGF to induce endoderm [16], high BMP4 with bFGF to induce mesoderm [39], and simultaneous activin inhibition (SB431542) and BMP4 inhibition (BMP receptor 1A; BMPR1A) with bFGF to induce ectoderm [50, 51] (Fig. 3.1B). The EBs appeared robust and morphologically similar to those grown in bacterial grade dishes and 6-well plates. 96-well flow cytometry was performed and the different populations of cells were defined from expression of the four biomarkers (Fig. 3.2A-B, Fig. 3.3). HES2 endoderm ($CXCR4^{+}KDR^{-}$), mesoderm ($KDR^{+}SSEA\text{-}3^{-}$), and ectoderm ($SSEA\text{-}3^{+}NCAM^{+}$) differentiation yields were 74 ± 9%, 74 ± 17%, and 57 ± 8%,

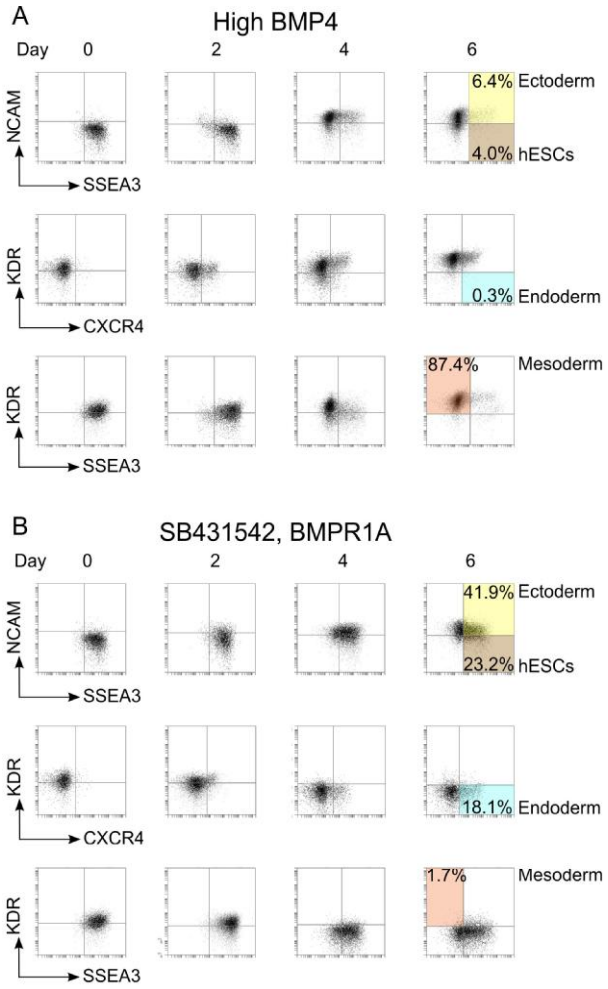

Figure 3.3. Mesoderm and ectoderm differentiation time course biomarker expression. Cells were harvested at days 0, 2, 4, and 6 from **(A)** mesoderm (high BMP4) and **(B)** ectoderm (SB431542, BMPR1A) differentiation cultures and assessed for SSEA-3, NCAM, CXCR4, and KDR expression. Colored quadrants represent undifferentiated cells (brown) and differentiation to endoderm (blue), ectoderm (yellow), and mesoderm (red). Abbreviations: SSEA-3, stage-specific embryonic antigen-3; CXCR, CXC chemokine receptor; KDR, kinase insert domain receptor; PDGFRα, platelet-derived growth factor-α; BMP, bone morphogenetic protein.

respectively (Fig. 3.4E). H9 cells demonstrated similar yields of 80 ± 11%, 78 ± 7%, and 41 ± 9% for endoderm, mesoderm, and ectoderm, respectively (Fig. 3.4F). Inter-well variability was remarkably low between identical induction conditions (Fig. 3.4A-D), with standard deviations consistently less than 4%. Activin-/BMP-inhibited media

retained expression characteristics of pluripotent hESCs (28 ± 17% SSEA-3^{+}NCAM^{-}), although NANOG and OCT4 transcript expression indicated this is likely due to retained expression of SSEA-3 in non-NCAM expressing ectoderm (Fig. 3.7A).

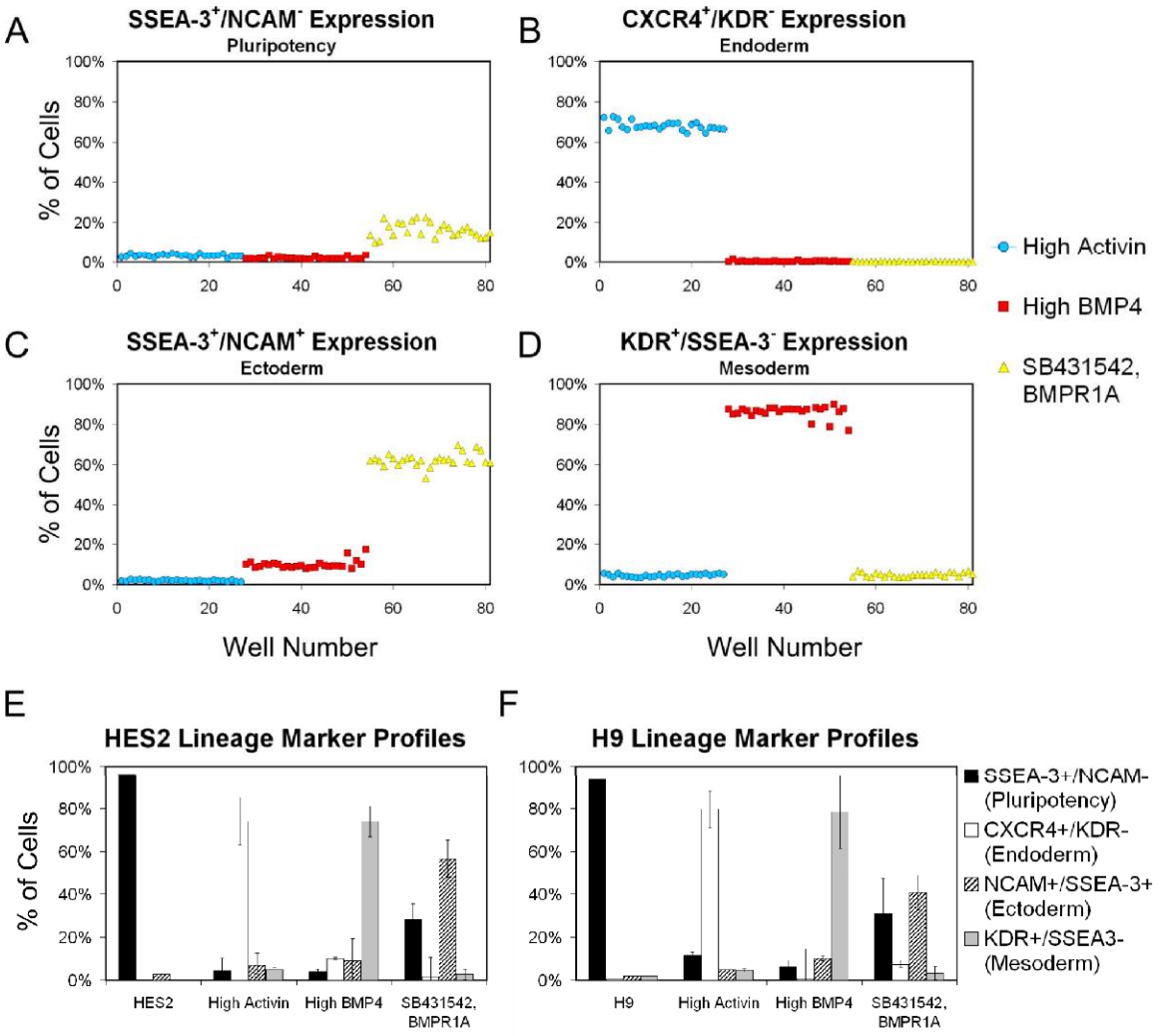

Figure 3.4. Day 6 phenotypes after differentiation to the three germ layers. **(A-D)** Inter-well variability for 96-well flow cytometry expression profiles. hESCs were seeded into a 96-well plate and differentiated to endoderm, mesoderm, or ectoderm. Cells were stained for SSEA-3, CXCR4, NCAM, and KDR after 6 days to assess inter-well variability and the ability to distinguish the separate germ layers. Plots show percentages of cells expressing the designated surface marker. **(E-F)** Biomarker profiles for HES2 and H9 differentiation. Each of the 4 cell types (hESCs, endoderm, mesoderm, ectoderm) was characterized by a unique biomarker expression profile. The 96-well format demonstrated highly efficient differentiation to all three lineages. Error bars represent well means of **(E)** 2 independent experiments (n = 2) ± SD and **(F)** 3 independent experiments (n = 3) ± SD. Each germ layer was significantly different for its appropriate biomarker at the $p < 0.01$ level (student's t-test).

Cells displayed some toxicity after being seeded at day 0 and then demonstrated proliferation after 2 days of differentiation (Fig. 3.5). Both endoderm and mesoderm conditions yielded 4 to 6 day cell counts similar to the initial seeding density of $2x10^4$ cells/well, indicating a potential population plateau for these media. Ectoderm cell yields (day 6 cell counts compared to day 0 seeding densities) were greater than 300% at day 6, possibly attributable to the addition of 20 ng/mL bFGF at day 4. In order to evaluate the

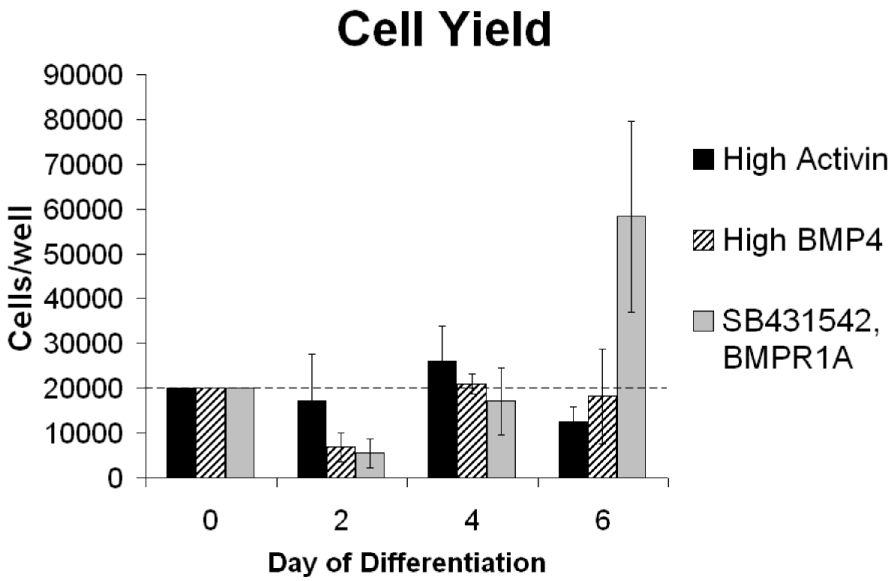

Figure 3.5. Differentiation culture cell yield analysis. H9 hESCs were seeded into 96-well plates at day 0 at 20,000 cells/well and differentiated utilizing one of the three differentiation media: High Activin (endoderm), high BMP4 (mesoderm), and SB431542, BMPR1A (ectoderm). Cell viability was assessed at days 2, 4, and 6. Error bars represent the mean ± SD of two independent experiments, each obtained from the mean of 6 wells on a single plate assay.

effect of seeding density upon differentiation efficiency, we evaluated day 6 marker expression levels for seeding densities of $8x10^3$ to $6x10^4$ cells/well (Fig. 3.6). The assay proved to be highly robust for differences in cell densities. Undifferentiated populations increased with increasing densities, as to be expected due to nutrient and cytokine depletion. Mesoderm and ectoderm differentiation efficiency showed a gradual

decreasing trend with increasing seeding density, whereas endoderm efficiency was essentially constant.

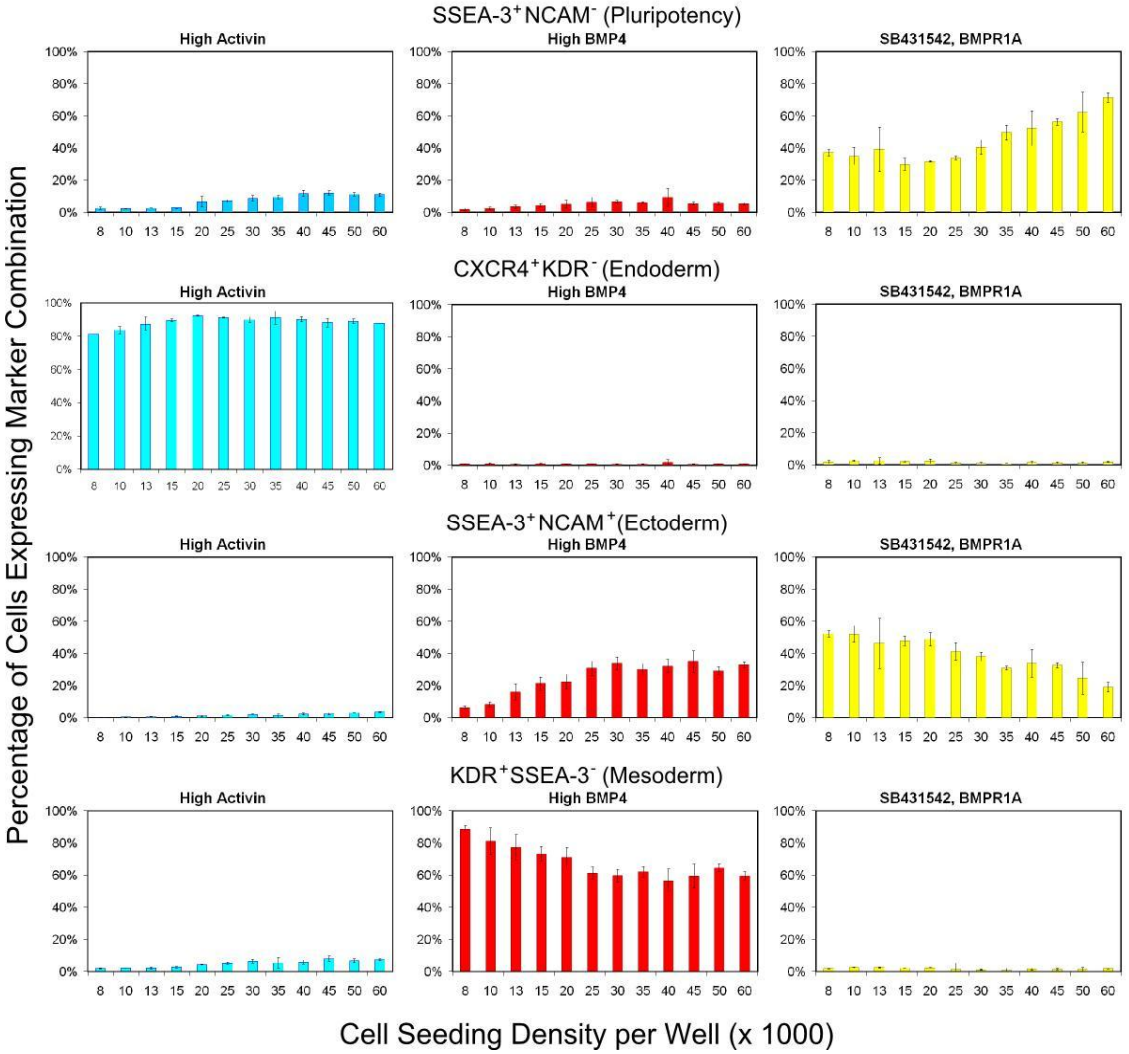

Figure 3.6. hESC seeding density analysis. H9 hESCs were seeded at the specified density into 96-well plates and differentiated to endoderm (high Activin), mesoderm (high BMP4), or ectoderm (SB431542, BMPR1A). Expression of SSEA-3, CXCR4, NCAM, and KDR was analyzed with 96-well plate flow cytometry at day 6. Error bars represent the mean ± SD of 3 wells from a single plate assay.

The differentiated populations of cells representative of each primary germ layer, as well as undifferentiated hESCs, display a unique biomarker profile (Fig. 3.4E-F). Each cell type was distinguished by increased expression of a combination of biomarkers.

These findings suggest that this 4-biomarker assay can be utilized to distinguish four unique cell types after 6 days of differentiation. Furthermore, the three differentiated cell types have a biomarker profile characteristic of either endodermal, mesodermal, or early ectodermal cells.

3.3.2 Gene expression verification of induced germ layers

In order to verify that the surface marker profiles obtained using flow cytometry corresponded to the anticipated lineages, real-time quantitative PCR (qPCR) was performed on RNA harvested from day 0 hESCs and from cells after 6 days of differentiation in the various differentiation conditions. The pluripotency genes *NANOG* and *OCT4* were expressed in undifferentiated cells and as expected were downregulated in the three conditions inducing cellular differentiation (Fig. 3.7A). The anterior primitive streak gene *FOXA2* was drastically upregulated in the high activin endoderm induction conditions, as were the anterior definitive endoderm genes *SOX17* and *CER1* (Fig. 3.7B). Figure 3.7C displays characteristic gene expression profiles representative of cells within the posterior primitive streak and differentiating toward mesoderm. These genes were upregulated in conditions using high BMP4, and are representative of early stage as well as paraxial (*PDGFRα*) and lateral progenitor mesoderm (*GATA2*). Dual BMP4 and activin A inhibition increased both *PAX6* and *SOX1* transcript expression (Fig. 3.7D). The neuronal marker *NESTIN* was not upregulated in the ectoderm induction conditions, indicating that these cells have not yet begun to undergo neuralization [52]. These gene expression data support the flow cytometry profiles showing that the three

defined induction conditions differentiate the cells into lineages representative of endodermal, mesodermal, and early ectodermal germ layers.

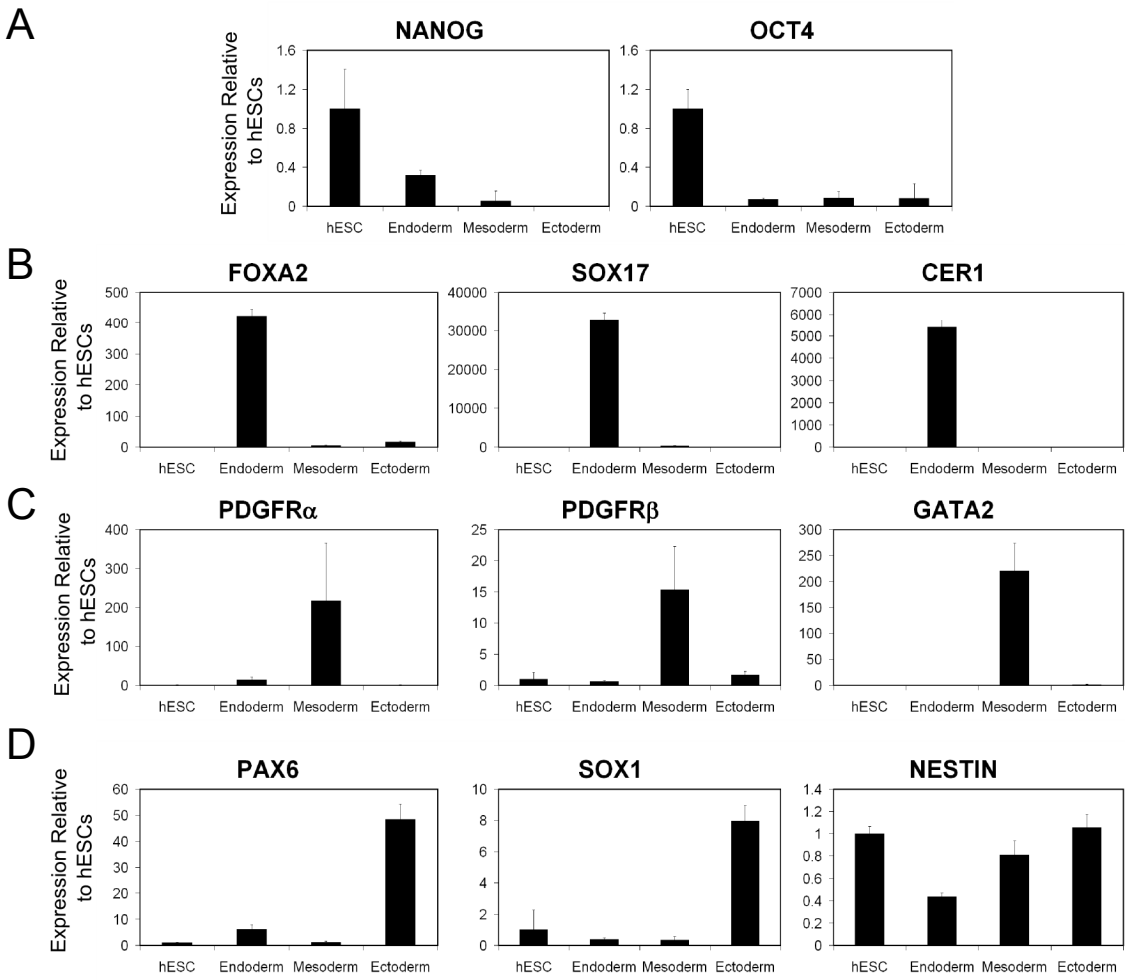

Figure 3.7. Germ layer gene expression analysis. Germ layer differentiation was initiated at day 0. (**A-D)** RNA was prepared from cells harvested at day 0 (hESCs) or day 6 and analyzed for genes characteristic of pluripotency **(A)**, endoderm **(B)**, mesoderm **(C)**, or ectoderm **(D)** by qPCR. Expression was normalized to the housekeeping gene *GAPDH* and all values are relative to hESC expression at day 0. Error bars represent mean ± SD of 3 pooled wells from a single plate assay.

3.3.3 96-well growth factor screening assay

We next sought to apply the 96-well flow cytometry assay to efficiently screen specific growth factors across a range of concentrations. The concentrations of 3 growth factors, activin A (0-100 ng/mL), BMP4 (0-40 ng/mL), and VEGF (± 10 ng/mL), were assessed for differentiation to endoderm and mesoderm over the course of 6 days. The expression of PDGFRα was assessed for an additional mesodermal marker and to indicate early progression towards the paraxial germ layer [43]. As discussed previously, $SSEA3^+$, $CXCR4^+KDR^-$, and $KDR^+SSEA\text{-}3^-$ expression was used to indicate undifferentiated cells and commitment of cells to endoderm and mesoderm, respectively. As expected, expression of the pluripotency marker, SSEA-3, steadily decreased in conditions with increasing concentrations of activin and BMP4 (Fig. 3.8A). $CXCR4^+KDR^-$ expression was nonexistent in the absence of activin A, whereas a low concentration of activin A (10 ng/mL) was sufficient to induce high (>60% of cells) CXCR4 expression (Fig. 3.8B). Increasing activin A from 10 to 100 ng/mL increased $CXCR4^+KDR^-$ expression for high BMP4 conditions, but otherwise did not have a notable effect upon $CXCR4^+KDR^-$ expression. For a constant activin A concentration, increasing BMP4 consistently reduced CXCR4 expression. $PDGFR\alpha^+$ and KDR^+ populations were greatest in the absence of activin A (Fig. 3.8C-D). Increasing the activin A concentration immediately abrogated PDGFRα expression. Activin A and BMP4 displayed a competitive relationship upon $KDR^+SSEA\text{-}3^-$ expression. Increasing BMP4 concentration increased KDR expression, whereas activin A consistently inhibited this expression. For most conditions, the additional supplementation of 10 ng/mL VEGF

had no notable effect upon the expression of this set of cell surface markers (Fig. 3.8A-D).

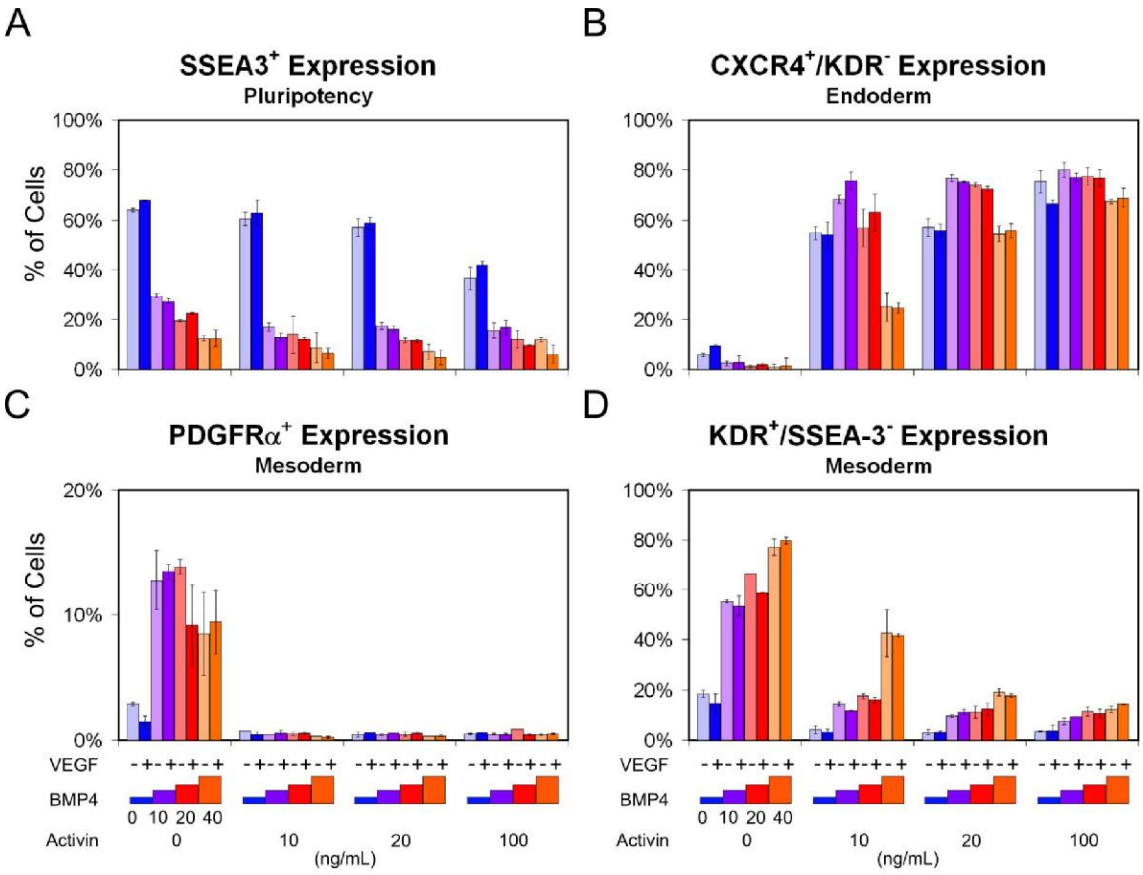

Figure 3.8. 96-well plate growth factor screening analysis. Activin A, BMP4, and VEGF concentrations were varied over a 96-well plate and SSEA-3$^+$ **(A)**, CXCR4$^+$KDR$^-$ **(B)**, PDGFRα$^+$ **(C)**, and KDR$^+$SSEA-3$^-$ **(D)** expression were analyzed using flow cytometry after 6 days of differentiation. All samples contained bFGF (days 1-4: 2.5 ng/mL; days 4-6: 5 ng/mL). VEGF concentration was ± 10 ng/mL. **(A)** Pluripotency decreased with increasing activin A and BMP4. **(B)** Endoderm populations increased with increasing activin A and decreased with increasing BMP4. **(C-D)** Mesoderm character was highest in the absence of activin A. PDGFRα$^+$ mesoderm was only detectable with no activin. KDR$^+$SSEA-3$^-$ mesoderm populations consistently increased with increasing BMP4 concentration and decreasing activin A concentration. All concentrations are ng/mL. Error bars represent the mean of 2 wells ± SD from a single plate assay.

These data suggest this 96-well flow cytometry assay can be utilized to screen for the effect of a spectrum of growth factor concentrations upon hESC differentiation in

serum-free conditions. Furthermore, increased concentrations of both activin A and BMP4 reduce pluripotency. Increasing activin A concentration increases $CXCR4^{+}KDR^{-}$ endoderm populations and reduces both $KDR^{+}SSEA\text{-}3^{-}$ and $PDGFR\alpha^{+}$ mesoderm populations. Conversely, increasing BMP4 concentration increases $KDR^{+}SSEA\text{-}3^{-}$ mesoderm populations but decreases $CXCR4^{+}KDR^{-}$ endoderm populations.

3.3.4 Tracking germ layer differentiation through gene expression kinetics

Kinetic analyses can also be performed during the differentiation assays. By keeping BMP-4 constant at 10 ng/ml, 4 of the previously screened induction conditions were chosen in which 2 were optimal for endoderm (activin A at 20 ng/ml ± 10 ng/mL VEGF) and 2 were optimal for mesoderm (activin A at 0 ng/ml ± 10 ng/mL VEGF). All conditions were carried out on a single 96-well plate. Gene expression profiles were determined from cells obtained during the six days of differentiation. Genes expressed during mesoderm and endoderm induction were analyzed, with the inclusion of *OCT4* as a marker of pluripotency in undifferentiated cells.

Mesoderm genes (*KDR*, *PDGFRα*, *MEOX1*, *CD34*) were consistently expressed at higher levels in the absence of activin A while endoderm genes (*FOXA2*, *CXCR4*, *SOX17*) were consistently expressed in the presence of activin A (Fig. 3.9). *OCT4* expression steadily decreased in all conditions over the 6 day period. *Brachyury* expression peaked rapidly at days 2-4 and then decreased in all samples, indicative of ESCs passing through the primitive streak stage [9, 53, 54]. Additionally, non-activin A conditions demonstrated a clear progression through a $Brachyury^{+}KDR^{-}$ stage to a

Brachyury^{+}*KDR*$^{+}$ stage, indicative of pre-mesoderm to mesoderm/hemangioblast differentiation [42, 53]. *PDGFRα* is a marker of mesendoderm [55] and was expressed in all samples at day 4 followed by increased expression in mesoderm inducing conditions. *CXCR4*, while expressed 100 fold higher in the activin A conditions, was still upregulated 10-fold in the absence of activin A when compared to undifferentiated cells. This is to be expected since *CXCR4* is not entirely endoderm specific but is also

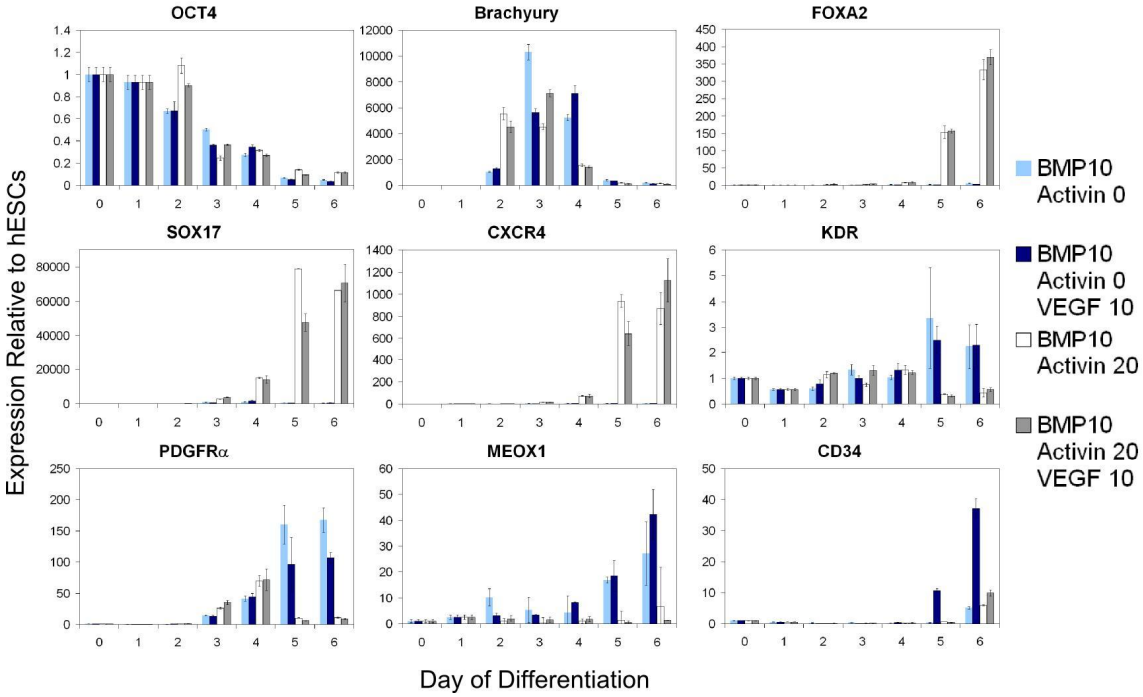

Figure 3.9. Gene expression kinetic analysis. 4 conditions (10 ng/mL BMP4, ± 20 ng/mL activin A, ± 10 ng/mL VEGF) were chosen from the results of the growth factor screening experiment (Fig. 4) and analyzed for transcript expression levels during the 6-day differentiation procedure. Pluripotency (*OCT4*) decreased over differentiation and *Brachyury* expression peaked between 2-4 days. Endoderm genes (*FOXA2*, *CXCR4*, *SOX17*) were expressed much higher for conditions supplemented with activin A, whereas mesoderm gene expression (*KDR*, *PDGFRα*, *MEOX1*, *CD34*) was highest for non-activin A conditions. VEGF increased *CD34* and decreased *PDGFRα* expression at late time-points. Expression was normalized to the housekeeping gene *GAPDH* and all values are relative to hESC expression at day 0. Error bars represent mean ± SD of 3 pooled wells from a single plate assay.

expressed by migrating mesoderm [41]. This result is consistent with CXCR4 protein expression detected by flow cytometry (Fig. 3.3A). Generally, the addition of VEGF had no notable effect upon gene expression, with the exception of lateral (CD34) and paraxial (PDGFRα) specific genes. The expression of *CD34*, a lateral mesoderm and hematopoietic cell marker, was induced in the absence of activin A but only in the presence of VEGF. Conversely, the expression of the paraxial gene, *PDGFRα*, was highest in the abscence of activin and VEGF, indicating that VEGF drives lateral or hematopoietic differentiation [43].

3.3.5 siRNA knockdown during endoderm differentiation

In addition to the amount of information that can be derived using this 96-well format in optimizing growth factor conditions and kinetics, this format is ideal as a high throughput siRNA screening platform during the differentiation of hESCs. To verify that siRNA knockdown can be achieved in this 96-well format without disrupting differentiation, hESCs that constitutively express an RFP protein [30] were utilized. These cells were induced to differentiate using endoderm conditions and transfected with a siRNA molecule targeting the *RFP* mRNA. Following 6 days of differentiation, cells were analyzed using flow cytometry and qPCR. Both control and mock-treated cells vividly fluoresced after 6 days, whereas cells exposed to the si*RFP* molecule only expressed very low levels of fluorescence (Fig. 3.10A). To evaluate RFP protein expression during endoderm induction, both RFP and CXCR4 expression were analyzed using flow cytometry (Fig. 3.10B). Approximately 85% of both the control cells and cells transfected with scrambled siRNA were RFP^+, compared to 4% of the cells

transfected with siRNA targeted to RFP. In all conditions, 75-80% of the cells in all conditions were $CXCR4^+$, with no notable decrease caused by siRFP knockdown. To further verify that siRNA knockdown had not altered endoderm differentiation, qPCR analysis was performed after 6 days of differentiation (Fig. 3.10C) to analyze *RFP* expression and the anterior primitive streak/definitive endoderm markers *FOXA2* and *CER1*. *RFP* transcript expression decreased by 96% as a result of siRNA knockdown. Neither *FOXA2* nor *CER1* expression were notably influenced by siRNA knockdown. These data suggest that siRNA knockdown can be performed in a 96-well format without significantly altering targeted differentiation.

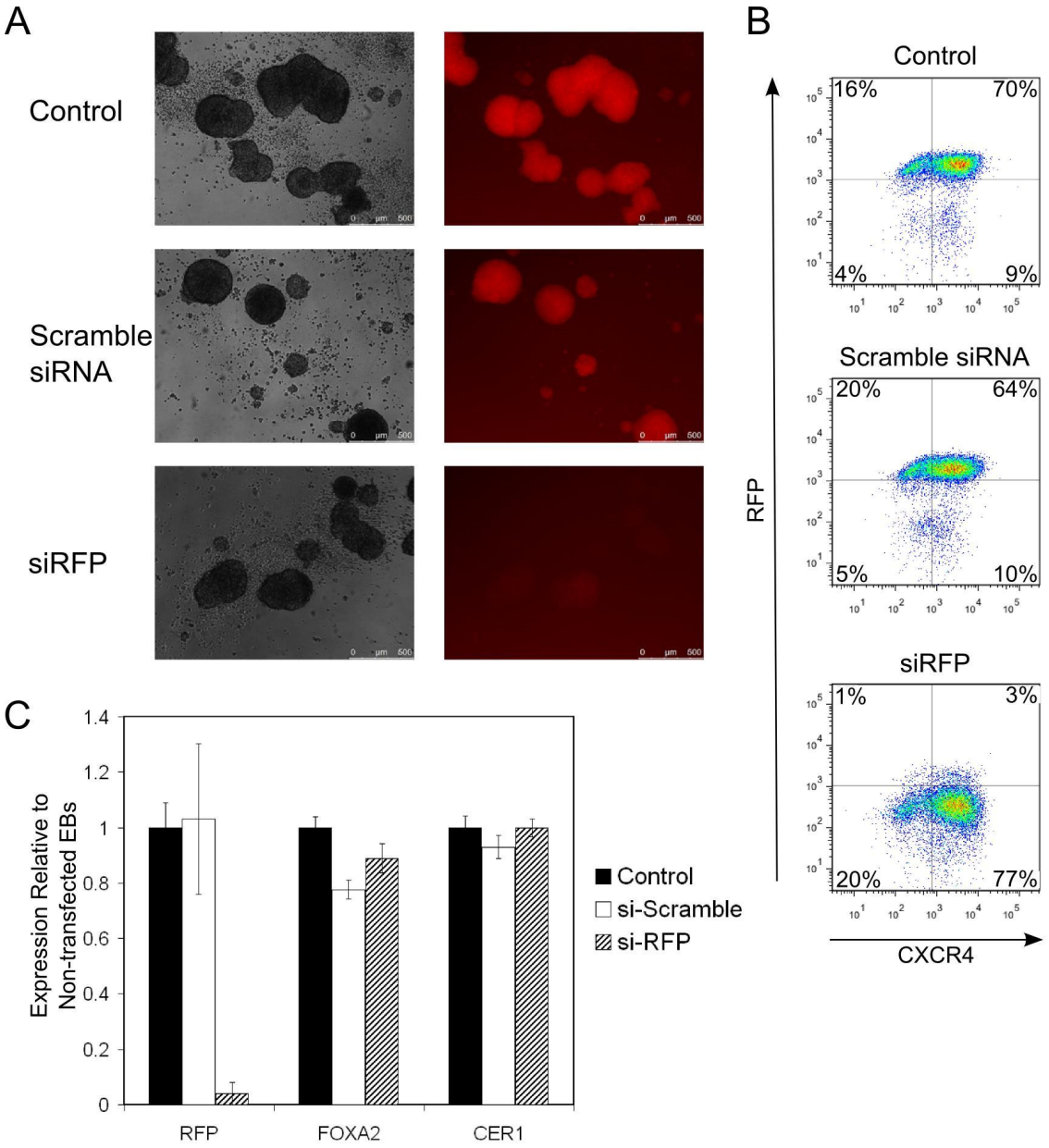

Figure 3.10. siRNA-mediated RFP knockdown during endoderm differentiation. hESCs were reverse transfected with siRFP or a scrambled control when seeded into 96-well plate format and induced to form endoderm in high activin A SFD media. **(A):** Fluorescence microscopy of day 6 EBs. **(B)** Flow cytometry of day 6 cells showing RFP (y-axis) vs. CXCR4 (x-axis) expression. CXCR4 expression was not diminished by siRNA-induced RFP knockdown. **(C)** Gene expression analysis. qPCR was performed at day 6 to analyze *RFP* transcript expression as well as the endoderm genes *FOXA2* and *CER1*. *RFP* knockdown had no notable effect upon endoderm differentiation. Error bars represent mean ± SD of 3 pooled wells from a single plate assay.

3.4 Discussion

Serum-free and feeder-free hESCs differentiation protocols are essential in order to 1) maximize experimental control and reproducibility and 2) develop clinically applicable regenerative therapies [56]. Many studies have focused on titrating growth factors and inhibitors within SFD cocktails to optimize target cell differentiation. As lineages are further explored, the possible combinations of factors will inevitably rise. Screening assays are extremely effective in this pursuit. We have developed a high throughput, multicolor flow cytometry assay of hESC differentiation that can be utilized to assess a range of SFD conditions. This small scale format requires approximately 92% less reagents and growth factors than 6-well culture conditions and occupies 6% of the incubator space. Additionally, this assay utilizes surface markers to allow for live-cell analysis and sorting.

We differentiated hESCs to the three primary germ layers in this system, identified extracellular biomarker profiles for each, and confirmed germ layer identity with gene expression analysis. A wide variety of extra- and intracellular markers have been previously utilized to identify each of the primary germ layers. Given the heterogeneous expression patterns of endoderm, mesoderm, and ectoderm, no four-marker combination will perfectly distinguish all cells within each lineage. CXCR4 is expressed in migrating early endoderm and mesoderm [41], developing vascular endothelial cells [57], as well as migrating neural stem cells [58]. Although typically 20-25% of mesodermal cells expressed CXCR4, our results showed that endoderm was uniquely distinguishable by $CXCR4^{+}KDR^{-}$ expression at this stage of differentiation. KDR is expressed on mesoderm cells after exiting the primitive streak [59] and has been

utilized to characterize hESC differentiation to general mesoderm as well as vascular and cardiac progenitors [42, 43, 60]. Although our results corresponded with previous studies that have found KDR expression in a portion of hESCs [39], mesodermal cells generated by high BMP4 conditions were uniquely identifiable by $KDR^{+}SSEA\text{-}3^{-}$ expression. Currently, no well-characterized extracellular early ectoderm surface markers have been validated. Ectoderm has typically been characterized by the intracellular markers Nestin, β-III Tubulin, or Sox1 [51, 61-65]. We exploited the delayed expression of SSEA-3 into the early neural stem cell stage [46] to overcome the confounding NCAM expression in endoderm and mesoderm. Transcript expression indicated that this stage is similar to the primitive anterior neuroectoderm/neuroepithelia stage defined by Pankratz et al. [66], namely that PAX6 expression is upregulated with SOX1 expression beginning to increase. This strategy carries the caveat that $SSEA\text{-}3^{+}NCAM^{+}$ phenotyping would not be applicable at a later stage in the ectoderm lineage due to the loss of SSEA-3 expression.

Although exact comparisons are difficult to make due to various time points, markers utilized, data reported, and host species differences, we obtained excellent yields in relation to previous studies. Serum-containing, high activin A protocols have produced $SOX17^{+}$ endoderm yields ranging from 55% [28] to greater than 80% [67] after 5-6 days of differentiation in hESCs. Our yield of 80% for H9 cells falls within the higher range of this spectrum. Day 6 KDR^{+} mesoderm populations 15-25% [68] and 52% [69] cells have been obtained from hESCs. We obtained greater than 74% $KDR^{+}SSEA\text{-}3^{-}$ mesoderm yields for multiple hESC lines. Patani et al. generated day 4 and day 8 yields of 51% and approximately 80%, respectively, for cells positive for the

neuroectoderm marker MUSASHI from hESCs [70]. Chambers et al. generated greater than 80% $HES5^{+}$ neuroectoderm after 11 days of hESC differentiation [50]. Our 6 day protocol generated yields of 41-57%, comparable to these studies given the shorter time duration.

Many cytokine conditions, small molecules, and transfection conditions may induce cellular toxicity. Additionally, seeding densities may be highly variable due to the inability to seed hESCs as single cell suspensions in many lines. It is vital to obtain consistent and reliable results from a screening assay despite these caveats. This small-scale culture system demonstrated remarkable inter-well repeatability and density-robustness, particularly since static EB differentiation systems have been reported to generate highly heterogeneous cell populations [11]. Since 96- and 384-plate assays can display variations due to edges, evaporation, thermal variations, and pipetting error [71-73], we utilized gas permeable membranes and stainless steel lids to minimize evaporation and ensure a uniform heat distribution[74]. All standard deviations were less than 4% for biomarker signals, which allowed for highly significant differences between conditions.

While many studies have utilized siRNA as a tool for studying ESC differentiation, there is limited data reporting the presence or absence of off-target siRNA effects upon differentiation outcome. Non-viral transfection of off-target siRNA molecules has been found to induce adipogenesis in human mesenchymal stem cells [75]. Hence, it is important to measure the effects that transfection or transduction may induce in ESC differentiation protocols. We found that siRNA-mediated knockdown of constitutively expressed RFP was highly efficient and induced no notable effects upon

endoderm differentiation. Cells were transfected with the siRNA molecules at Day 1 of differentiation and exhibited significant RFP knockdown at Day 6. This assay provides a siRNA screening platform that can potentially be utilized for differentiation pathway analysis.

In an effort to demonstrate the efficiency and power of this 96-well assay system, we conducted a growth factor screening assay utilizing a single 96-well plate and analyzed 32 conditions in duplicate. We then extended the capabilities of this small-scale system to analyze time-course gene expression profiles for four of these conditions, again, within a single 96-well plate. bFGF in combination with activin A or BMP4 drove differentiation and reduced pluripotency. In particular, the greatest number of $CXCR4^{+}KDR^{-}$ cells was induced by low to high activin A with no BMP4. Gene profiles over the 6 day time period for the activin A + BMP4 conditions confirmed that these $CXCR4^{+}KDR^{-}$ cells were characteristic of definitive endoderm. These results correspond to previous studies that found increased CXCR4 expression and increased definitive endoderm yields by differentiating cells in high activin A containing SFD conditions [67, 76]. Our results are similar to those of Vallier et al. in which high activin A in combination with bFGF and BMP4 induced mesendoderm [51]. Several studies have previously reported that activin A + bFGF blocks differentiation and maintains pluripotency [51, 77], whereas our results demonstrated increased endoderm production. Our protocol includes a BMP4 exposure step at day 0-1 to serve as a "jumpstart" to differentiation. The decrease in pluripotent marker expression in subsequent activin A + bFGF SFD conditions is likely attributable to this step. Activin A and BMP4 exhibited a competitive effect upon mesoderm marker expression. The presence of activin A alone

eliminated PDGFRα expression at day 6, although all samples demonstrated transcript expression through the day 2-4 primitive streak stage. This PDGFRα reducing effect of activin A has been previously observed [51]. Similarly, activin A reduced $KDR^{+}SSEA\text{-}3^{-}$ expression, with highest expression levels seen in high BMP4 SFD conditions with no activin A. These results also corroborate previous studies that have induced mesoderm and vascular progenitors through BMP4 activation [33, 78] and noted reduced KDR expression with increasing activin A supplementation [39, 42, 51].

The addition of VEGF to SFD had no notable effect upon surface marker expression at day 6. However, *CD34* transcript expression increased and *PDGFRα* expression decreased, indicating a role in inducing early mesoderm cells towards a hematopoietic lineage. Indeed, several studies have utilized VEGF to induce mesendoderm or mesoderm progenitors towards a hematopoietic or cardiovascular state [24, 39, 79], and VEGF inclusion has been shown to improve subsequent hematopoietic blast colony formation [42].

Elucidating the optimal serum-free protocols for EB differentiation of hESCs will require exploring a vast combinatorial field of growth factors, inhibitors, and cytokines. This small scale culture platform and live-cell flow assay provides a more efficient and more cost-effective approach to analyzing a large number of conditions. It can additionally be utilized to discover biological pathways or optimize differentiation through RNAi or miRNA screens. By varying biomarkers, this assay can be adopted to various stages of lineage differentiation to significantly enhance progress towards hESC-derived clinical therapies.

4. Optimizing Hematopoietic Differentiation

4.1 Abstract

An *in vitro* method of generating functional hematopoietic cells would alleviate the strain on the limited availability of donor-supplied cells caused by the widespread prevalence of hematopoietic malignancies. Embryonic stem cells offer hematopoietic generating potential, but reported protocols are either not clinically translatable or inefficient. Additionally, a reliable, defined protocol would allow controversial and unknown nuances of human embryonic hematopoiesis to be resolved. We have applied a high throughput hESC differentiation assay to both study hematopoietic differentiation and optimize the generation of primitive hematopoietic progenitor cells. Specifically, we performed numerous cytokine and inhibitor screens to develop a stepwise protocol that utilizes serum-free differentiation medium supplemented with defined concentrations of growth factors BMP4, VEGF, bFGF, TPO, and IL-3 and the kinase inhibitors Y-27632 and Chir-99021 to generate $CD43^{+}CD41^{+}CD235^{+}$ primitive megakaryocyte-erythromyeloid progenitors and $CD41^{+}CD42^{+}$ megakaryocytes after 8 and 11 days of embryoid body differentiation, respectively. We obtain approximately 1 day 8 progenitor and 1 day 11 megakaryocyte for every 2 initial hESCs. This highly efficient differentiation protocol will allow a greater understand of primitive hematopoietic differentiation.

4.2 Introduction

4.2.1 Primitive hematopoiesis

Embryogenesis is characterized by two waves of erythrocyte production. The initial wave, primitive hematopoiesis, occurs in the extraembryonic yolk sac between embryonic days 7.25 and 9 (E7.25-9) in the murine embryo [80]. This stage is primarily characterized by the production of transient, large, nucleated "primitive" erythrocytes that express embryonic globin (ε-globin) but not adult globin (β-globin). The second wave, definitive hematopoiesis, begins around E9.5 within the embryo proper, continues throughout post-natal life, and is characterized by the production of enucleated, adult globin-expressing erythrocytes, as well as all adult hematopoietic cells [81].

Primitive hematopoiesis remains an incompletely understood phenomenon, particularly in humans in which *in vivo* are essentially not possible. The hallmark of this process is the production of a hemangioblast, a progenitor cell with both erythrocytic and endothelial potential. The hemangioblast first originates in the most posterior region of the primitive streak prior to migrating to the extraembryonic yolk sac [82]. Studies have also demonstrated myeloid [80] and megakaryocyte [83] potential from early yolk-sac derived cells, indicating that hemangioblasts can differentiate to these lineages as well. Although the exact transition from primitive to definitive hematopoiesis is debated, primitive erythrocytes have disappeared by E9, around the time of definitive onset. Multipotent progenitors have been found in the yolk sac at E8.5 [84], and hematopoietic stem cells (HSCs) with long term engraftment potential have been found in the embryo proper by E10.5 [85].

Due to ethical and practical difficulties, far less is understood regarding hematopoiesis in the human embryo. Much of the knowledge of the hemangioblast and primitive hematopoiesis has now come from ESC studies. Kennedy et al. found that a progenitor cell with erythrocytic, macrophage, and endothelial differentiation potential arose within a KDR^+ population after 7 days of differentiation [19]. Klimchenko et al. proved the emergence of a primitive megakaryocyte-erythroid progenitor arising after 9 days of differentiation that could generate primitive erythrocytes and a primitive form of megakaryocyte whose ploidy remained typically less than 8N [86].

Inducing definitive hematopoiesis in ESC studies has proven much more elusive. An unknown mechanism must occur to "mature" hematopoietic progenitor cells from primitive to definitive. This mechanism has so far been provided either by feeder cells or by serum supplementation. Co-culture of mESCs upon an OP9 murine stromal layer, characterized by its inability to produce macrophage colony-stimulating factor (M-CSF), induces differentiation of all hematopoietic lineages [87]. Co-culture upon OP9 cells along with forced expression of definitive gene HoxB4 induces a definitive HSC capable of long-term engraftment in adult mice [17, 20]. Undirected EB differentiation in serum-containing medium induces two sequential waves of primitive followed by definitive hematopoiesis [18]. Exact pathways involved in these systems have yet to be determined.

4.2.2 In vitro hematopoietic hESC systems

Due to the paucity of available HSCs for clinical therapies, there is a large need for *in vitro* protocols that can reliably produce functional HSCs capable of engraftment in

humans. *In vitro* systems also offer the ability to study developmental mechanisms in a controllable environment. Vodyanik et al. developed an OP9 bone marrow stromal line coculture system and studied the progression of hESC hematopoietic differentiation [88]. They generated $CD34^+$ primitive hematopoietic cells after 8-9 days of differentiation capable of generating primitive erythroid, megakaryocytic, and myeloid colonies. Additionally, after further coculture on MS-5 stromal cells, these cells produced myeloid and select lymphoid cells. After further study, it was determined that the $CD43^+$ subpopulation of $CD34^+$ cells generated with this system differentiated committed hematopoietic progenitors from endothelial and mesenchymal cells [89]. While these systems shed light on hematopoietic differentiation of hESCs, coculture with animal cells prohibits translating protocols to the clinic. Furthermore, due to the unknown factors produced by feeder layers, a thorough understanding of requisite signaling cues was not possible.

The feeder-free methylcellulose EB differentiation system developed by Zambidis et al. demonstrated a wave or primitive hematopoietic progenitors characterized by $CD34^+CD31^+$ expression and a second definitive wave from $CD45^+$ cells [18]. While shedding light on hematopoiesis of hESCs, the use of serum in this system still presented a need for serum-free systems to be created.

Several studies have developed serum-free hESC hematopoietic differentiation systems, although hematopoietic progenitor yields have been modest. Pick et al. assessed combinations of cytokines to optimize hematopoietic differentiation and obtained a 16% yield after 10 days of differentiation [24]. Chicha et al. utilized an EB based system to produce $CD34^+$ cells after 8 days capable primitive erythroid and myeloid colony

forming ability. Up to 20% of total day 8 cells expressed CD34, although no reference to initial seeding density was made [90]. Niwa et al. utilized a stepwise procedure to induce $KDR^{+}CD34^{+}$ progenitors, representing less than 10% of total cell population after 6 days of differentiation [91].

For clinical translation, protocols will need to generate large quantities of target hematopoietic cells. This represents a need for high yielding differentiation protocols. The lack of an efficient serum-free EB protocol to generate hematopoietic progenitors motivated us to apply the EB differentiation screen to optimize hematopoietic differentiation of hESCs. Furthermore, we sought to establish a stepwise protocol to generate megakaryocytes in suspension culture.

4.3 Results

4.3.1 VEGF hematopoietic differentiation screen

Having established conditions to optimize the differentiation of KDR^{+} mesoderm cells [92], we initially aimed to investigate inducing cells further down the hematopoietic lineage. Although VEGF had no effect upon KDR^{+} expression in our system, it did induce higher CD34 transcript expression and has been demonstrated to be requisite for hematopoietic differentiation of ESCs [42]. While previous results had demonstrated the ability of BMP4 to effectively induce KDR^{+} mesoderm, we also sought to explore its relationship upon inducing hematopoietic cells. Therefore, we performed an EB differentiation screen by supplementing with 0-40 ng/mL BMP4 and 0-100 ng/mL VEGF. bFGF was supplemented at 5 ng/mL from days 3-6 (Fig. 4.1A). As opposed to

prior experiments, BMP4 was removed at day 3 to avoid the differentiation towards trophoblast and extraembryonic endoderm caused by long term exposure [69]. The pan-hematopoietic marker CD34 and the hemato-endothelial marker CD31 are the first hematopoietic markers expressed during OP co-culture of hESCs [88] and were thus assessed by flow cytometry after 6 days of differentiation.

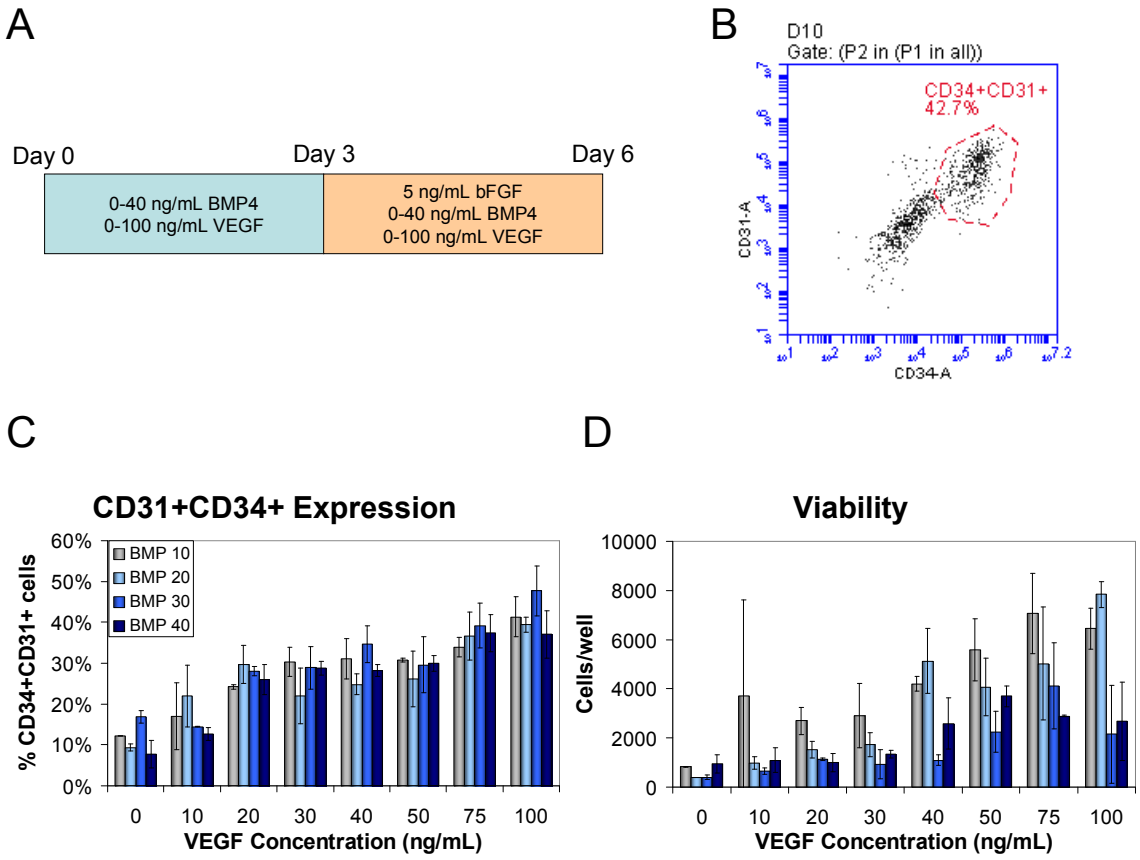

Figure 4.1. VEGF and BMP4 hematopoiesis screen. **(A)** Schematic of the 6-day differentiation screen with growth factor concentrations. Medium was replaced after 3 days of differentiation. **(B)** Representative flow cytometry plot of conditions inducing $CD34^{+}CD31^{+}$ cells. **(C)** Percentage of $CD34^{+}CD31^{+}$ cells for the assayed BMP4 and VEGF conditions. Results are given as percentages of total cells within each condition. **(D)** Cell viability for the assayed conditions. Bars represent the mean ± SD of two wells.

Both markers were expressed at approximately the same rates in cells, as demonstrated by the double positive population in Figure 4.1B. Hematopoietic character was proportional to the concentration of VEGF in the differentiation medium (Fig. 4.1C). Conditions lacking VEGF induced roughly 10% of cells toward the hematopoietic lineage. Increasing concentrations steadily induced higher percentages of total day 6 $CD34^{+}CD31^{+}$ cells, with approximately 40% of cells in 100 ng/mL VEGF medium expressing both markers. There was no clear relationship between BMP concentration and early hematopoietic character.

In contrast to general mesoderm conditions from previous experiments, hematopoietic differentiation conditions were characterized by low and highly variable viability (Fig. 4.1C). Viability generally increased with increasing concentrations of VEGF. BMP4, conversely, induced lower cell counts, although trends were not consistent. These data suggest that the 96-well assay could be utilized to screen hematopoietic differentiation conditions. Additionally, VEGF supplementation concentration is proportional to the percentage of cells characteristic of early hematopoietic cells and induces higher viability after 6 days of differentiation. Increasing BMP4 concentrations tends to result in lower viability.

4.3.2 Hematopoietic differentiation in 96-well format

Having established the capability and basic conditions for early hematopoietic differentiation in 96-well format, we next sought to explore cell phenotype over a longer period of differentiation. Cells were seeded into 96-well plates at day 0 with 25 ng/mL BMP4 and 50 ng/mL VEGF, and medium supplemented with 5 ng/mL bFGF was added

at days 2 and 6 (Fig. 4.2A-B). In an effort to increase viability following differentiation, the Rho-associated protein kinase (ROCK) inhibitor Y-27632 was added to differentation medium for the first 48 hours [93]. EBs were dissociated and various hematopoietic markers were assayed by flow cytometry at days 4 and 8.

After 4 days of differentiation, EBs ranged in size from 50-300 μM in diameter (Fig. 4.2D). A distinct $KDR^{+}CD31^{+}CD34^{+}$ population of cells had emerged (Fig 4.2C). These cells were absent of CD43 and CD41 expression. Most cells were KDR^{+} and 33% ± 3% had begun expressing CD34. As observed previously, $CD34^{+}$ cells typically expressed CD31 as well. Few cells had begun to express the pan-hematopoietic marker CD43 or the erythrocytic marker CD235a. Essentially all $CD31^{+}$ cells were also KDR^{+} (Fig. 4.2C). CD31 expression was preceded by KDR^{+} expression by about 24 hours (data not shown).

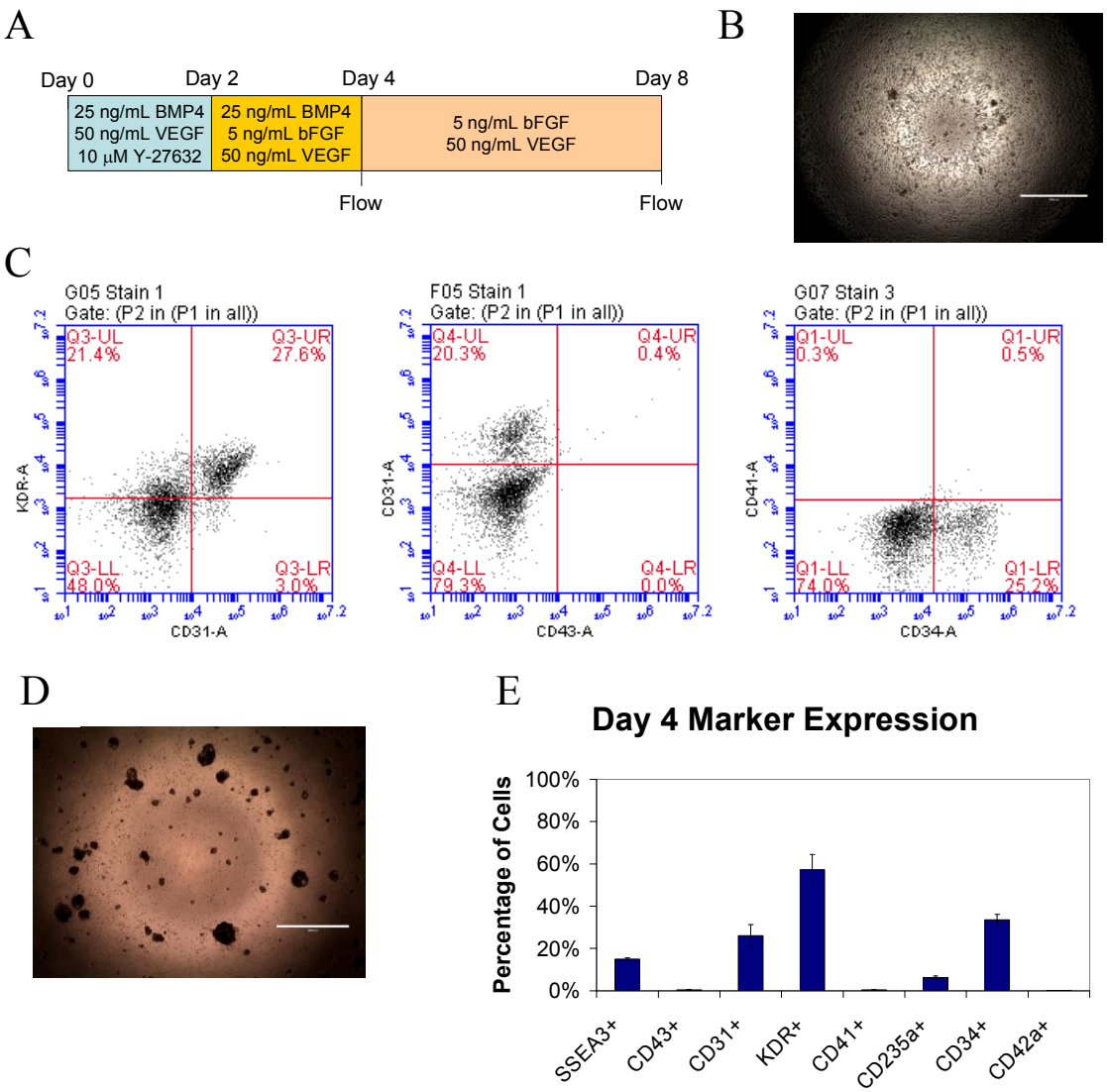

Figure 4.2. 96-well hematopoietic differentiation setup and day 4. **(A)** Schematic of 8 day hematopoietic differentiation. **(B)** Cells at Day 0 after seeding in suspension into 96-well format. Scalebar, 1000 μM. **(C)** Day 4 flow cytometry profiles demonstrating the $KDR^{+}CD31^{+}CD34^{+}$ population. **(D)** Day 4 EBs. **(E)** Day 4 hematopoietic marker profiles. Bars represent mean ± SD of 3 wells.

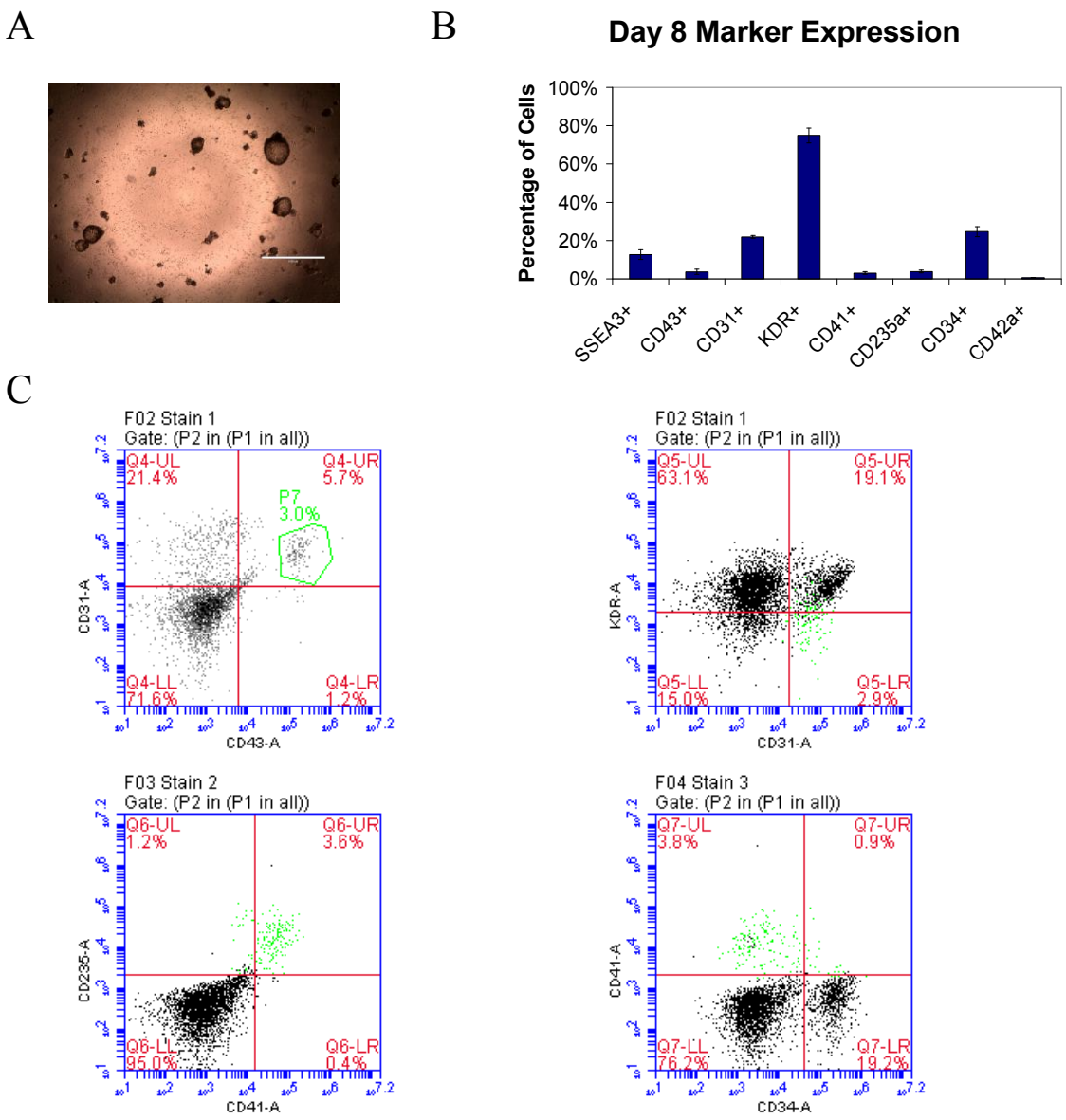

Figure 4.3. Day 8 hematopoietic cells. **(A)** Day 8 EBs. **(B)** Day 8 hematopoietic marker profiles. Bars represent mean ± SD of 3 wells. **(C)** Day 8 flow cytometry profiles. Cells within the gated $CD31^{+}CD43^{+}$ population in the upper left plot are highlighted in green in remaining plots.

After 8 days of differentiation, EBs had adopted a much larger cystic, vacuolated morphology with some EBs measuring 400 μM in diameter (Fig.4.3A). EBs also appeared to be emitting single cells in suspension. While the $KDR^{+}CD31^{+}CD34^{+}$ population was still present, a small $CD43^{+}CD31^{+}KDR^{low/-}$ population had emerged (Fig.

4.3C). These cells also expressed CD235a and the megakaryocytic marker CD41 and were $CD34^{+/-}$. This population only represented approximately 3% of total cells.

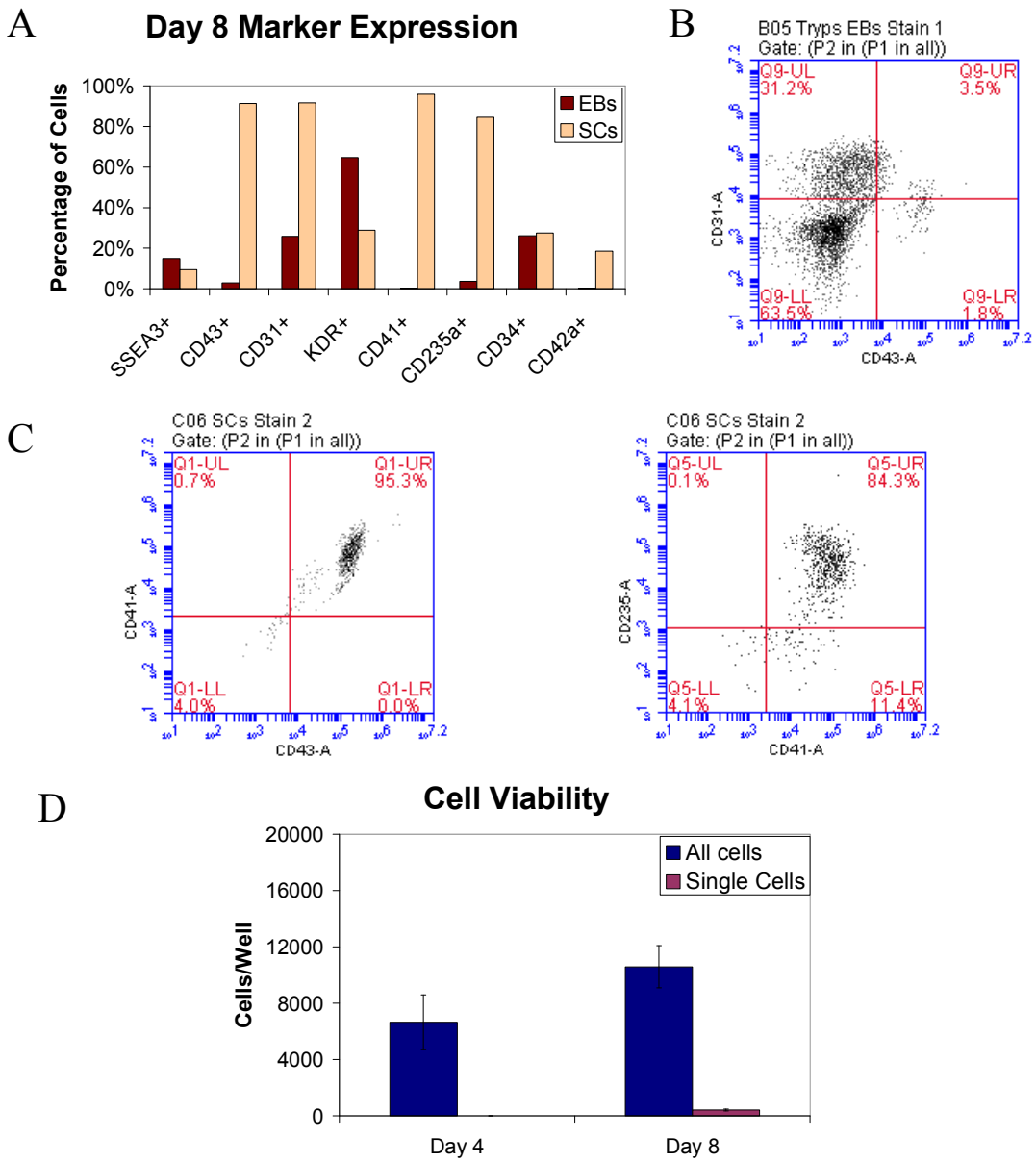

Figure 4.4. Day 8 separated EBs and single cells. **(A)** Day 8 flow cytometry profiles. **(B)** CD31, CD43 expression for EB cells. **(C)** Flow cytometry plots for single cells demonstrating CD43, CD41, and CD235a expression. **(D)** Cell viability over 8 days of differentiation.

It was hypothesized that this $CD43^+$ population consisted of single cells released from EBs. In order to evaluate this possibility, wells were pooled and EBs were allowed to settle for several minutes. The supernatant was then withdrawn, EBs were dissociated, and flow cytometry was performed on both sets of cells. EBs exhibited almost no expression of the hematopoietic markers CD43, CD41, and CD235a, whereas more than 90% of single cells expressed CD43 (Fig. 4.4A-C). Approximately 20% of single cells had also begun expressing the committed megakaryocytic marker CD42a.

Cell viability immediately decreased following seeding at Day 0. Day 4 populations were still less than 40% of the initial number of hESCs seeded (Fig. 4.4D). Yield had grown to higher than 50% at day 8, although the magnitude of single cells was lower than 500 cells/well, representing less than a 2.5% yield.

This data suggests that as hematopoietic differentiation proceeds, an early population of $KDR^+CD31^+CD34^+$ cells is generated by day 4 and gives rise to a $CD31^+CD43^+CD41^+CD235a^+$ population by day 8. This day 8 population emerges predominantly as single cells released by EBs. Although not shown, a very small amount of these cells (several cells per well) was observed at day 6.

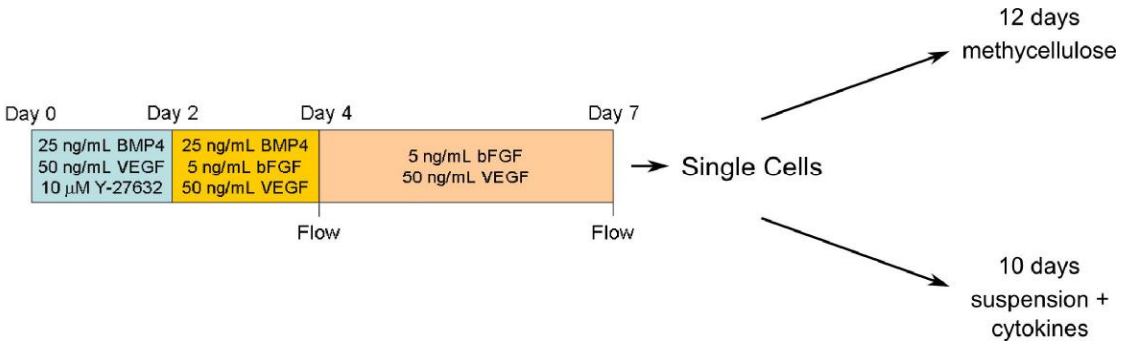

Figure 4.5. Schematic of 6-well scaled up procedure and single cell progenitor assays. Single cells were isolated at day 7 of differentiation and either cultured in methylcellulose for CFC analysis or re-suspended in differentiation medium supplemented with various cytokines to monitor differentiation progression.

In order to characterize the hematopoietic potential of the day 7-8 single cells and verify the scalability of this system, hESCs were differentiated in identical conditions in 6-well culture format. Single cells were isolated after 7 days of differentiation and seeded into methycellulose and supplemented with hematopoietic cytokines to test colony forming potential (Fig. 4.5). At day 7, heterogenous EBs and single cells were both visible in cultures (Fig. 4.6A). Over 90% of single cells were $CD43^{+}CD31^{+}$ (Fig. 4.6B). 41% were $CD41^{+}CD235a^{+}$, with some cells already expressing single lineage markers. Cells were $KDR^{low/-}$ and approximately 70% were $CD34^{-}$. Approximately 10% of cells expressed a $CD41^{-}CD34^{+}$ phenotype.

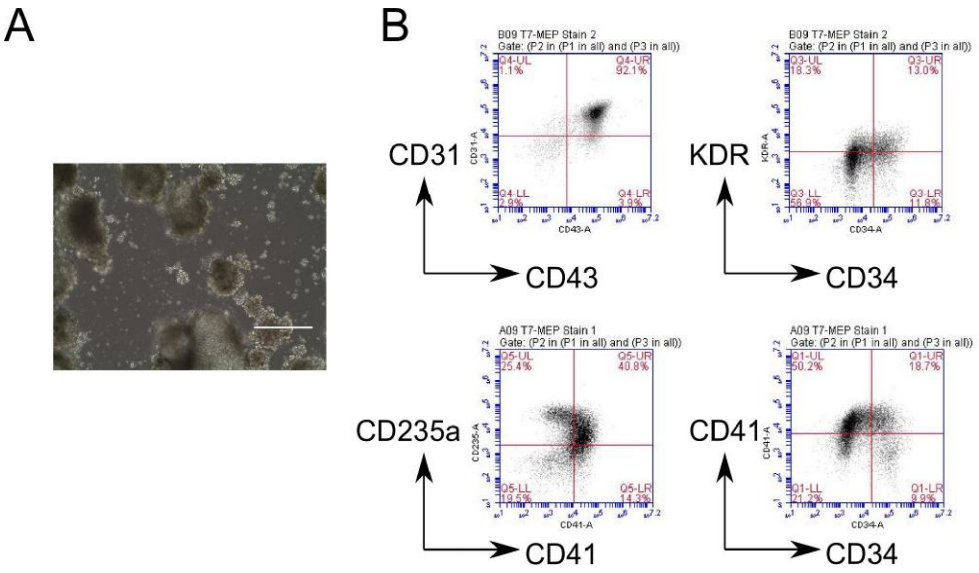

Figure 4.6. Phenotype of day 7 cells. **(A)** Day 7 EBs and single cells. Scalebar, 400 μM. **(B)** Flow cytometric marker profiles of day 7 single cells.

After 12 days of methylcellulose culture, cells had given rise to colonies of primitive erythrocytic, macrophage, and mixed morphology (Fig. 4.7A, B). Cytospins and May-Grunwald-Giemsa staining were then performed on selected colonies and demonstrated primarily primitive erythroblast and macrophage cells. These results suggest that differentiation conditions identified by the 96-well assay are scalable to 6-well plate or larger formats and that single cells produced after 7 days of differentiation have erythromyeloid potential.

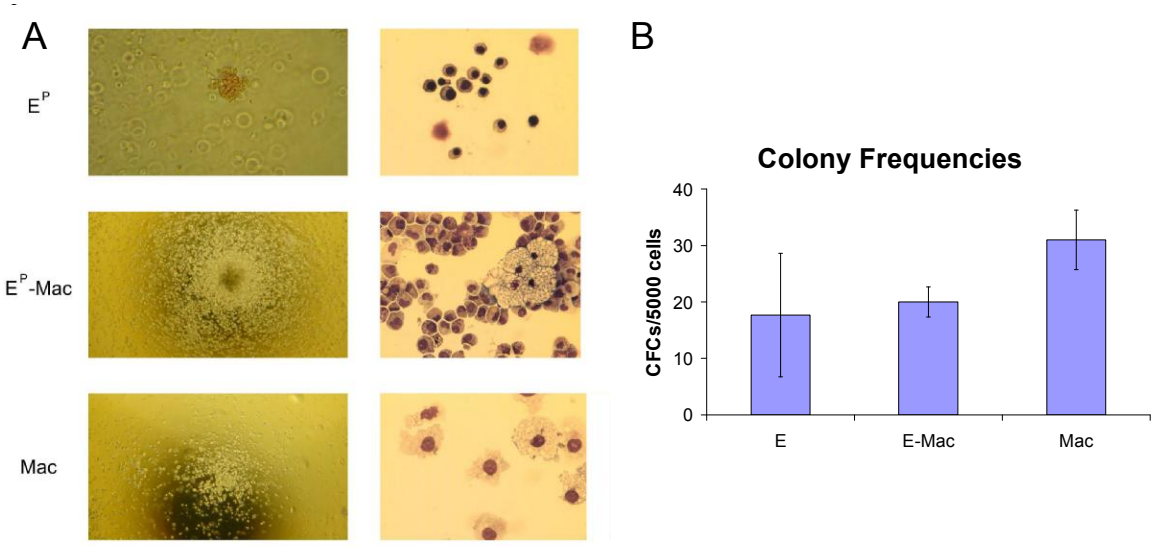

Figure 4.7. Hematopoietic colony potential of isolated day 7 single cells. **(A)** Colonies observed after 12 days of methycellulose culture and corresponding cytospins demonstrating primitive erythroblasts and macrophages. E^P: primitive erythrocyte colony; Mac: macrophage colony **(B)** Colony frequencies after 12 days. Bars represent mean ± SD of three assays.

Differentiating day 7 suspension single cells for a further 4 days in hematopoietic medium (containing SCF, TPO, EPO, Flt3-L, IL-6, and IL-3) produced cells morphologically characteristic of blast cells, primitive erythrocytes, and myeloid cells (Fig. 4.8A). At least three distinct populations were evident based off of marker expression profiles (Fig. 4.8B). A $CD41^{high}CD42a^{+}CD235a^{-}CD43^{high}$ population indicated the presence of committed megakaryocytes (approximately 25% of cells). A $CD235a^{+}CD41^{-}CD43^{mid/low}$ population indicated committed erythrocytes. A separate $CD41^{low/-}CD235a^{-}CD43^{high/mid}CD31^{high/mid}KDR^{mid}$ population also existed, although it was not clear what these represented. Almost all cells were $CD34^{-}$ and slight CD18 and CD45 expression indicated progression towards myeloid lineages. This suggests that day 7 single cells are capable of further differentiating down the erythroid, megakaryocytic, and myeloid lineages.

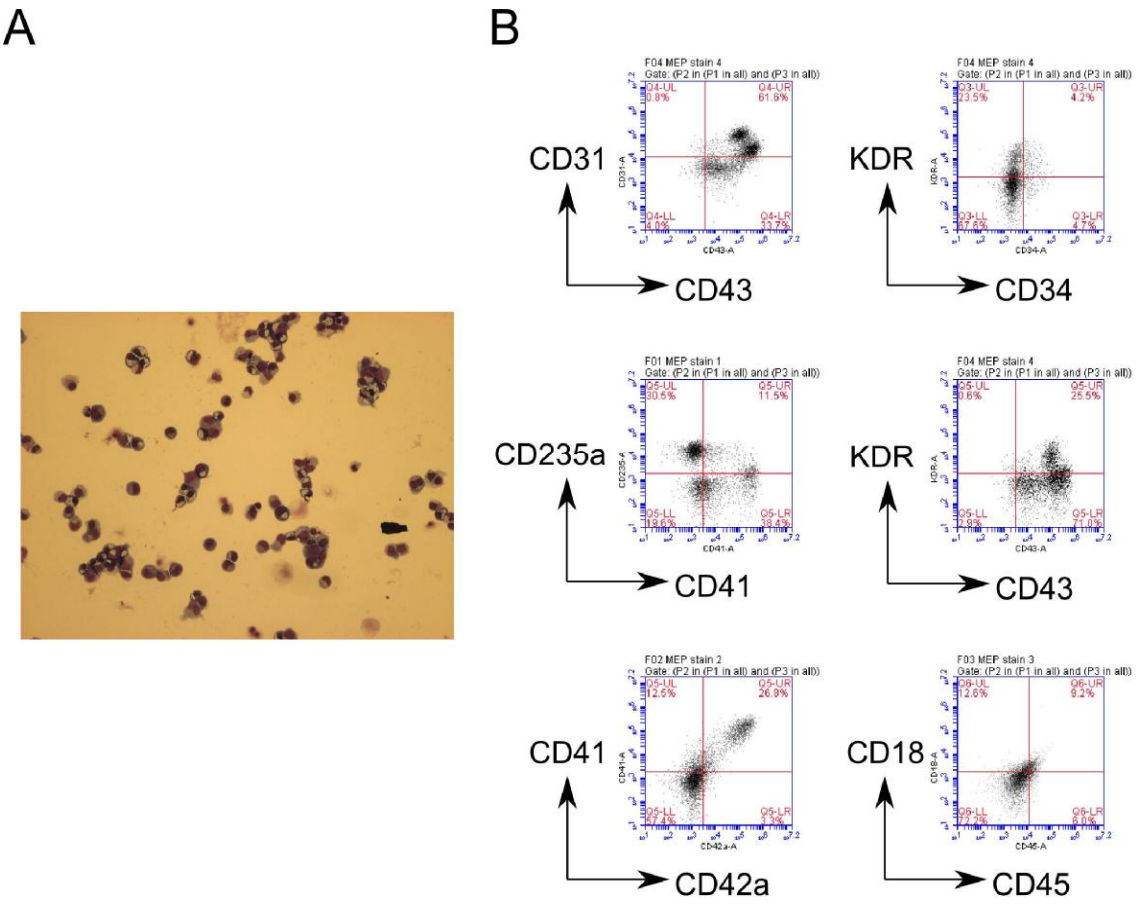

Figure 4.8. Hematopoietic differentiation phenotypes of day 7 + 4 cells. **(A)** Cytospin of day 7 suspension cells showing blast cell morphology. **(B)** Flow cytometry marker profiles.

After 10 days of differentiation of isolated single cells, populations began to appear less distinct. Committed $CD235a^{+}$ erythroid and $CD41^{+}CD42a^{+/-}$ megakaryocytic populations were still evident, although both had declined (Fig. 4.9B). A new $CD43^{low}CD41^{-}CD235a^{-}$ population was evident. Myeloid populations, characterized by CD18 and CD45 expression, had increased. Cytospins revealed multilineage cells resembling mature erythrocytes, megakaryocytes, and myeloid cells (Fig. 4.9A). These

data suggest that multipotent day 7 progenitors do not continue to self-renew and produce new committed progeny when cultured in the utilized differentiation medium.

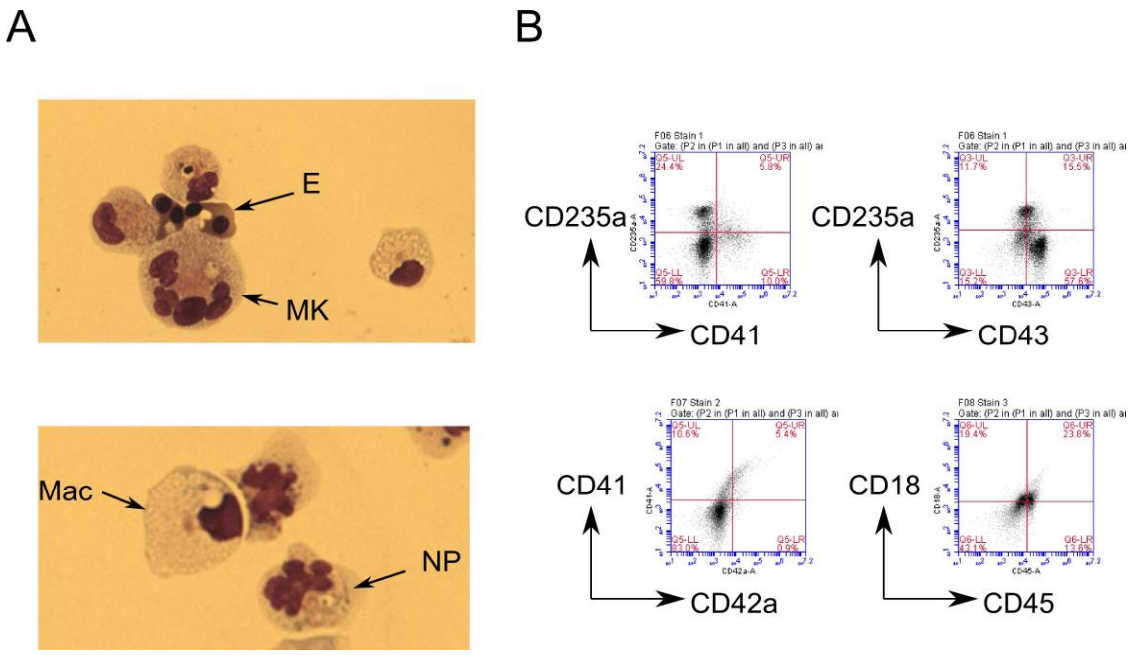

Figure 4.9. Hematopoietic differentiation phenotypes of day 7 + 10 cells. **(A)** Cytospin of day 7 suspension cells, showing cells characteristic of erythrocytes (E), megakaryocytes (MK), macrophages (Mac), and neutrophils (NP). **(B)** Flow cytometry marker profiles.

4.3.3 Optimizing KDR$^+$CD31$^+$ and CD31$^+$CD43$^+$ differentiation

These experiments indicated that during EB hematopoietic differentiation of hESCs, cells progress first through a KDR$^+$CD31$^+$ stage before CD43$^+$ primitive megakaryocyte-erythromyeloid progenitors are produced and that BMP4 followed by VEGF supplementation was required to induce CD31$^+$ expression. However, yields of CD43$^+$ single cells remained modest. We next sought to optimize the yield of these populations by increasing differentiation percentages and viability.

During mesoderm differentiation, BMP4 activates the Wnt pathway indirectly and Wnt signaling is required for primitive streak and mesoderm differentiation of mESCs

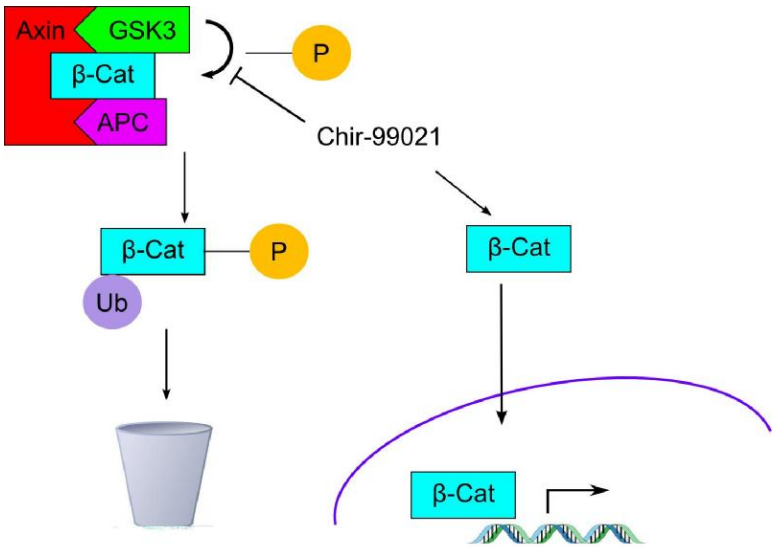

Figure 4.10. Simplified schematic of Chir-induced β-Catenin nuclear translocation. Chir inhibits phosphorylation of β-catenin by GSK3, preventing ubiquitination in inducing nuclear translocation and subsequent mediation of downstream genes.

[42, 94]. However, addition of exogenous Wnt to BMP4-supplemented conditions does not significantly improve hematopoietic differentiation [42]. Prior to differentiation, Wnt supplementation induces proliferation in undifferentiated hESCs [95]. The canonical WNT pathway relies on the nuclear translocation of the transcription factor β-catenin to the nucleus [96]. In the absence of exogenous WNT signaling, β-catenin is phosphorylated by the glycogen synthase kinase 3 (GSK3) and subsequently ubiquitinated and degraded. The small molecule Chir-99021 (herein referred to as Chir) is a highly selective inhibitor of GSK3β [97]. Inhibition of GSK3 activates the WNT pathway by preventing the degredation of β-catenin (Fig. 4.10). We hypothesized that GSK3 inhibition during concomitant BMP4 supplementation may enhance yields by inducing proliferation during differentiation. Our first objective was to evaluate the

effect of GSK3 inhibition, and consequently WNT activation, upon EB-based hematopoietic differentiation of hESCs.

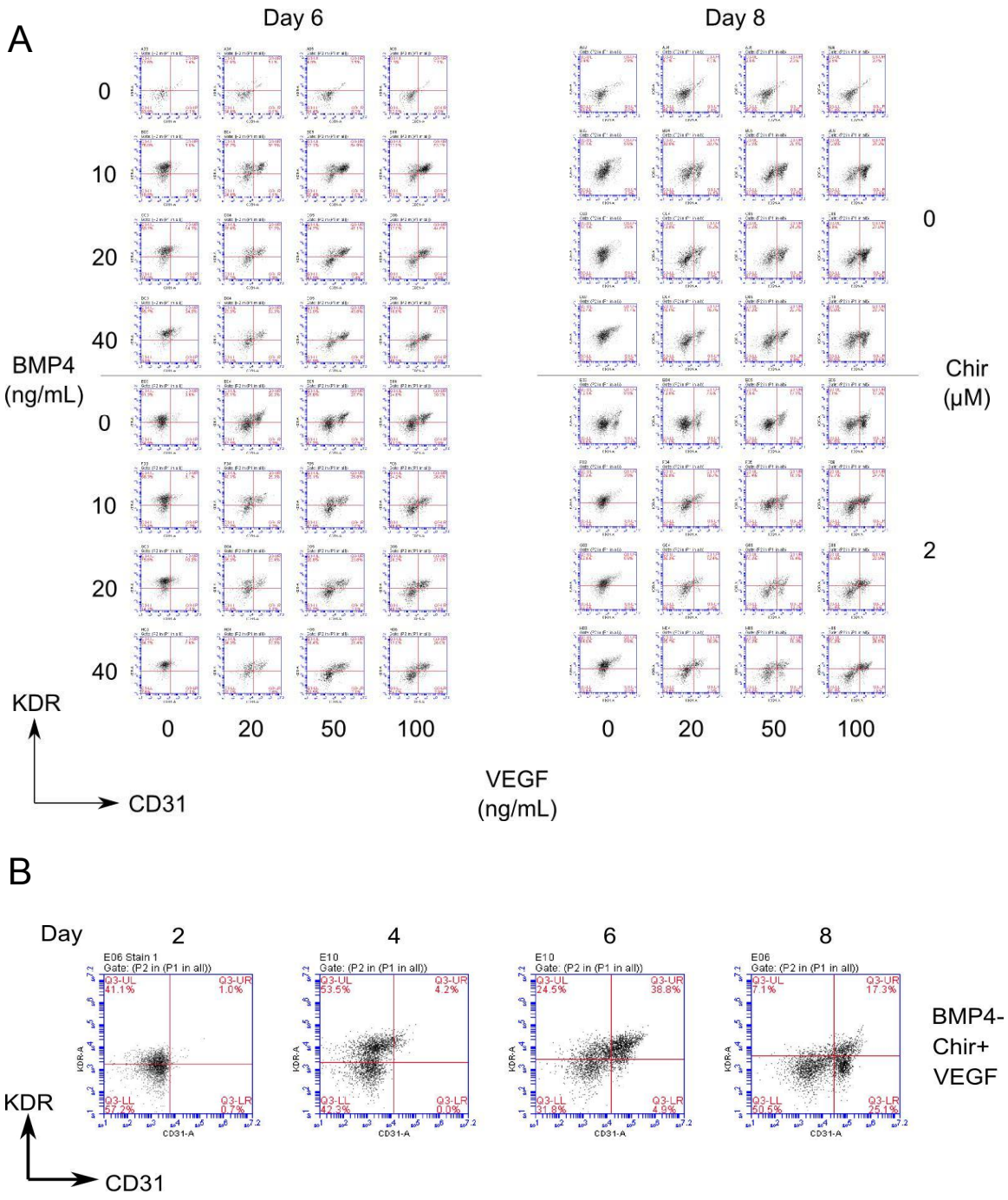

Figure 4.11. KDR-CD31 profiles for Chir, BMP4, VEGF Screen. **(A)** Day 6 and 8 profiles for all conditions. The double positive population is clear at day 6 and the $CD31^{+}KDR^{low/-}$ population is evident at day 8. **(B)** Time-course flow plots over 8 days of differentiation for medium supplemented with 2 μM Chir and 0 ng/mL BMP4.

We performed a screen to evaluate the effects of Chir supplementation upon a range of BMP4 and VEGF concentrations. hESCs were seeded at day 0 with ± Chir in conditions supplemented with 0-40 ng/mL BMP4 and 0-100 ng/mL VEGF. Chir was removed after 48 hours by replacement with bFGF-containing medium. After 6 days of differentiation, the $KDR^{+}CD31^{+}$ early hematopoietic population was observed in all VEGF and BMP4 containing conditions, as expected, and additionally in the Chir-supplemented conditions with 0 ng/mL BMP4 (Fig. 4.11A). $CD31^{+}KDR^{low/-}$ cells were evident in all VEGF and BMP4-containing conditions at day 8 and in Chir-exposed conditions without BMP4. Additionally, in Chir-conditions, this population surprisingly declined with increasing BMP4 concentrations. Smaller populations of these cells were also observed in wells containing both Chir and BMP4. Time course flow cytometry demonstrated that $CD31^{+}$ expression was delayed by up to 2 days by replacing BMP4 with Chir (Fig. 4.11B). Chir also greatly enhanced post-seeding cell viability, particularly in the absence of BMP4 (data not shown). This observation indicated that Chir supplementation may compliment or replace BMP4 supplementation and may enhance viability. Smaller $CD31^{+}KDR^{low/-}$ for increasing BMP4 concentrations in Chir-exposed conditions indicated that higher concentrations of BMP4 may inhibit hematopoietic differentiation.

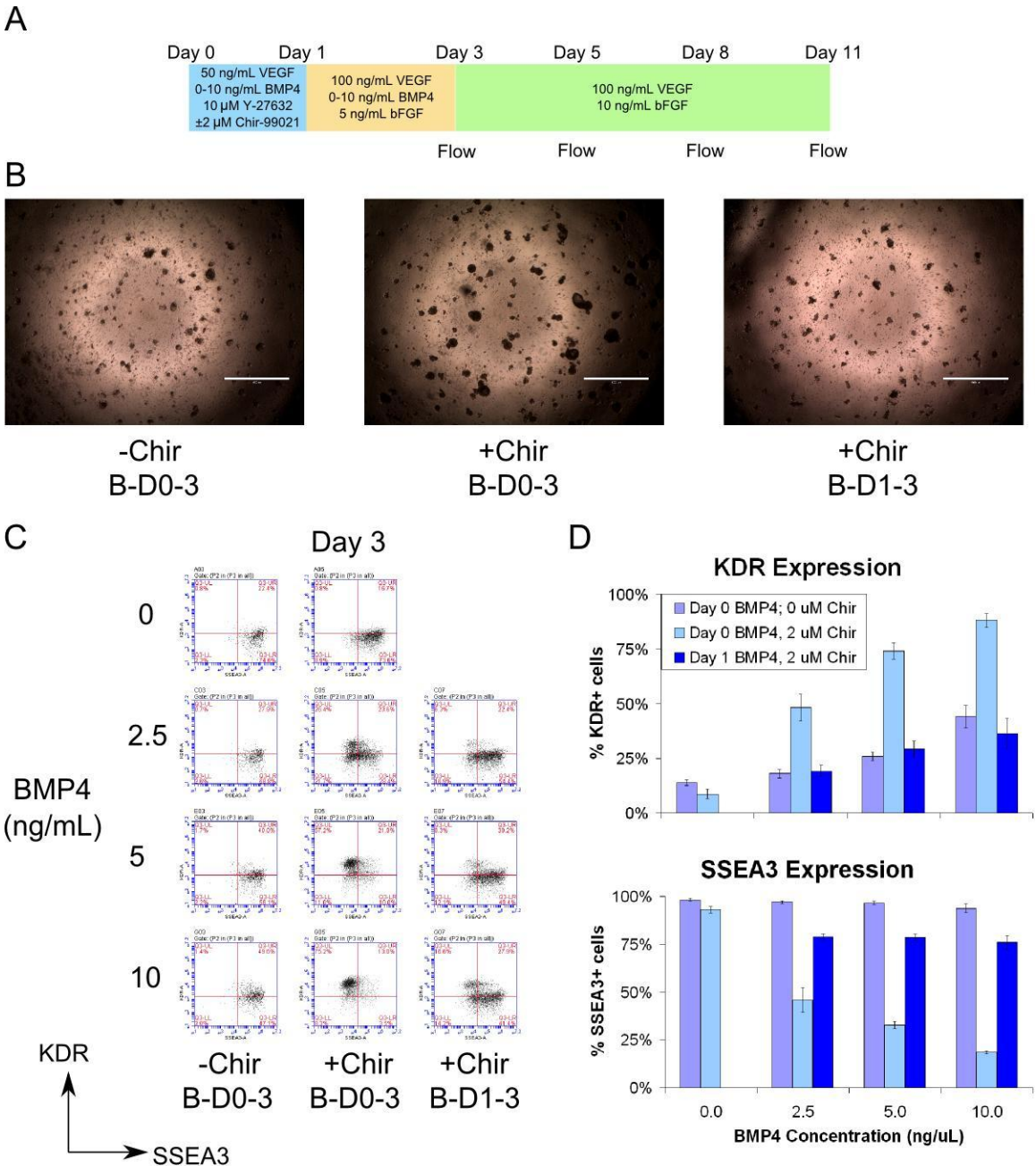

Figure 4.12. Day 3 results of the hematopoietic screen with Chir. **(A)** Experiment schematic **(B)** Images of EBs for the three conditions, all with 2.5 ng/mL BMP4. Scalebar, 1000 µM. **(C)** KDR, SSEA3 flow cytometry profiles of conditions. **(D)** Flow cytometry marker expression profiles. Expression values are given as percent of total live cells. Bars represent the mean ± SD of 4 wells. B-D0-3: BMP4 supplementation from Days 0-3. Chir concentration was 2 µM.

To evaluate these possibilities, a repeat screen was performed upon BMP4 concentrations of 0-10 ng/mL. Unlike the previous experiment, Chir was replaced with bFGF containing medium at day 1. BMP4 was supplemented for either days 0-3 or days 1-3 (Fig 4.12A). After 3 days and throughout differentiation, EBs in Chir-containing conditions were more defined and exhibited less surrounding apoptotic cells (Fig 4.12B). After 3 days of differentiation, Chir notably induced greater differentiation, as evidenced by lower SSEA3 expression (Fig 4.12C). Dual BMP4 and Chir supplementation induced the early mesoderm KDR^+ population, whereas this population had yet to emerge in conditions without Chir. A smaller KDR^+ population was evident in conditions without BMP4 for the first 24 hours. In Chir-containing conditions, KDR expression was proportional to the concentration of BMP4, with over 80% of cells KDR^+ when supplemented with Chir and 10 ng/mL BMP4.

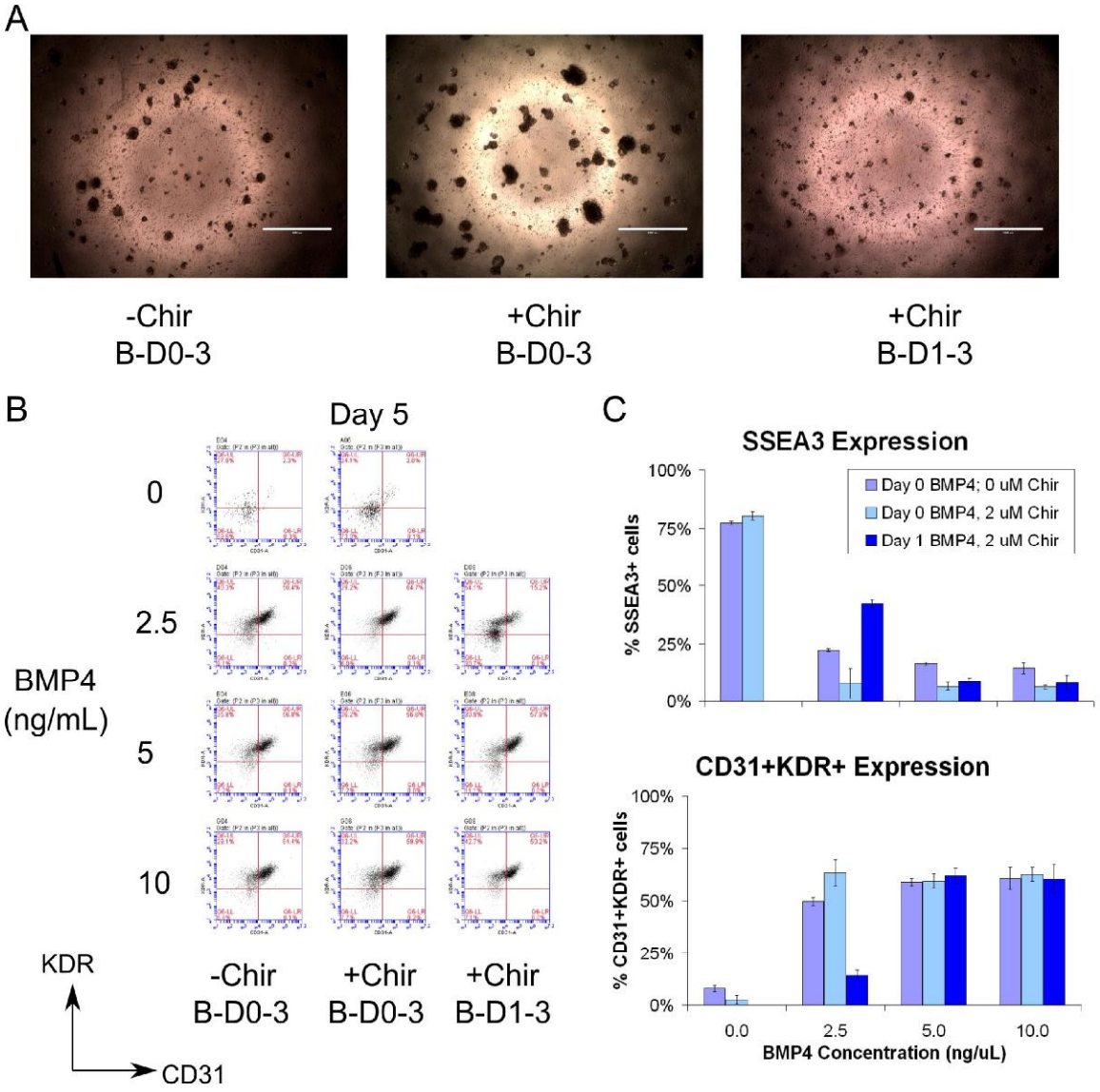

Figure 4.13. Day 5 results of the hematopoietic screen with Chir. **(A)** Images of EBs for the three conditions, all with 2.5 ng/mL BMP4. Scalebar, 1000 μM. **(B)** CD31, KDR flow cytometry profiles of conditions. **(C)** $SSEA3^+$ and $CD31^+KDR^+$marker expression profiles. Expression values are given as percent of total live cells. Bars represent the mean ± SD of 4 wells. Day 0 cell seeding density is represented by the red dashed line. Chir concentration was 2 μM. B-D0-3: BMP4 supplementation from Days 0-3.

After 5 days of differentiation, Chir EBs continued to remain larger than BMP4 alone EBs (Fig. 4.13A). Postponing BMP4 supplementation by 24 hours resulted in smaller EBs. BMP4-containing conditions displayed similar KDR^+CD31^+ populations,

with efficiencies generally ranging 50-65% (Fig. 4.13B, C). This population appeared to plateau for BMP4 concentrations greater than 2.5 ng/mL. Delaying BMP4 addition in small concentrations by 24 hours again delayed differentiation, as noted by increased SSEA-3 expression and decreased CD31 expression. Although Chir induced higher

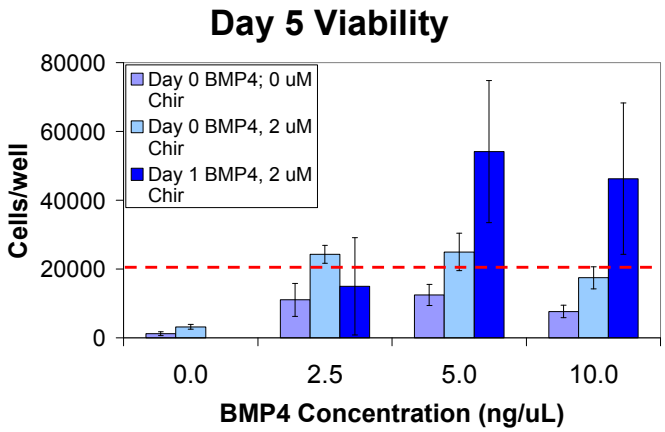

Figure 4.14. Day 5 viability. Expression values are given as percent of total live cells. Bars represent the mean ± SD of 4 wells. Day 0 cell seeding density is represented by the red dashed line.

KDR^+ populations at day 3, there was no corresponding increase in $CD31^+KDR^+$ cells at day 5. Yields, however, were significantly higher for Chir containing conditions due to higher viability (Fig. 4.14). Samples exposed to Chir without BMP4 for 24 hours were extremely variable. For BMP4 concentrations greater than 5 ng/mL administered at day 1, Chir supplementation increased cell counts by an average of 5-fold. However, viability was similar to BMP4 alone conditions for lower concentrations. Simultaneous Chir and BMP4 supplementation at day 0 increased viability by approximately 100% over BMP4 supplementation alone.

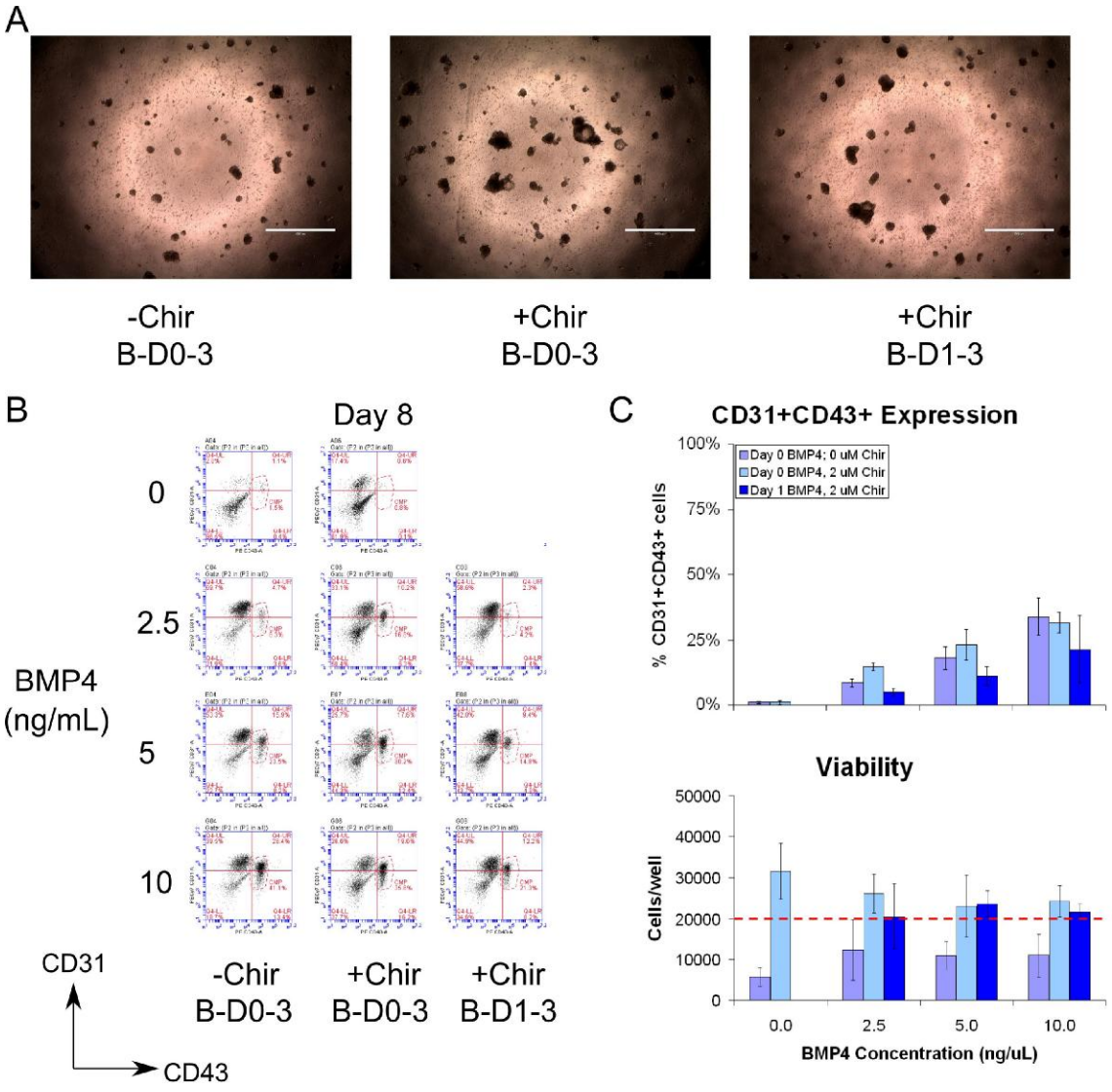

Figure 4.15. Day 8 results of the hematopoietic screen with Chir. **(A)** Images of EBs for the three conditions, all with 2.5 ng/mL BMP4. Scalebar, 1000 μM. **(B)** CD31, CD43 flow cytometry profiles of conditions. **(C)** $CD31^{+}CD43^{+}$marker expression profiles and cell viability. Expression values are given as percent of total live cells. Bars represent the mean ± SD of 4 wells. Day 0 cell seeding density is represented by the red dashed line. Chir concentration was 2 μM. B-D0-3: BMP4 supplementation from Days 0-3.

As seen previously, $CD43^{+}$ cells had begun to emerge by day 8, most predominantly in BMP4-containing conditions EBs were typically more frequent and larger for Chir conditions (Fig. 4.15A). For small concentrations of BMP4 (2.5-5

ng/mL), Chir enhanced $CD43^+$ differentiation, whereas no difference in induction percentage was seen at 10 ng/mL (Fig. 4.15B-C). Postponing BMP4 supplementation by 24 hours had no significant effect upon $CD43^+$ differentiation percentages. In all samples, BMP4 concentration was proportional to the size of this population. Although large variances were observed, Chir induced higher total cell viabilities than BMP4 alone (Fig. 4.15C). Cell counts were generally at least double those of BMP4 alone.

The $CD43^+$ populations were still present at day 11, indicating that these cells either remain viable over this period or are replaced by newly differentiating cells. EBs were similar to day 8, although larger cystic EBs were more frequent in Chir containing conditions (Fig. 4.16A). The KDR^+CD31^+ population was still present and relatively larger than day 8 for Chir conditions. CD43 relative population sizes were generally similar to day 8, although the day 0 BMP4 + Chir conditions demonstrated decreases. Notably, Chir supplementation with no BMP4 induced a population of $CD43^+$ cells unobserved at day 8 (Fig 4.16B). Similar to day 8, viability remained increased in Chir-containing conditions.

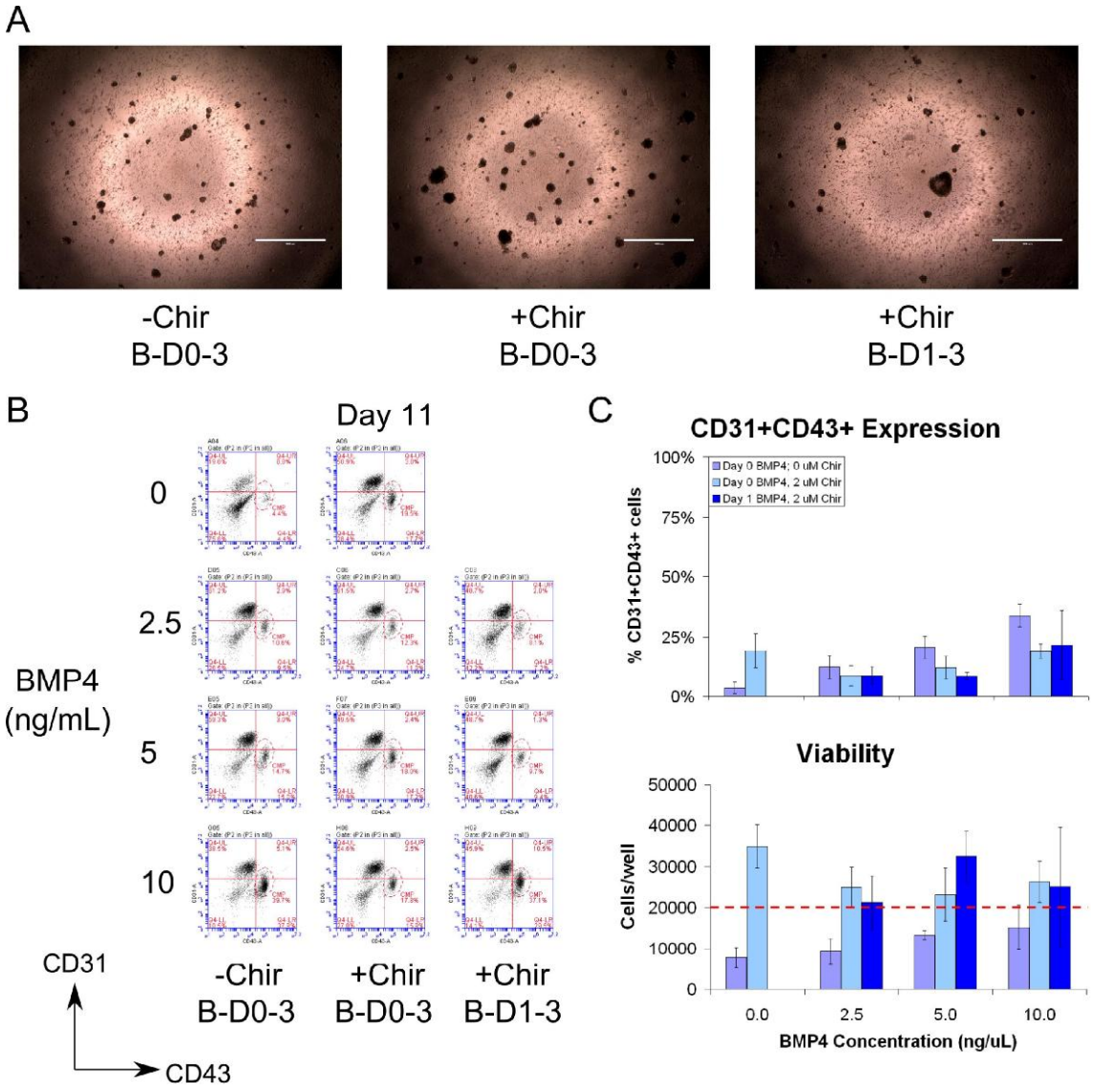

Figure 4.16. Day 11 results of the hematopoietic screen with Chir. **(A)** Images of EBs for the three conditions, all with 2.5 ng/mL BMP4. Scalebar, 1000 μM. **(B)** CD31, CD43 flow cytometry profiles of conditions. **(C)** $CD31^{+}CD43^{+}$marker expression profiles and cell viability. Expression values are given as percent of total live cells. Bars represent the mean ± SD of 4 wells. Day 0 cell seeding density is represented by the red dashed line. Chir concentration was 2 μM. B-D0-3: BMP4 supplementation from Days 0-3.

Differentiation percentages and absolute cell counts were utilized to determine yields of target cells over the course of differentiation (Fig. 4.17). In particular, we assessed the yields of target hematopoietic cell populations at different timepoints in

comparison to the initial seeding density of 20,000 cells per well. Early hematopoietic populations were significantly increased for all BMP4 conditions in the presence of Chir. At day 3, yields were greater than 80% of cells expressing KDR when BMP4 concentrations greater than 5 ng/mL were supplemented with Chir, compared with less than 5% of cells in the corresponding conditions without Chir ($p<0.01$). Subsequently at day 5, mid-range BMP4 and Chir concentrations demonstrated approximately 75% yields for $KDR^{+}CD31^{+}$, compared to less than 40% in the absence of Chir. Similarly at day 8, $CD43^{+}$ yields greater than 45% were observed when BMP4 concentration was at least 5 ng/mL in the presence of Chir, compared to less than 25% in its absence. Surprisingly, at day 11, conditions with Chir and no BMP4 demonstrated a yield of 34 ± 2%.

These results indicate that 24 hour exposure to Chir in the presence of concentrations of BMP4 less than 10 ng/mL enhances EB hematopoietic differentiation, resulting in more early-stage hematopoietic cells emerging at earlier time points. Additionally, Chir supplementation in the absence of BMP4 induces efficient hematopoietic differentiation, albeit at a delayed scale. Initial Chir supplementation during hematopoietic differentiation greatly increases cell viability in 96-well format.

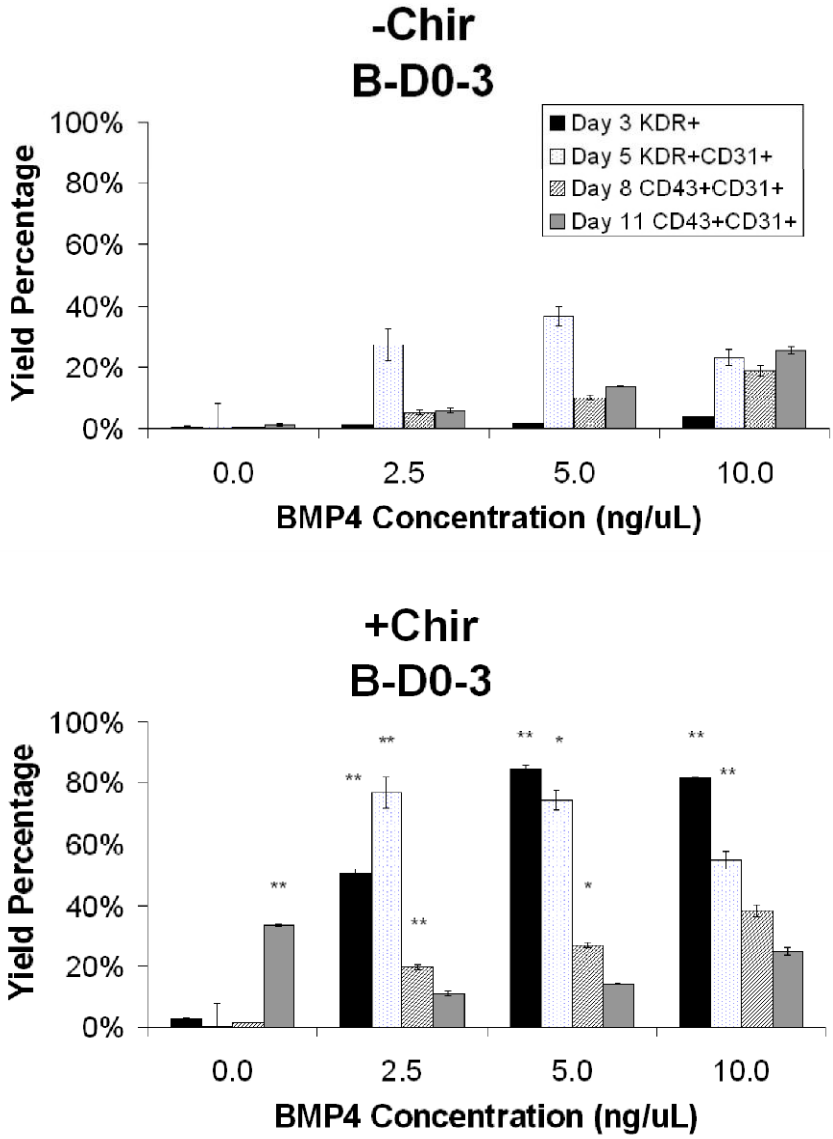

Figure 4.17. Differentiation yields throughout 11 days of differentiation. Yields are given for conditions supplemented with BMP4 from days 0-3 with and without 2 μM Chir. Percentages are relative to the initial day 0 seeding density of 20,000 cells/well. Asterisks in lower graph represent significant differences when compared to the corresponding condition without Chir in the top graph (*: $p<0.05$; **: $p<0.01$). B-D0-3: BMP4 supplementation from Days 0-3.

4.3.4 Cytokine screen to enhance $CD43^+$ progenitor differentiation and megakaryopoiesis

We established a step-wise procedure to differentiate hESCs down the hematopoietic lineage to obtain $CD43^+CD41^+CD235^+$ cells characteristic of common myeloid progenitors. This procedure demonstrated that the growth factors BMP4, VEGF, and bFGF were sufficient to induce this cell population. We also found that an initial 24 hour exposure to the GSK3β inhibitor Chir-99021 enhanced viability and hematopoietic differentiation. Prior studies have shown that supplementation with various hematopoietic cytokines further enhances hematopoietic differentiation and is required for commitment to several specific lineages [86, 98, 99]. However, requirements of these factors to hemopoietic differentiation of hESCs in serum-free medium have not been assessed. Many hematopoietic differentiation protocols of ESCs have included cytokines at various stages without detailing their contribution. Additionally, reports have included such factors in differentiation medium and noted no apparent benefit in blast colony formation [100]. We sought to perform a screen of various hematopoietic cytokines to assess their potential enhancement to production of $CD43^+$ progenitors and $CD41^+CD42^+$ megakaryocytes.

hESCs were differentiated according to the previously established stepwise protocol, including an initial 24 hour exposure to Chir-99012 (Fig. 4.18A). At day 6, cells were exposed to medium supplemented with 10 ng/mL bFGF, 100 ng/mL VEGF, and various cytokine combinations: ± 25 ng/mL FLT3-L, ± 10 ng/mL IL-3, ± 10 ng/mL IL-6, and ± 50 ng/mL TPO. Cell identity and viability were assessed at days 8 and 11. After 8 days of differentiation, $CD31^+CD43^+$ yields were similar amongst all conditions,

ranging between 40-65%, with no clear trends due to the presence or absence of different growth factors (Fig. 4.18B). Viability was above the seeding density of 20,000 cells per well for most conditions (Fig. 4.18C).

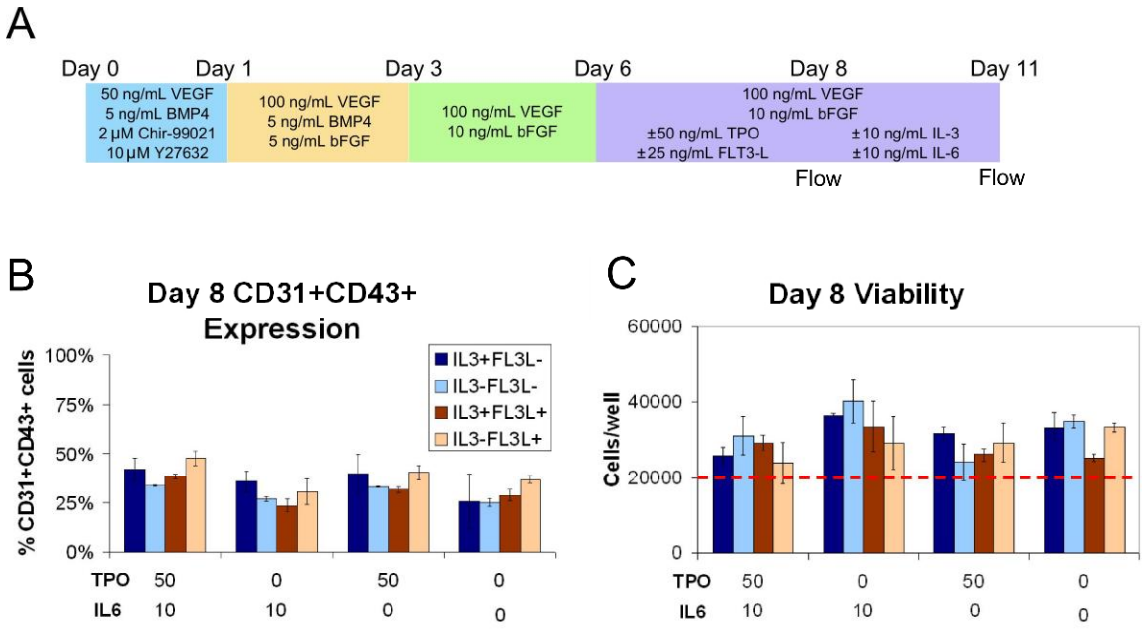

Figure 4.18. Experiment schematic and day 8 hematopoietic cells. **(A)** Schematic of hematopoietic cytokine screen. **(B)** $CD31^{+}CD43^{+}$ populations. Percentages represent percentage of total cells. **(C)** Total cell viability. Bars represent mean ± SD of two wells.

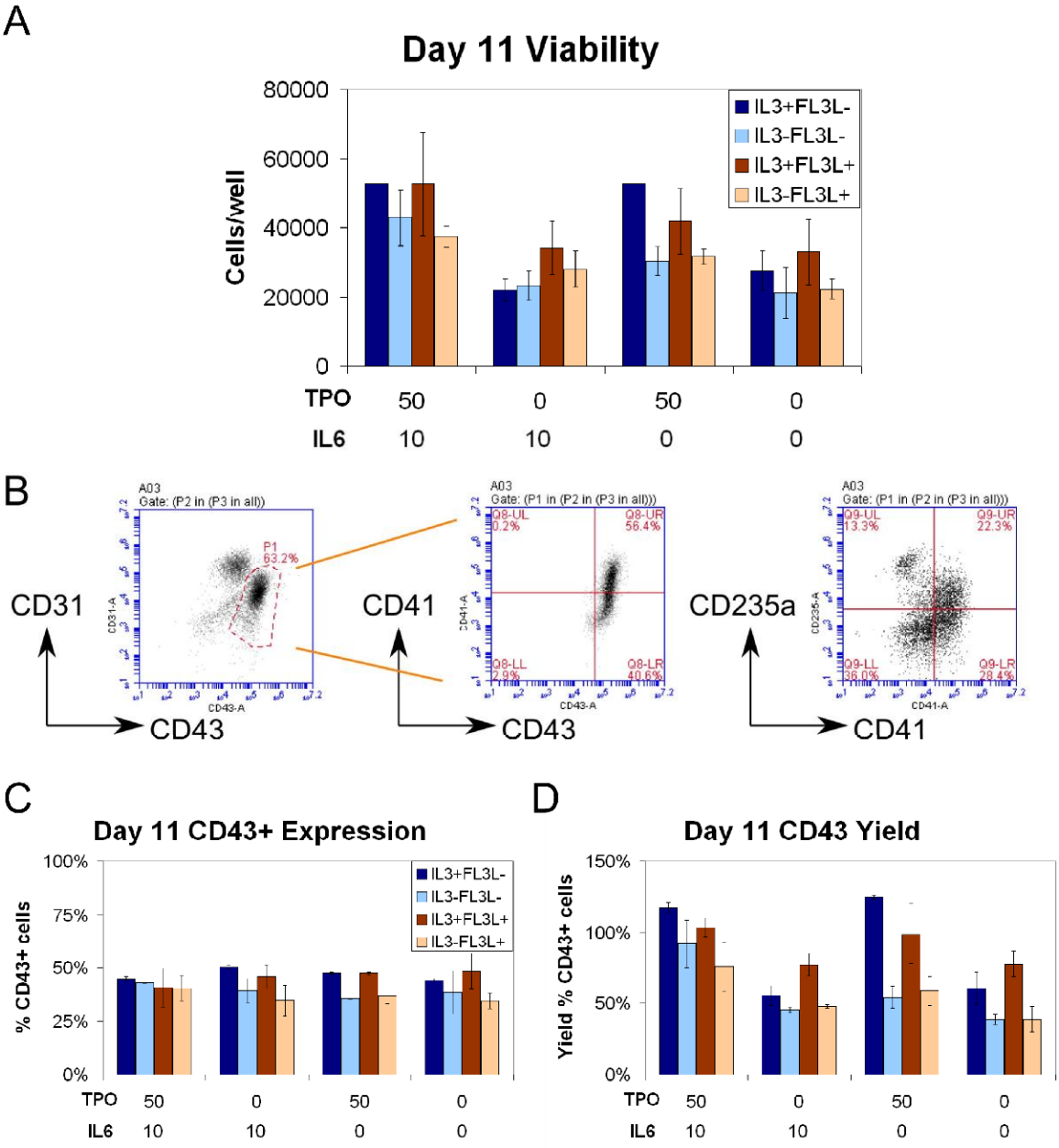

Figure 4.19. Day 11 CD43+ hematopoietic populations. **(A)** Marker profiles demonstrating gated $CD43^{+}CD31^{low/-}$ hematopoietic cells out of total cells (left) and CD41 and CD235a expression for those gated cells. **(B)** $CD43^{+}$ populations. Percentages represent percentage of total cells. **(C)** $CD43^{+}$ percentage yields. Values are given as percentage of 20,000 cells/well seeded at day 0. Bars represent mean ± SD of two wells.

After 11 days of differentiation, cells had begun to differentiate down more committed lineages. Viability was higher for cells exposed to both TPO and IL-3 (Fig. 4.19A). IL-6 appeared to increase viability in the absence of IL-3. Several general marker expression trends were evident for all samples. The hematopoietic progenitor population maintained CD43 but began to express lower CD31 expression than observed at day 8 (Fig. 4.19B). A subpopulation of $CD43^+$ cells had lost CD41 expression, indicating commitment to a non-megakaryocytic lineage. Approximately one-third of these cells expressed CD235a, indicating differentiation toward the erythrocytic lineage. $CD41^+CD235a^+$ cells were still observed, although a population of $CD41^+$ cells had lost CD235a expression, indicating progression towards the megakaryocytic lineage. Population sizes began to vary between the various cytokine conditions. $CD43^+$ differentiation percentages were increased for IL-3-containing conditions (Fig. 4.19C). When viability was taken into account, $CD43^+$ yields were greater for cells exposed to both TPO and IL-3 and to cells exposed to both TPO and IL-6 (Fig. 4.19D). This phenomenon emphasized the need to assess both marker expression percentages and yields. Differences in the former imply an influence upon differentiation efficiency; in the latter, upon proliferation.

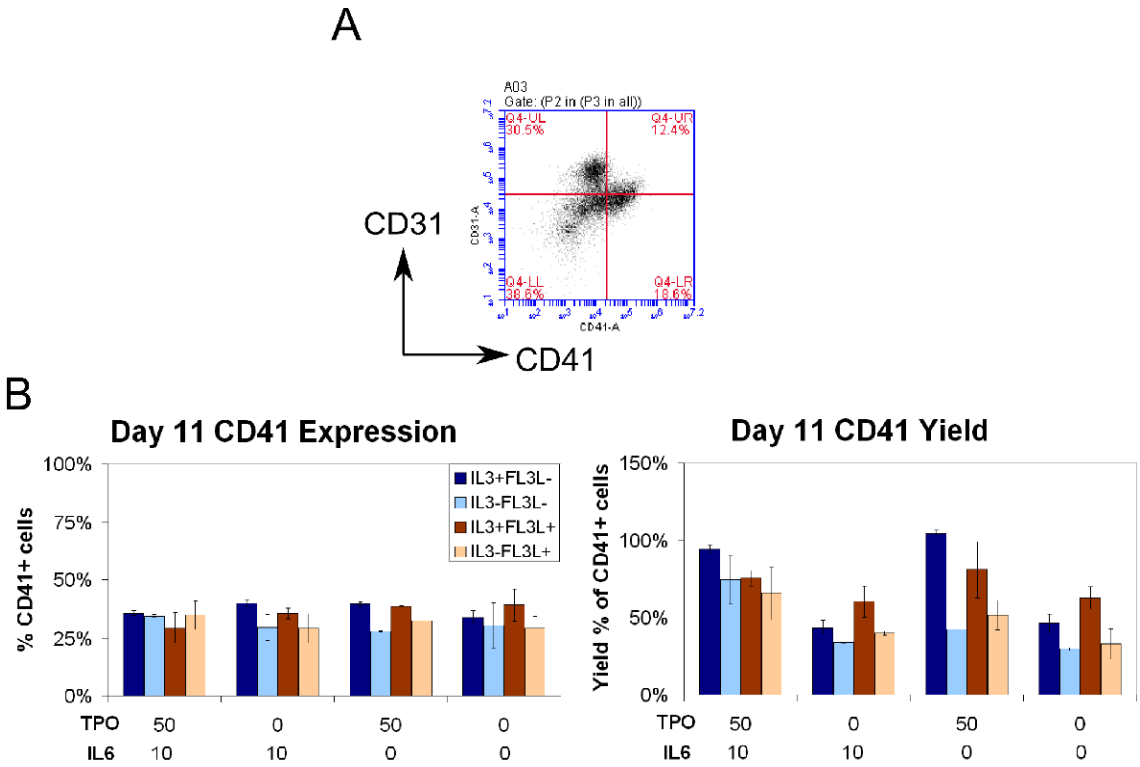

Figure 4.20. Day 11 CD41+ hematopoietic populations. **(A)** Marker profile demonstrating the $CD41^{+}CD31^{low/-}$ population. **(B)** Differentiation percentages and yields for total $CD41^{+}$. Percentages represent percentage of total cells (left) and percentages of 20,000 cells/well seeded at day 0 (right). Bars represent mean ± SD of two wells.

$CD41^{+}$ cells exhibited the $CD31^{low/-}$ phenotype (Fig. 4.20A). Differentiation percentages ranged between 28-40% of total cells, with TPO and IL3 inducing more efficient differentiation although not significantly (Fig. 4.20B). The greatest cell counts were obtained for conditions supplemented with only TPO and IL-3, with a yield of 21,900 ± 350 cells/well, or approximately 110% of the initial hESC cell density. When used in combination with TPO and IL-3, IL-6 and FLT3-L appeared to decrease yield slightly, but not significantly so. Removing either TPO or IL-3 significantly reduced $CD41^{+}$ cell generation.

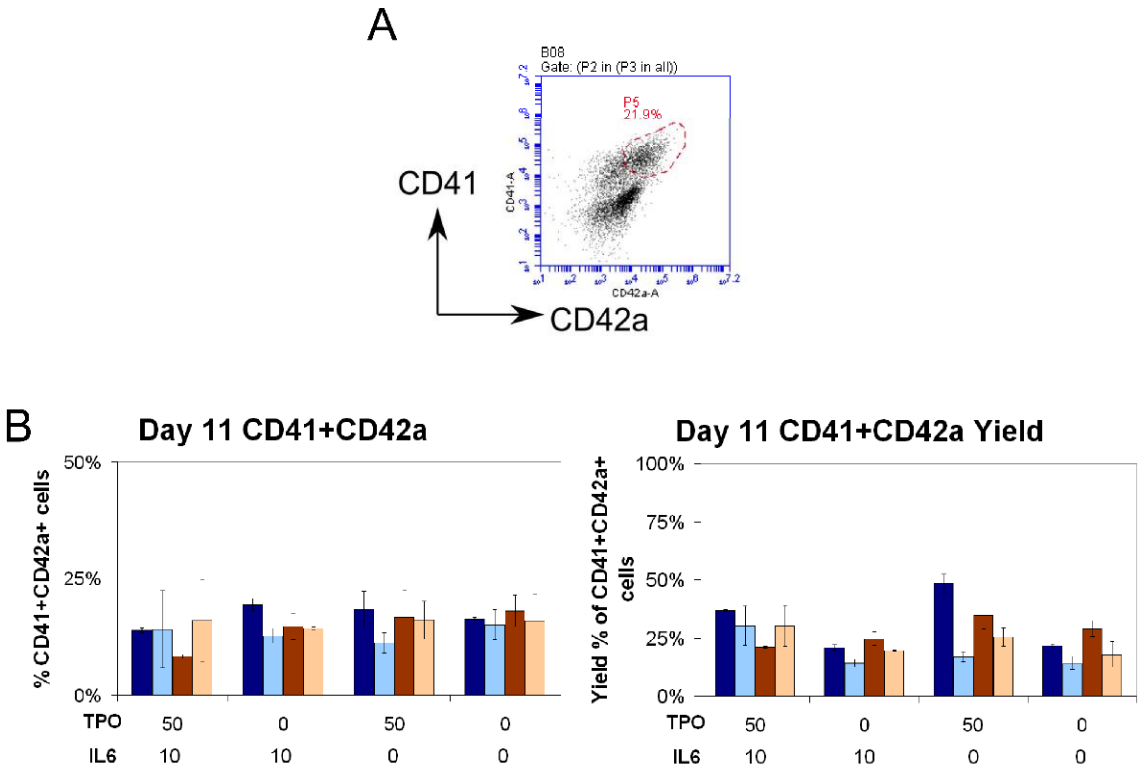

Figure 4.21. Day 11 CD42+ megakaryocyte populations. **(A)** Marker profile demonstrating the $CD41^{+}CD42a^{+}$ population. **(B)** Differentiation percentages and yields for total $CD42a^{+}$. Percentages represent percentage of total cells (left) and percentages of 20,000 cells/well seeded at day 0 (right). Bars represent mean ± SD of two wells.

A portion of $CD41^{+}$ cells had begun to express CD42a, indicating commitment to the megakaryocyte lineage (Fig. 4.21A). These cells generally represented 40-50% of total $CD41^{+}$ cells. Due to variability, various cytokine combinations failed to significant affect $CD42^{+}$ differentiation efficiency (Fig. 4.21B). However, as with $CD43^{+}$ and $CD41^{+}$ cells, $CD42a^{+}$ megakaryocyte yields were higher for TPO and IL-3 containing conditions, with TPO and IL-3 together generating a yield of 48 ± 4% (Fig. 4.21B). FLT3-L again appeared to inhibit $CD42a^{+}$ cell production in the presence of TPO and IL-3, although this trend was true for $CD43^{+}$ hematopoietic cells in general (Fig. 4.19D). IL-6 appeared to inhibit CD42a expression in the presence of TPO and IL-3.

These data suggest that supplementing the stepwise differentiation protocol with hematopoietic cytokines enhances hematopoietic progenitor generation after 11 days of differentiation by influencing both differentiation efficiency and cell proliferation. More specifically, TPO and IL-3 increased the proportion of $CD43^+$ cells. These two cytokines also increased $CD43^+$, $CD41^+$, and $CD42a^+$ yields by inducing greater proliferation between days 8 and 10. For conditions containing only TPO and IL-3, $CD41^+$ and $CD42a^+$ cell yields were approximately 100% and 50%, respectively.

4.4 Discussion

Here, we applied the 96-well EB differentiation assay to optimize distinct stages of hematopoietic differentiation of hESCs. Specifically, we developed a stepwise serum-free protocol to efficiently differentiate hESCs toward $CD41^+$ primitive common myeloid progenitors and $CD42^+$ megakaryocytes (Fig. 4.22). Combinations of BMP4, VEGF, bFGF, TPO, and IL-3, along with the ROCK inhibitor Y-27632 and the GSK-3β inhibitorChir-99021, are utilized at distinct times during an 11 day differentiation in serum-free medium. Along the procedure, cells transition from pluripotent ESCs to KDR^+ early mesoderm, KDR^+CD31^+ hematopoietic cells, $CD43^+CD41^+CD235^+$ progenitor cells, and $CD41^+CD42^+$ megakaryocytes.

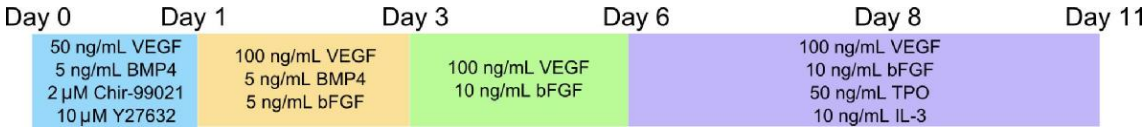

Figure 4.22. The final stepwise hematopoietic and megakaryocyte differentiation protocol.

Initially BMP4 and Chir-99021 are utilized to push the hESCs to the primitive streak stage. BMP4 has been shown to induce primitive streak differentiation and have a "posteriorizing effect" upon streak cells, further pushing them toward KDR^+ mesoderm [33, 42]. In our system, BMP4 effectively induced KDR^+ mesoderm and KDR^+CD31^+ mesoderm, but cell death was high, limiting the information content of endpoint flow cytometry results. Wnt signalling is required for both primitive streak and KDR^+ mesoderm formation [42, 94]. However, Wnt supplementation in addition to BMP4 has been shown to have little contributory effect toward either streak formation or KDR^+ mesoderm [42]. Our results demonstrated that simultaneous Chir and BMP4 supplementation increased viability by approximately two-fold and notably enhanced differentiation yields of hematopoietic cells throughout differentiation. Chir supplementation prior to BMP4 exposure drastically increased cell counts in some conditions, consistent with the previous observation of Wnt-stimulated hESC proliferation [95].

The exact mechanisms underlying Chir-induced enhanced primitive hematopoietic differentiation are unclear. The requirement of Wnt signaling in the mesoderm-to-hematopoietic transition is more established. In murine ESCs, BMP activates Wnt3a, which in turn promotes hematopoiesis via the Cdx-Hox pathway [101].

Wnt signaling has also been shown to be required for post-mesoderm primitive but not definitive hematopoiesis in mESCs [42]. Our results demonstrated enhanced hematopoietic differentiation following an initial 24-hour activation of the Wnt pathway, as indicated by the action of Chir. These results conflict with those of a previous study showing that Wnt treatment prior to primitive streak formation induces a mesoderm to cardiomyocyte route in mESCs [102]. However, these results were obtained in undirected, serum-containing medium, obfuscating the underlying mechanisms. Indeed, human induced pluripotent stem cells (iPSCs) generated KDR^+ progenitors with erythro-myeloid potential after 8 days of differentiation in WNT3a-containing serum-free medium [103]. In agreement with our results, co-culture of hESCs on a Wnt1-producing stromal line, which activates canonical Wnt signaling, enhanced differentiation of $KDR^+CD31^+CD34^+$ cells. This was not observed by activation of the non-canonical pathway [104].

The ROCK inhibitor Y-27632 is known to increase viability during hESC passaging [105] and has been shown to increase cell survival within the first 24 hours of differentiation initiation [93]. Due to the low viability observed during hematopoietic differentiation and the heightened concern due to the small culture format, Y-27632 was added for initially 48 hours and subsequently 24 hours at day 0 in the stepwise protocol. Although Y-27632 has been reported to decrease post-thawing viability and expansion of frozen $CD34^+$ cord blood cells [106], we observed no negative effects upon hematopoietic differentiation.

Previous studies have documented the requirement of VEGF for hematopoietic differentiation of ESCs [42, 107, 108], but to our knowledge none had characterized the

relationship between concentration and differentiation efficiency. We directly demonstrated that VEGF is required for generating $CD34^+CD31^+$ cells and that its concentration is proportional to differentiation efficiency. Furthermore, we showed that these cells are also KDR^+. Although we did not characterize the exact identity and potential of these cells, it is likely that, prior to emergence of the $CD43^+$ cells, this population contains the KDR^+ hemangioblast previously described that exhibits primitive-erythroid and myeloid potential [19].

CD43 expression marks the commitment of differentiating hESCs to the hematopoietic lineage [89]. We first detected $CD43^+$ expression within a population of $CD43^+CD41^+CD235^+$ single cells that emerged between days 7-8 in this system. We found these cells to have primitive-erythroid, megakaryocyte, and myeloid potential. Past studies have defined a $CD41^+CD235^+$ bipotent primitive erythroid-megakaryocyte progenitor (MEP) capable of differentiating towards the primitive erythroid or megakaryocyte lineages in both murine embryogenesis [83] and hESC OP9 coculture [86]. However, these studies did not assess myeloid potential. The primitive MEP generated by OP9 coculture expressed CD34 shortly after emergence, whereas our progenitor did not. Macrophage potential arises within the murine yolk sac at the same time as primitive erythroid potential [80], indicating that these lines share a common progenitor. Thus, it is difficult to state definitively whether the cell we have generated represents an identical or analogous cell type to previous studies. It is perhaps better described as a primitive version the common adult myeloid progenitor [109].

In this study, hematopoietic potential was evaluated based off of entire populations of single cells without sorting. Thus, we can not definitely state which cell

possesses common myeloid potential. Prior studies have demonstrated that unilineage $CD235^+$ erythrocytes and $CD41^+$ megakaryocytes arise from $CD235^+CD41^+$ bipotential progenitors [83], and thus it is reasonable to hypothesize the same here. We observed both $CD34^+$ and $CD34^-$ cells within CD41 populations at day 7. It is not clear if either offers more progenitor capabilities. Zambidis et al. found more colony forming potential in $CD143^+CD34^-$ than in $CD143^+CD34^+$ early hematopoietic cells [108]. Chicha et al. reported a differentiation system in which $CD34^+$ cells generated myeloid and mature erythroid colonies whereas as $CD34^-$ cells produced only small immature erythoid colonies [90]. The relationship between CD34 expression and progenitor potential is clearly not fully understood.

IL-3 has been previously shown to enhance primitive erythroid colony formation from hESC derived primitive MEPs and has frequently been used in hematopoietic differentiation protocols [86, 91]. TPO promotes megakaryopoiesis by binding to its receptor c-Mpl [99] and is also commonly utilized in protocols [90, 91, 100, 110]. We found that Chir-99021, BMP4, VEGF, and bFGF supplementation were sufficient to generate $CD43^+$ committed hematopoietic progenitors and megakaryocytes, but highest yields were generated when TPO and IL-3 cytokines were added in combination to the differentiation medium. FLT3L had no apparent effect after 11 days of differentiation. In the absence of IL3, IL6 increased hematopoietic yields when used in combination with TPO.

5. Conclusions, Limitations, and Future Work

5.1 Conclusions

Many clinical therapies could benefit from an *in vitro* protocol of generating hematopoietic cells in a reproducible manner. Methods to produce both HSCs and megakaryocytes, and subsequently platelets, would greatly advance treatment of hematopoietic diseases. Additionally, these protocols could allow further study of hematopoiesis during human development. Many hematopoietic differentiation protocols have been published. However, only a small portion of these are feeder-free and serum-free, thus allowing clinical translation. Even fewer allow for target cells to be harvested in bulk, and none present an efficient method of producing primitive erythromyeloid progenitors and megakaryocytes. We have created a high throughput assay capable of optimizing EB based differentiation of hESCs toward one of the three primary germ layers, and applied this assay to create a stepwise serum-free, feeder-free protocol for the highly efficient generation of $CD41^{+}CD235^{+}$ erythromyeloid progenitors and $CD41^{+}CD42a^{+}$ megakaryocytes.

We have shown that the 4-color differentiation assay itself can distinguish between the three primary germ layers and from undifferentiated pluripotent stem cells using the 4 markers as described. Differentiation toward any lineage could potentially be examined by selection of the proper combination of biomarkers. The use of 4 colors is determined by the technical capability of the flow cytometer. At this point, no commercially available instruments exist that allow 96-well plate flow cytometry and are capable of more colors. This is likely to be overcome within several years. Naturally,

more colors would allow for more markers to be assessed, allowing for greater cell specification and more elaborate experiments. At least one 384-well plate flow cytometer is available. However, at this point, in our opinion, EB differentiation within a 384-well plate would not be possible. Cell counts would be too low to allow for reliable differentiation and accurate analysis.

To our knowledge, two other groups have created small-scale differentiation optimization assays [23, 26]. Both of these rely upon culturing single EBs within 96-well plates. This allows for precise experiments upon culture conditions and signaling pathways to be performed. Both methods also ensure uniform EB size. However, hESCs undoubtedly release factors into surrounding medium during differentiation. This cross-talk between EBs most assuredly would have effects upon differentiation progress, course, or efficiency. Neither method is directly scalable to larger platforms, which limits the ability to design a system to supply hematopoietic cells for clinical purposes. Our system accomplishes both of these goals. We have shown scalability to 6-well culture for hematopoietic differentiation. This system also allows highly efficient staining and flow cytometry without the need to pool cells.

We have defined a primitive hematopoietic EB differentiation protocol using stepwise addition of defined differentiation media at specified stages. By inhibiting GSK-3β through the supplementation of Chir-99021, we observed differentiation yields of over 80% for Day 3 KDR^+ cells, over 70% for day 5 KDR^+CD31^+ cells, and over 25% for day 8 $CD43^+$ $CD41^+CD235^+$ primitive progenitors. We then performed a screen of all combinations of four cytokines to enhance day 8 and day 11 $CD43^+$ yields to approximately 64% and 104%, respectively. In summary, we obtained yields of about

two $CD41^{+}CD235^{+}$ primitive hematopoietic progenitors and one $CD41^{+}CD42^{+}$ megakaryocyte for every hESC plated.

5.2 Limitations & pitfalls

As with all techniques, this differentiation assay has advantages and disadvantages. It is relevant to highlight the limitations in order to properly interpret results and design future experiments accordingly.

5.2.1 Flow cytometry

This protocol relies upon a commercially available 96-well flow cytometry unit. As previously discussed, only four markers can be assessed simultaneously, limiting the conclusions that can be drawn from a single sample. Furthermore, if markers are only expressed transiently, then a given marker combination will only be applicable for a brief period of time. This places limitations on abilities to accurately detect complex arrangements of differentiation kinematics. For ectoderm detection, a $NCAM^{+}/SSEA3^{+}$ identity was utililized. This is clearly transient as SSEA3 is only expressed within early ectoderm. Thus, if a given condition enhances ectoderm differentiation by quickening its pace, the observer may be oblivious due to absence of SSEA3 expression. If more than four colors are desirable, multiple samples must be run and stained separately. Protocols exist for assessing 5 colors simultaneously from a 4 color system, but these were never tried.

Generally, it would require 60-90 minutes to read an entire 96-well plate. Consequently, some samples would be analyzed 90 minutes apart. Given the small volume, this creates concerns for sample temperature, evaporation, viability, and potential differentiation. Additionally, cells would easily settle during this time, ensuring the need for frequent plate agitation. In order to minimize these confounding variables, plates were covered with a lid and kept on ice after staining. Columns would be transferred to a new 96-well round bottom plate one at a time and acquired immediately. Round bottom plates were utilized because, according to the manufacturer's instructions, V-bottom plates are not accurate for absolute cell counts. If only a few columns were needed, plate transfer would not be performed, but wells would be agitated by trituration with a pipet multichannel just prior to acquisition.

5.2.2 EB dissociation

In order to perform accurate flow cytometry, EBs must be dissociated to single cells. In many standard 6-well culture protocols, then entails enzymatic cleavage of cellular bonds followed by rigorous trituration with a syringe and needle. A 96-well plate system renders this single sample technique impractical. Hence, EB dissociation is all the more difficult. For early stage EBs (less than 7-8 days), 0.25% trypsin-EDTA will suffice for dissociation. For larger, later stage EBs, a collagenase incubation period must be performed initially, followed by incubation with a harsher agent (such as trypsin). We have observed two caveats that arise from either of these dissociation options.

First, some antigens, such as CD41, are especially to trypsin and will be cleaved off within several minutes. This can easily confound results if not expected. Second, if

EBs are not completely dissociated, flow cytometer occlusion will likely occur. Additionally, cells within EBs will not be analyzed. If samples mixed with EBs and single cells are dissociated together, this will give a reading that 100% of cells in the sample are single cells and artificially inflating differentiation efficiency. The latter is also true if EBs are improperly enzymatically dissociated and too rigoursly mechanically separated, resulting in cell death. Thus, trial experiments should be performed to test antigen sensitivity to the applied dissociation agent. For hematopoietic experiments, we found that incubation of cells with Collagenase B for one hour at 37ºC, followed by 5-15 minutes of accutase incubation at 37ºC with occasional trituration would generally suffice. EBs should be examined with a microscope to ensure disruption.

5.3 Future work

5.3.1 Hematopoietic differentiation

We utilized flow cytometry to characterize cell populations capable of multilineage primitive hematopoietic potential. As a first more thorough assessment of the identity of these cells, transcript expression analysis should be performed. Chir-99021 supplementation generated quicker differentiation of KDR^{+} mesoderm cells. *Brachyury* expression should be monitored in the first 3 days to assess the effect of Chir upon differentiation to the primitive streak. Throughout the differentiation process, gene expression should be evaluated to verify lineage commitment. Genes to be evaluated include: *SCL* (hematopoietic commitment), *LMO2* (hematopoietic commitment, erythro-megakaryocytic specification), *RUNX1* (hematopoietic commitment, definitive

hematopoietic potential), *C-MYB* (definitive hematopoietic potential, lymphomyeloid lineages), *GATA2* (hematopoietic commitment), GATA1 (erythro-megakaryocytic specification) [89], the megakaryocyte specific genes *MPL, FLI1*, and the erythrocytic specific genes *EPOR and KLF1* [86].

In order to further understand the mechanism behind Chir-induced enhancement, experiments should be performed to verify that β-catenin phosphorylation is prevented and that nuclear translocation occurs. First, β -catenin phosphorylation could be evaluated by staining with a p-β-catenin specific antibody. Nuclear translocation can be verified by immunofluorescence staining of hESCs 24 hours after Chir supplementation. B-catenin functionality can be evaluated by evaluating the subsequent activation of downstream genes, such as *SP5* or *AXIN2* [111]. Enhanced proliferation after Chir supplementation could be assessed by evaluating BrdU incorporation. Decreased apoptosis could be evaluated by using TUNEL analysis. Furthermore, colony potential of hematopoietic progenitors produced following Chir supplementation should be evaluated.

By screening 4 hematopoietic cytokines, we drastically increased the yield of progenitors and megakaryocytes. This yield could likely be increased further by screening other commonly utilized cytokines. A first screen should evaluate EPO and SCF. We observed IL-6 to potentially decrease megakaryocyte specification. Thus, FP6, a soluble form of the IL-6 receptor, could be added to remove any soluble IL-6 [112]. Additionally, the Notch ligand Delta-like1 (DL-1) has been demonstrated to induce megakaryopoiesis from adult HSCs [113]. It would be interesting to conduct a screen with recombinant IL-6. While trends identified by the hematopoietic cytokine screen

were consistent and convincing, conclusions drawn from screens should be interpreted cautiously. Future studies will involve follow-up and further validation of these results.

Due to the fact that megakaryocytes are difficult to detect in standard methycellulose cultures such as that used here, a megakaryocyte-specific culture assay (MegaCult, StemCell Technologies) could be utilized. Additionally, in order to assess functionality, fibrin clot assays should be performed upon harvested megakaryocytes [86].

5.3.2 Differentiation assay

By utilization of fluorescent or luminescent reporter genes, this culture system could be adapted to endstage readouts other than flow cytometry. For instance, by using Gadue et al.'s Brachyury-driven GFP system, we could perform screens to assess effect upon differentiation to the primitive streak [9]. Promoter-specific luciferase cell lines would offer the ability to lyse cells and perform efficient viability and luciferase measurements by utilization of a plate reader.

6. References

[1] J.A. Thomson, J. Itskovitz-Eldor, S.S. Shapiro, M.A. Waknitz, J.J. Swiergiel, V.S. Marshall, J.M. Jones, Embryonic stem cell lines derived from human blastocysts, Science, 282 (1998) 1145-1147.

[2] J. Itskovitz-Eldor, M. Schuldiner, D. Karsenti, A. Eden, O. Yanuka, M. Amit, H. Soreq, N. Benvenisty, Differentiation of human embryonic stem cells into embryoid bodies compromising the three embryonic germ layers, Molecular Medicine, 6 (2000) 88-95.

[3] B.E. Reubinoff, M.F. Pera, C.Y. Fong, A. Trounson, A. Bongso, Embryonic stem cell lines from human blastocysts: somatic differentiation in vitro, Nat Biotechnol, 18 (2000) 399-404.

[4] J.G. Chenoweth, R.D. McKay, P.J. Tesar, Epiblast stem cells contribute new insight into pluripotency and gastrulation, Dev Growth Differ, 52 293-301.

[5] P. Gadue, T.L. Huber, M.C. Nostro, S. Kattman, G.M. Keller, Germ layer induction from embryonic stem cells, Experimental Hematology, 33 (2005) 955-964.

[6] C.E. Murry, G. Keller, Differentiation of embryonic stem cells to clinically relevant populations: lessons from embryonic development, Cell, 132 (2008) 661-680.

[7] H. Kurosawa, Methods for inducing embryoid body formation: in vitro differentiation system of embryonic stem cells, Journal of Bioscience & Bioengineering, 103 (2007) 389-398.

[8] T. Yamada, M. Yoshikawa, S. Kanda, Y. Kato, Y. Nakajima, S. Ishizaka, Y. Tsunoda, In vitro differentiation of embryonic stem cells into hepatocyte-like cells identified by cellular uptake of indocyanine green, Stem Cells, 20 (2002) 146-154.

[9] P. Gadue, T.L. Huber, P.J. Paddison, G.M. Keller, Wnt and TGF-beta signaling are required for the induction of an in vitro model of primitive streak formation using embryonic stem cells, Proceedings of the National Academy of Sciences of the United States of America, 103 (2006) 16806-16811.

[10] S.M. Dang, M. Kyba, R. Perlingeiro, G.Q. Daley, P.W. Zandstra, Efficiency of embryoid body formation and hematopoietic development from embryonic stem cells in different culture systems, Biotechnology & Bioengineering, 78 (2002) 442-453.

[11] R.L. Carpenedo, C.Y. Sargent, T.C. McDevitt, Rotary suspension culture enhances the efficiency, yield, and homogeneity of embryoid body differentiation, Stem Cells, 25 (2007) 2224-2234.

[12] M.D. Ungrin, C. Joshi, A. Nica, C. Bauwens, P.W. Zandstra, Reproducible, ultra high-throughput formation of multicellular organization from single cell suspension-derived human embryonic stem cell aggregates, PLoS ONE [Electronic Resource], 3 (2008) e1565.

[13] M.V. Wiles, G. Keller, Multiple hematopoietic lineages develop from embryonic stem (ES) cells in culture, Development, 111 (1991) 259-267.

[14] B.C. Zandstra PW, Yin T, Liu Q, Schiller H, Zweigerdt R, Pasumarthi KB, Field LJ., Scalable production of embryonic stem cell-derived cardiomyocytes, Tissue Engineering, 9 (2003) 767-778.

[15] I. Orlovskaya, I. Schraufstatter, J. Loring, S. Khaldoyanidi, Hematopoietic differentiation of embryonic stem cells, Methods, 45 (2008) 159-167.

[16] K.A. D'Amour, A.G. Bang, S. Eliazer, O.G. Kelly, A.D. Agulnick, N.G. Smart, M.A. Moorman, E. Kroon, M.K. Carpenter, E.E. Baetge, Production of pancreatic hormone-expressing endocrine cells from human embryonic stem cells, Nature Biotechnology, 24 (2006) 1392-1401.

[17] M. Kyba, R.C. Perlingeiro, G.Q. Daley, HoxB4 confers definitive lymphoid-myeloid engraftment potential on embryonic stem cell and yolk sac hematopoietic progenitors, Cell, 109 (2002) 29-37.

[18] E.T. Zambidis, B. Peault, T.S. Park, F. Bunz, C.I. Civin, Hematopoietic differentiation of human embryonic stem cells progresses through sequential hematoendothelial, primitive, and definitive stages resembling human yolk sac development, Blood, 106 (2005) 860-870.

[19] M. Kennedy, S.L. D'Souza, M. Lynch-Kattman, S. Schwantz, G. Keller, Development of the hemangioblast defines the onset of hematopoiesis in human ES cell differentiation cultures, Blood, 109 (2007) 2679-2687.

[20] K. Matsumoto, T. Isagawa, T. Nishimura, T. Ogaeri, K. Eto, S. Miyazaki, J. Miyazaki, H. Aburatani, H. Nakauchi, H. Ema, Stepwise development of hematopoietic stem cells from embryonic stem cells, PLoS One, 4 (2009) e4820.

[21] M. Nakanishi, A. Kurisaki, Y. Hayashi, M. Warashina, S. Ishiura, M. Kusuda-Furue, M. Asashima, Directed induction of anterior and posterior primitive streak by Wnt from embryonic stem cells cultured in a chemically defined serum-free medium, FASEB Journal, 23 (2009) 114-122.

[22] E.S. Ng, R. Davis, E.G. Stanley, A.G. Elefanty, A protocol describing the use of a recombinant protein-based, animal product-free medium (APEL) for human embryonic stem cell differentiation as spin embryoid bodies, Nat Protoc, 3 (2008) 768-776.

[23] E.S. Ng, R.P. Davis, L. Azzola, E.G. Stanley, A.G. Elefanty, Forced aggregation of defined numbers of human embryonic stem cells into embryoid bodies fosters robust, reproducible hematopoietic differentiation, Blood, 106 (2005) 1601-1603.

[24] M. Pick, L. Azzola, A. Mossman, E.G. Stanley, A.G. Elefanty, Differentiation of human embryonic stem cells in serum-free medium reveals distinct roles for bone morphogenetic protein 4, vascular endothelial growth factor, stem cell factor, and fibroblast growth factor 2 in hematopoiesis, Stem Cells, 25 (2007) 2206-2214.

[25] R.P. Davis, E.S. Ng, M. Costa, A.K. Mossman, K. Sourris, A.G. Elefanty, E.G. Stanley, Targeting a GFP reporter gene to the MIXL1 locus of human embryonic stem cells identifies human primitive streak-like cells and enables isolation of primitive hematopoietic precursors, Blood, 111 (2008) 1876-1884.

[26] M. Koike, H. Kurosawa, Y. Amano, A Round-bottom 96-well Polystyrene Plate Coated with 2-methacryloyloxyethyl Phosphorylcholine as an Effective Tool for Embryoid Body Formation, Cytotechnology, 47 (2005) 3-10.

[27] M. Koike, S. Sakaki, Y. Amano, H. Kurosawa, Characterization of embryoid bodies of mouse embryonic stem cells formed under various culture conditions and estimation of differentiation status of such bodies, J Biosci Bioeng, 104 (2007) 294-299.

[28] M. Borowiak, R. Maehr, S. Chen, A.E. Chen, W. Tang, J.L. Fox, S.L. Schreiber, D.A. Melton, Small molecules efficiently direct endodermal differentiation of mouse and human embryonic stem cells, Cell Stem Cell, 4 (2009) 348-358.

[29] S.C. Desbordes, D.G. Placantonakis, A. Ciro, N.D. Socci, G. Lee, H. Djaballah, L. Studer, High-throughput screening assay for the identification of compounds regulating self-renewal and differentiation in human embryonic stem cells, Cell Stem Cell, 2 (2008) 602-612.

[30] S. Irion, H. Luche, P. Gadue, H.J. Fehling, M. Kennedy, G. Keller, Identification and targeting of the ROSA26 locus in human embryonic stem cells, Nat Biotechnol, 25 (2007) 1477-1482.

[31] J.T. Outten, P. Gadue, D.L. French, S.L. Diamond, High-throughput screening assay for embryoid body differentiation of human embryonic stem cells, Curr Protoc Stem Cell Biol, Chapter 1 (2012) Unit 1D 6.

[32] M. Zhao, H. Yang, X. Jiang, W. Zhou, B. Zhu, Y. Zeng, K. Yao, C. Ren, Lipofectamine RNAiMAX: an efficient siRNA transfection reagent in human embryonic stem cells, Mol Biotechnol, 40 (2008) 19-26.

[33] C. Park, I. Afrikanova, Y.S. Chung, W.J. Zhang, E. Arentson, G. Fong Gh, A. Rosendahl, K. Choi, A hierarchical order of factors in the generation of FLK1- and SCL-expressing hematopoietic and endothelial progenitors from embryonic stem cells, Development, 131 (2004) 2749-2762.

[34] L. Vallier, P.J. Rugg-Gunn, I.A. Bouhon, F.K. Andersson, A.J. Sadler, R.A. Pedersen, Enhancing and diminishing gene function in human embryonic stem cells, Stem Cells, 22 (2004) 2-11.

[35] D.C. Hay, L. Sutherland, J. Clark, T. Burdon, Oct-4 knockdown induces similar patterns of endoderm and trophoblast differentiation markers in human and mouse embryonic stem cells, Stem Cells, 22 (2004) 225-235.

[36] H. Zaehres, M.W. Lensch, L. Daheron, S.A. Stewart, J. Itskovitz-Eldor, G.Q. Daley, High-efficiency RNA interference in human embryonic stem cells, Stem Cells, 23 (2005) 299-305.

[37] R.T. Rodriguez, J.M. Velkey, C. Lutzko, R. Seerke, D.B. Kohn, K.S. O'Shea, M.T. Firpo, Manipulation of OCT4 levels in human embryonic stem cells results in induction of differential cell types, Experimental Biology & Medicine, 232 (2007) 1368-1380.

[38] N. Izumi, T. Era, H. Akimaru, M. Yasunaga, S. Nishikawa, Dissecting the molecular hierarchy for mesendoderm differentiation through a combination of embryonic stem cell culture and RNA interference, Stem Cells, 25 (2007) 1664-1674.

[39] L. Yang, M.H. Soonpaa, E.D. Adler, T.K. Roepke, S.J. Kattman, M. Kennedy, E. Henckaerts, K. Bonham, G.W. Abbott, R.M. Linden, L.J. Field, G.M. Keller, Human cardiovascular progenitor cells develop from a KDR+ embryonic-stem-cell-derived population, Nature, 453 (2008) 524-528.

[40] M. Yasunaga, S. Tada, S. Torikai-Nishikawa, Y. Nakano, M. Okada, L.M. Jakt, S. Nishikawa, T. Chiba, T. Era, S. Nishikawa, Induction and monitoring of definitive and visceral endoderm differentiation of mouse ES cells, Nat Biotechnol, 23 (2005) 1542-1550.

[41] K.E. McGrath, A.D. Koniski, K.M. Maltby, J.K. McGann, J. Palis, Embryonic expression and function of the chemokine SDF-1 and its receptor, CXCR4, Developmental Biology, 213 (1999) 442-456.

[42] M.C. Nostro, X. Cheng, G.M. Keller, P. Gadue, Wnt, activin, and BMP signaling regulate distinct stages in the developmental pathway from embryonic stem cells to blood, Cell Stem Cell, 2 (2008) 60-71.

[43] H. Sakurai, T. Era, L.M. Jakt, M. Okada, S. Nakai, S. Nishikawa, S. Nishikawa, In vitro modeling of paraxial and lateral mesoderm differentiation reveals early reversibility, Stem Cells, 24 (2006) 575-586.

[44] T. Enver, S. Soneji, C. Joshi, J. Brown, F. Iborra, T. Orntoft, T. Thykjaer, E. Maltby, K. Smith, R.A. Dawud, M. Jones, M. Matin, P. Gokhale, J. Draper, P.W. Andrews, Cellular differentiation hierarchies in normal and culture-adapted human embryonic stem cells, Hum Mol Genet, 14 (2005) 3129-3140.

[45] R. Kannagi, N.A. Cochran, F. Ishigami, S. Hakomori, P.W. Andrews, B.B. Knowles, D. Solter, Stage-specific embryonic antigens (SSEA-3 and -4) are epitopes of a unique globo-series ganglioside isolated from human teratocarcinoma cells, Embo J, 2 (1983) 2355-2361.

[46] J. Pruszak, K.C. Sonntag, M.H. Aung, R. Sanchez-Pernaute, O. Isacson, Markers and methods for cell sorting of human embryonic stem cell-derived neural cell populations, Stem Cells, 25 (2007) 2257-2268.

[47] I.H. Park, R. Zhao, J.A. West, A. Yabuuchi, H. Huo, T.A. Ince, P.H. Lerou, M.W. Lensch, G.Q. Daley, Reprogramming of human somatic cells to pluripotency with defined factors.[see comment], Nature, 451 (2008) 141-146.

[48] P.M. Lackie, C. Zuber, J. Roth, Polysialic acid of the neural cell adhesion molecule (N-CAM) is widely expressed during organogenesis in mesodermal and endodermal derivatives, Differentiation, 57 (1994) 119-131.

[49] C.J. Moller, S. Christgau, M.R. Williamson, O.D. Madsen, Z.P. Niu, E. Bock, S. Baekkeskov, Differential expression of neural cell adhesion molecule and cadherins in

pancreatic islets, glucagonomas, and insulinomas, Molecular Endocrinology, 6 (1992) 1332-1342.

[50] S.M. Chambers, C.A. Fasano, E.P. Papapetrou, M. Tomishima, M. Sadelain, L. Studer, Highly efficient neural conversion of human ES and iPS cells by dual inhibition of SMAD signaling, Nat Biotechnol, 27 (2009) 275-280.

[51] L. Vallier, T. Touboul, Z. Chng, M. Brimpari, N. Hannan, E. Millan, L.E. Smithers, M. Trotter, P. Rugg-Gunn, A. Weber, R.A. Pedersen, Early cell fate decisions of human embryonic stem cells and mouse epiblast stem cells are controlled by the same signalling pathways, PLoS One, 4 (2009) e6082.

[52] U. Lendahl, L.B. Zimmerman, R.D. McKay, CNS stem cells express a new class of intermediate filament protein, Cell, 60 (1990) 585-595.

[53] H.J. Fehling, G. Lacaud, A. Kubo, M. Kennedy, S. Robertson, G. Keller, V. Kouskoff, Tracking mesoderm induction and its specification to the hemangioblast during embryonic stem cell differentiation, Development, 130 (2003) 4217-4227.

[54] Y. Wang, N. Nakayama, WNT and BMP signaling are both required for hematopoietic cell development from human ES cells, Stem Cell Res, 3 (2009) 113-125.

[55] S. Tada, T. Era, C. Furusawa, H. Sakurai, S. Nishikawa, M. Kinoshita, K. Nakao, T. Chiba, S. Nishikawa, Characterization of mesendoderm: a diverging point of the definitive endoderm and mesoderm in embryonic stem cell differentiation culture, Development, 132 (2005) 4363-4374.

[56] L.G. Chase, M.T. Firpo, Development of serum-free culture systems for human embryonic stem cells, Current Opinion in Chemical Biology, 11 (2007) 367-372.

[57] K. Tachibana, S. Hirota, H. Iizasa, H. Yoshida, K. Kawabata, Y. Kataoka, Y. Kitamura, K. Matsushima, N. Yoshida, S. Nishikawa, T. Kishimoto, T. Nagasawa, The chemokine receptor CXCR4 is essential for vascularization of the gastrointestinal tract, Nature, 393 (1998) 591-594.

[58] J. Imitola, K. Raddassi, K.I. Park, F.J. Mueller, M. Nieto, Y.D. Teng, D. Frenkel, J. Li, R.L. Sidman, C.A. Walsh, E.Y. Snyder, S.J. Khoury, Directed migration of neural stem cells to sites of CNS injury by the stromal cell-derived factor 1alpha/CXC chemokine receptor 4 pathway, Proc Natl Acad Sci U S A, 101 (2004) 18117-18122.

[59] M. Ema, S. Takahashi, J. Rossant, Deletion of the selection cassette, but not cis-acting elements, in targeted Flk1-lacZ allele reveals Flk1 expression in multipotent mesodermal progenitors, Blood, 107 (2006) 111-117.

[60] S.J. Kattman, T.L. Huber, G.M. Keller, Multipotent flk-1+ cardiovascular progenitor cells give rise to the cardiomyocyte, endothelial, and vascular smooth muscle lineages, Dev Cell, 11 (2006) 723-732.

[61] F.W. King, C. Ritner, W. Liszewski, H.C. Kwan, A. Pedersen, A.D. Leavitt, H.S. Bernstein, Subpopulations of human embryonic stem cells with distinct tissue-specific fates can be selected from pluripotent cultures, Stem Cells Dev, 18 (2009) 1441-1450.

[62] M. Nakagawa, M. Koyanagi, K. Tanabe, K. Takahashi, T. Ichisaka, T. Aoi, K. Okita, Y. Mochiduki, N. Takizawa, S. Yamanaka, Generation of induced pluripotent stem cells without Myc from mouse and human fibroblasts, Nat Biotechnol, 26 (2008) 101-106.

[63] B. Parekkadan, Y. Berdichevsky, D. Irimia, A. Leeder, G. Yarmush, M. Toner, J.B. Levine, M.L. Yarmush, Cell-cell interaction modulates neuroectodermal specification of embryonic stem cells, Neuroscience Letters, 438 (2008) 190-195.

[64] J.R. Smith, L. Vallier, G. Lupo, M. Alexander, W.A. Harris, R.A. Pedersen, Inhibition of Activin/Nodal signaling promotes specification of human embryonic stem cells into neuroectoderm, Developmental Biology, 313 (2008) 107-117.

[65] K. Watanabe, D. Kamiya, A. Nishiyama, T. Katayama, S. Nozaki, H. Kawasaki, Y. Watanabe, K. Mizuseki, Y. Sasai, Directed differentiation of telencephalic precursors from embryonic stem cells, Nature Neuroscience, 8 (2005) 288-296.

[66] M.T. Pankratz, X.J. Li, T.M. Lavaute, E.A. Lyons, X. Chen, S.C. Zhang, Directed neural differentiation of human embryonic stem cells via an obligated primitive anterior stage, Stem Cells, 25 (2007) 1511-1520.

[67] K.A. D'Amour, A.D. Agulnick, S. Eliazer, O.G. Kelly, E. Kroon, E.E. Baetge, Efficient differentiation of human embryonic stem cells to definitive endoderm, Nature Biotechnology, 23 (2005) 1534-1541.

[68] O. Goldman, O. Feraud, J. Boyer-Di Ponio, C. Driancourt, D. Clay, M.C. Le Bousse-Kerdiles, A. Bennaceur-Griscelli, G. Uzan, A boost of BMP4 accelerates the commitment of human embryonic stem cells to the endothelial lineage, Stem Cells, 27 (2009) 1750-1759.

[69] P. Zhang, J. Li, Z. Tan, C. Wang, T. Liu, L. Chen, J. Yong, W. Jiang, X. Sun, L. Du, M. Ding, H. Deng, Short-term BMP-4 treatment initiates mesoderm induction in human embryonic stem cells, Blood, 111 (2008) 1933-1941.

[70] R. Patani, A. Compston, C.A. Puddifoot, D.J. Wyllie, G.E. Hardingham, N.D. Allen, S. Chandran, Activin/Nodal inhibition alone accelerates highly efficient neural conversion from human embryonic stem cells and imposes a caudal positional identity, PLoS ONE [Electronic Resource], 4 (2009) e7327.

[71] S. Armknecht, M. Boutros, A. Kiger, K. Nybakken, B. Mathey-Prevot, N. Perrimon, High-throughput RNA interference screens in Drosophila tissue culture cells, Methods Enzymol, 392 (2005) 55-73.

[72] G.A. Barker, S.L. Diamond, RNA interference screen to identify pathways that enhance or reduce nonviral gene transfer during lipofection, Mol Ther, 16 (2008) 1602-1608.

[73] H.M. Faessel, L.M. Levasseur, H.K. Slocum, W.R. Greco, Parabolic growth patterns in 96-well plate cell growth experiments, In Vitro Cell Dev Biol Anim, 35 (1999) 270-278.

[74] E. Lucumi, C. Darling, H. Jo, A.D. Napper, R. Chandramohanadas, N. Fisher, A.E. Shone, H. Jing, S.A. Ward, G.A. Biagini, W.F. DeGrado, S.L. Diamond, D.C. Greenbaum, Discovery of potent small-molecule inhibitors of multidrug-resistant Plasmodium falciparum using a novel miniaturized high-throughput luciferase-based assay, Antimicrob Agents Chemother, 54 3597-3604.

[75] Y. Xu, S.H. Mirmalek-Sani, F. Lin, J. Zhang, R.O. Oreffo, Adipocyte differentiation induced using nonspecific siRNA controls in cultured human mesenchymal stem cells, Rna, 13 (2007) 1179-1183.

[76] S. Yao, S. Chen, J. Clark, E. Hao, G.M. Beattie, A. Hayek, S. Ding, Long-term self-renewal and directed differentiation of human embryonic stem cells in chemically

defined conditions, Proceedings of the National Academy of Sciences of the United States of America, 103 (2006) 6907-6912.

[77] L. Xiao, X. Yuan, S.J. Sharkis, Activin A maintains self-renewal and regulates fibroblast growth factor, Wnt, and bone morphogenic protein pathways in human embryonic stem cells, Stem Cells, 24 (2006) 1476-1486.

[78] H. Bai, Y. Gao, M. Arzigian, D.M. Wojchowski, W.S. Wu, Z.Z. Wang, BMP4 regulates vascular progenitor development in human embryonic stem cells through a smad-dependent pathway, J Cell Biochem, 109 363-374.

[79] G. Narazaki, H. Uosaki, M. Teranishi, K. Okita, B. Kim, S. Matsuoka, S. Yamanaka, J.K. Yamashita, Directed and systematic differentiation of cardiovascular cells from mouse induced pluripotent stem cells, Circulation, 118 (2008) 498-506.

[80] J. Palis, S. Robertson, M. Kennedy, C. Wall, G. Keller, Development of erythroid and myeloid progenitors in the yolk sac and embryo proper of the mouse, Development, 126 (1999) 5073-5084.

[81] J.C. Boisset, C. Robin, On the origin of hematopoietic stem cells: progress and controversy, Stem Cell Res, 8 (2012) 1-13.

[82] T.L. Huber, V. Kouskoff, H.J. Fehling, J. Palis, G. Keller, Haemangioblast commitment is initiated in the primitive streak of the mouse embryo, Nature, 432 (2004) 625-630.

[83] J. Tober, A. Koniski, K.E. McGrath, R. Vemishetti, R. Emerson, K.K. de Mesy-Bentley, R. Waugh, J. Palis, The megakaryocyte lineage originates from hemangioblast precursors and is an integral component both of primitive and of definitive hematopoiesis, Blood, 109 (2007) 1433-1441.

[84] I. Godin, F. Dieterlen-Lievre, A. Cumano, Emergence of multipotent hemopoietic cells in the yolk sac and paraaortic splanchnopleura in mouse embryos, beginning at 8.5 days postcoitus, Proc Natl Acad Sci U S A, 92 (1995) 773-777.

[85] A. Medvinsky, E. Dzierzak, Definitive hematopoiesis is autonomously initiated by the AGM region, Cell, 86 (1996) 897-906.

[86] O. Klimchenko, M. Mori, A. Distefano, T. Langlois, F. Larbret, Y. Lecluse, O. Feraud, W. Vainchenker, F. Norol, N. Debili, A common bipotent progenitor generates the erythroid and megakaryocyte lineages in embryonic stem cell-derived primitive hematopoiesis, Blood, 114 (2009) 1506-1517.

[87] T. Nakano, H. Kodama, T. Honjo, Generation of lymphohematopoietic cells from embryonic stem cells in culture, Science, 265 (1994) 1098-1101.

[88] M.A. Vodyanik, J.A. Bork, J.A. Thomson, Slukvin, II, Human embryonic stem cell-derived CD34+ cells: efficient production in the coculture with OP9 stromal cells and analysis of lymphohematopoietic potential, Blood, 105 (2005) 617-626.

[89] M.A. Vodyanik, J.A. Thomson, Slukvin, II, Leukosialin (CD43) defines hematopoietic progenitors in human embryonic stem cell differentiation cultures, Blood, 108 (2006) 2095-2105.

[90] L. Chicha, A. Feki, A. Boni, O. Irion, O. Hovatta, M. Jaconi, Human pluripotent stem cells differentiated in fully defined medium generate hematopoietic CD34- and CD34+ progenitors with distinct characteristics, PLoS One, 6 (2011) e14733.

[91] A. Niwa, T. Heike, K. Umeda, K. Oshima, I. Kato, H. Sakai, H. Suemori, T. Nakahata, M.K. Saito, A novel serum-free monolayer culture for orderly hematopoietic

differentiation of human pluripotent cells via mesodermal progenitors, PLoS ONE [Electronic Resource], 6 (2011) e22261.

[92] J.T. Outten, X. Cheng, P. Gadue, D.L. French, S.L. Diamond, A high-throughput multiplexed screening assay for optimizing serum-free differentiation protocols of human embryonic stem cells, Stem Cell Res, 6 (2011) 129-142.

[93] S.R. Braam, R. Nauw, D. Ward-van Oostwaard, C. Mummery, R. Passier, Inhibition of ROCK improves survival of human embryonic stem cell-derived cardiomyocytes after dissociation, Ann N Y Acad Sci, 1188 (2010) 52-57.

[94] R.C. Lindsley, J.G. Gill, M. Kyba, T.L. Murphy, K.M. Murphy, Canonical Wnt signaling is required for development of embryonic stem cell-derived mesoderm, Development, 133 (2006) 3787-3796.

[95] L.G. Villa-Diaz, C. Pacut, N.A. Slawny, J. Ding, K.S. O'Shea, G.D. Smith, Analysis of the factors that limit the ability of feeder cells to maintain the undifferentiated state of human embryonic stem cells, Stem Cells Dev, 18 (2009) 641-651.

[96] E.H. Lee, R. Chari, A. Lam, R.T. Ng, J. Yee, J. English, K.G. Evans, C. Macaulay, S. Lam, W.L. Lam, Disruption of the non-canonical WNT pathway in lung squamous cell carcinoma, Clin Med Oncol, 2008 (2008) 169-179.

[97] M. Radinger, D. Smrz, D.D. Metcalfe, A.M. Gilfillan, Glycogen synthase kinase-3beta is a prosurvival signal for the maintenance of human mast cell homeostasis, J Immunol, 187 (2011) 5587-5595.

[98] D. Metcalf, L. Di Rago, S. Mifsud, Synergistic and inhibitory interactions in the in vitro control of murine megakaryocyte colony formation, Stem Cells, 20 (2002) 552-560.

[99] M. Yu, A.B. Cantor, Megakaryopoiesis and thrombopoiesis: an update on cytokines and lineage surface markers, Methods Mol Biol, 788 (2012) 291-303.

[100] S.J. Lu, Q. Feng, S. Caballero, Y. Chen, M.A. Moore, M.B. Grant, R. Lanza, Generation of functional hemangioblasts from human embryonic stem cells, Nat Methods, 4 (2007) 501-509.

[101] C. Lengerke, S. Schmitt, T.V. Bowman, I.H. Jang, L. Maouche-Chretien, S. McKinney-Freeman, A.J. Davidson, M. Hammerschmidt, F. Rentzsch, J.B. Green, L.I. Zon, G.Q. Daley, BMP and Wnt specify hematopoietic fate by activation of the Cdx-Hox pathway, Cell Stem Cell, 2 (2008) 72-82.

[102] S. Ueno, G. Weidinger, T. Osugi, A.D. Kohn, J.L. Golob, L. Pabon, H. Reinecke, R.T. Moon, C.E. Murry, Biphasic role for Wnt/beta-catenin signaling in cardiac specification in zebrafish and embryonic stem cells, Proc Natl Acad Sci U S A, 104 (2007) 9685-9690.

[103] Y. Wang, K. Umeda, N. Nakayama, Collaboration between WNT and BMP signaling promotes hemoangiogenic cell development from human fibroblast-derived iPS cells, Stem Cell Res, 4 223-231.

[104] P.S. Woll, J.K. Morris, M.S. Painschab, R.K. Marcus, A.D. Kohn, T.L. Biechele, R.T. Moon, D.S. Kaufman, Wnt signaling promotes hematoendothelial cell development from human embryonic stem cells, Blood, 111 (2008) 122-131.

[105] K. Gauthaman, C.Y. Fong, A. Bongso, Effect of ROCK inhibitor Y-27632 on normal and variant human embryonic stem cells (hESCs) in vitro: its benefits in hESC expansion, Stem Cell Rev, 6 (2010) 86-95.

[106] C. Bueno, R. Montes, P. Menendez, The ROCK inhibitor Y-27632 negatively affects the expansion/survival of both fresh and cryopreserved cord blood-derived CD34+ hematopoietic progenitor cells: Y-27632 negatively affects the expansion/survival of CD34+HSPCs, Stem Cell Rev, 6 (2010) 215-223.

[107] S. Pearson, P. Sroczynska, G. Lacaud, V. Kouskoff, The stepwise specification of embryonic stem cells to hematopoietic fate is driven by sequential exposure to Bmp4, activin A, bFGF and VEGF, Development, 135 (2008) 1525-1535.

[108] E.T. Zambidis, T.S. Park, W. Yu, A. Tam, M. Levine, X. Yuan, M. Pryzhkova, B. Peault, Expression of angiotensin-converting enzyme (CD143) identifies and regulates primitive hemangioblasts derived from human pluripotent stem cells, Blood, 112 (2008) 3601-3614.

[109] M.G. Manz, T. Miyamoto, K. Akashi, I.L. Weissman, Prospective isolation of human clonogenic common myeloid progenitors, Proc Natl Acad Sci U S A, 99 (2002) 11872-11877.

[110] A.E. Grigoriadis, M. Kennedy, A. Bozec, F. Brunton, G. Stenbeck, I.H. Park, E.F. Wagner, G.M. Keller, Directed differentiation of hematopoietic precursors and functional osteoclasts from human ES and iPS cells, Blood, 115 (2010) 2769-2776.

[111] M. Takahashi, Y. Nakamura, K. Obama, Y. Furukawa, Identification of SP5 as a downstream gene of the beta-catenin/Tcf pathway and its enhanced expression in human colon cancer, Int J Oncol, 27 (2005) 1483-1487.

[112] Y. Yokoyama, T. Suzuki, M. Sakata-Yanagimoto, K. Kumano, K. Higashi, T. Takato, M. Kurokawa, S. Ogawa, S. Chiba, Derivation of functional mature neutrophils from human embryonic stem cells, Blood, 113 (2009) 6584-6592.

[113] T. Mercher, M.G. Cornejo, C. Sears, T. Kindler, S.A. Moore, I. Maillard, W.S. Pear, J.C. Aster, D.G. Gilliland, Notch signaling specifies megakaryocyte development from hematopoietic stem cells, Cell Stem Cell, 3 (2008) 314-326.